NTNU – Trondheim
Norwegian University of
Science and Technology

Long Term Hydropower Scheduling under Price and Inflow Uncertainty

A Linear Decision Rules Approach

Ajla Hadziomerovic
Nina Ingvoldstad
Ida Alexandra Utheim Grønvik

Industrial Economics and Technology Management
Submission date: June 2013
Supervisor: Stein-Erik Fleten, IØT
Co-supervisor: Rudolf Egging, IØT

Norwegian University of Science and Technology
Department of Industrial Economics and Technology Management

NTNU
Det skapende universitet

MASTERKONTRAKT

- uttak av masteroppgave

1. Studentens personalia

Etternavn, fornavn **Utheim Grønvik, Ida Alexandra**	Fødselsdato **03. sep 1989**
E-post **idaalexa@stud.ntnu.no**	Telefon **41764902**

2. Studieopplysninger

Fakultet **Fakultet for Samfunnsvitenskap og teknologiledelse**	
Institutt **Institutt for industriell økonomi og teknologiledelse**	
Studieprogram **Industriell økonomi og teknologiledelse**	Hovedprofil **Anvendt økonomi og optimering**

3. Masteroppgave

Oppstartsdato **15. jan 2013**	Innleveringsfrist **11. jun 2013**
Oppgavens (foreløpige) tittel **Hydropower scheduling under price- and inflow uncertainty**	
Oppgavetekst/Problembeskrivelse Operational planning of a hydropower plant with reservoir capacity must weigh the benefits of current release of water against the opportunity cost associated with having less water for future generation. The benefit of having water in the reservoirs depends on future electricity price levels and future inflow, both of which are uncertain. This thesis will develop a decision model based on optimization for the scheduling problem. To the extent it is useful, both price and inflow uncertainty will be taken into account. The decision model will be demonstrated on several Norwegian hydropower plants. The goal is to analyse the hydropower scheduling problem.	
Hovedveileder ved institutt **Professor Stein-Erik Fleten**	Medveileder(e) ved institutt **Rudolf Egging**
Merknader **1 uke ekstra p.g.a påske.**	

4. Underskrift

Student: Jeg erklærer herved at jeg har satt meg inn i gjeldende bestemmelser for mastergradsstudiet og at jeg oppfyller kravene for adgang til å påbegynne oppgaven, herunder eventuelle praksiskrav.

Partene er gjort kjent med avtalens vilkår, samt kapitlene i studiehåndboken om generelle regler og aktuell studieplan for masterstudiet.

Trondheim 25.01.2013

Sted og dato

Ida Grønvik — **Student**

Stein-E. Fleten — **Hovedveileder**

Originalen lagres i NTNUs elektroniske arkiv. Kopi av avtalen sendes til instituttet og studenten.

NTNU
Det skapende universitet

MASTERKONTRAKT

- uttak av masteroppgave

1. Studentens personalia

Etternavn, fornavn	Fødselsdato
Hadziomerovic, Ajla	**30. jul 1989**
E-post **hadziome@stud.ntnu.no**	Telefon **92454001**

2. Studieopplysninger

Fakultet **Fakultet for Samfunnsvitenskap og teknologiledelse**	
Institutt **Institutt for industriell økonomi og teknologiledelse**	
Studieprogram **Industriell økonomi og teknologiledelse**	Hovedprofil **Investering, finans og økonomistyring**

3. Masteroppgave

Oppstartsdato **15. jan 2013**	Innleveringsfrist **11. jun 2013**
Oppgavens (foreløpige) tittel **Hydropower scheduling under price- and inflow uncertainty**	
Oppgavetekst/Problembeskrivelse Operational planning of a hydropower plant with reservoir capacity must weigh the benefits of current release of water against the opportunity cost associated with having less water for future generation. The benefit of having water in the reservoirs depends on future electricity price levels and future inflow, both of which are uncertain. This thesis will develop a decision model based on optimization for the scheduling problem. To the extent it is useful, both price and inflow uncertainty will be taken into account. The decision model will be demonstrated on several Norwegian hydropower plants. The goal is to analyse the hydropower scheduling problem.	
Hovedveileder ved institutt **Professor Stein-Erik Fleten**	Medveileder(e) ved institutt **Rudolf Egging**
Merknader **1 uke ekstra p.g.a påske.**	

4. Underskrift

Student: Jeg erklærer herved at jeg har satt meg inn i gjeldende bestemmelser for mastergradsstudiet og at jeg oppfyller kravene for adgang til å påbegynne oppgaven, herunder eventuelle praksiskrav.

Partene er gjort kjent med avtalens vilkår, samt kapitlene i studiehåndboken om generelle regler og aktuell studieplan for masterstudiet.

Trondheim, 25.01.2013
Sted og dato

Ajla Hadziomerovic
Student

Stein-E. Fleten
Hovedveileder

Originalen lagres i NTNUs elektroniske arkiv. Kopi av avtalen sendes til instituttet og studenten.

NTNU
Det skapende universitet

MASTERKONTRAKT
- uttak av masteroppgave

1. Studentens personalia

Etternavn, fornavn **Ingvoldstad, Nina**	Fødselsdato **13. jan 1989**
E-post **ninain@stud.ntnu.no**	Telefon **99010975**

2. Studieopplysninger

Fakultet **Fakultet for Samfunnsvitenskap og teknologiledelse**	
Institutt **Institutt for industriell økonomi og teknologiledelse**	
Studieprogram **Industriell økonomi og teknologiledelse**	Hovedprofil **Anvendt økonomi og optimering**

3. Masteroppgave

Oppstartsdato **15. jan 2013**	Innleveringsfrist **11. jun 2013**
Oppgavens (foreløpige) tittel **Hydropower scheduling under price- and inflow uncertainty**	
Oppgavetekst/Problembeskrivelse Operational planning of a hydropower plant with reservoir capacity must weigh the benefits of current release of water against the opportunity cost associated with having less water for future generation. The benefit of having water in the reservoirs depends on future electricity price levels and future inflow, both of which are uncertain. This thesis will develop a decision model based on optimization for the scheduling problem. To the extent it is useful, both price and inflow uncertainty will be taken into account. The decision model will be demonstrated on several Norwegian hydropower plants. The goal is to analyse the hydropower scheduling problem.	
Hovedveileder ved institutt **Professor Stein-Erik Fleten**	Medveileder(e) ved institutt **Rudolf Egging**
Merknader **1 uke ekstra p.g.a påske.**	

4. Underskrift

Student: Jeg erklærer herved at jeg har satt meg inn i gjeldende bestemmelser for mastergradsstudiet og at jeg oppfyller kravene for adgang til å påbegynne oppgaven, herunder eventuelle praksiskrav.

Partene er gjort kjent med avtalens vilkår, samt kapitlene i studiehåndboken om generelle regler og aktuell studieplan for masterstudiet.

Trondheim, 25/01 - 2013

Sted og dato

Nina Ingvoldstad

Student

Stein-E. Fleten

Hovedveileder

Originalen lagres i NTNUs elektroniske arkiv. Kopi av avtalen sendes til instituttet og studenten.

Preface

This master thesis is the final assignment in the Master of Science degree in Industrial Economics and Technology Management at the Norwegian University of Science and Technology (NTNU) in Trondheim, Norway. This thesis has been written during the spring of 2013 and is a part of the specialization in Financial Engineering and Managerial Economics and Operational Research.

We would like to thank our supervisor, professor Stein-Erik Fleten, and co-supervisor associate professor Rudolf Egging, for advice and support during the writing of the thesis. A special thanks also goes to the hydropower producers for providing data.

Trondheim, June 11th 2013

Ida Grønvik Ajla Hadžiomerović Nina Ingvoldstad

Abstract

This thesis takes the perspective of a hydropower producer facing the task of determining a long term reservoir management strategy that maximizes the expected market value of production. This task is complicated by the uncertainty in future electricity price and inflow. Linear Stochastic Programming and Stochastic Dynamic Programming are traditionally used for solving these type of problems. The size of these problems grows exponentially with the number of stages and the number of state variables, respectively. Hence the problems may become computationally cumbersome. In this thesis, a multistage stochastic scheduling model is developed based on the Linear Decision Rules (LDR) approximation. This approximation is effective at reducing computational complexity, and permits scalability to multistage models (Kuhn et al., 2011). By restricting the decision variables to be affine functions of the realisations of the uncertain parameters, the original intractable problem is transformed into a tractable one with short computational time. In order to estimate the loss of optimality incurred by the complexity reduction, the approximation is applied to both the primal version and the dual version of the problem. The approach is demonstrated on four Norwegian hydropower plants, and is proven to give an acceptable trade-off between accuracy and tractability. It is shown that both the length of the scheduling horizon considered and the relation between the size of the reservoirs, the amount and distribution of inflow and the production capacity of the power stations affect the reservoir management strategies.

Sammendrag

Denne masteroppgaven tar perspektivet til en vannkraftprodusent som skal bestemme en langsiktig reservoarhåndteringsstrategi som maksimerer produksjonens forventede markedsverdi. Usikkerhet i framtidig strømpris og tilsig kompliserer denne beslutningsprosessen. Lineær stokastisk programmering og stokastisk dynamisk programmering er metoder som vanligvis brukes for å løse denne typen problemer. Størrelsen på disse problemene vokser eksponentielt med henholdsvis antall steg og antall tilstandsvariable, noe som kan resultere i uhåndterbare dimensjoner. I denne masteroppgaven utvikles en stokastisk flerstegs planleggingsmodell basert på lineære beslutningsregler. Ved å begrense beslutningsvariablene til å være funksjoner av de ukjente parameterne kan det uløselige problemet transformeres til et løsbart et. Metoden reduserer kompleksiteten til det opprinnelige problemet, noe som medfører korte regnetider. For å estimere optimalitetstapet som følger av kompleksitetsreduksjonen, brukes lineære beslutningsregler både på den primale og duale versjonen av problemet. Metoden demonstreres på fire norske vannkraftverk, og det er vist at både lengden på planleggingsperioden og forholdet mellom reservoarstørrelse, mengde og distribusjon av tilsig og produksjonskapasiteten til kraftstasjonene påvirker reservoarhåndteringsstrategien.

Contents

1 Introduction

This thesis takes the perspective of a hydropower producer with one or several reservoirs and power stations, aiming to maximize the expected market value of production. When deciding a scheduling strategy, there is a trade-off between releasing water now, receiving the spot price of electricity, or saving the water for future release (Fleten et al., 2011). The producers flexibility in choosing when to release the available water depends on the size of the reservoir(s), the amount and distribution of inflow and the production capacity of the power station(s). The scheduling task is complicated by the presence of uncertainties and the span in time in which the scheduling takes place.

The scheduling problem is normally separated into three parts with different degree of detail and different scheduling horizon; long term, seasonal term and short term scheduling (Wallace and Fleten, 2003). The focus of this thesis is on long term scheduling, in which the objective is to obtain optimal use of resources with a time horizon of one to five years. Long term scheduling represents the strategic reservoir management, and initialises boundary conditions for the more detailed seasonal or short term models.

The Nordic countries have a liberialised common market, in which hydropower constitutes about 50 % of total generation (Gjelsvik et al. 2010). In Norway, hydropower accounts for 99 % of the total power generation. Due to the high fraction of hydro, market prices will depend on the hydrological situation, and taking the stochasticity in inflow into account is therefore essential. Assuming that the individual producers can not influence the market price, it is also necessary to model stochasticity in price. In this thesis, stochastic models for price and inflow are developed in order to provide forecasts for the long term scheduling. Parameters for these models are computed based on historical spot prices, forward and futures prices and historical inflow data collected from four Norwegian hydropower producers.

A traditional approach for solving reservoir management problems under uncertainty is Stochastic Dynamic Programming. This approach offer convenient and efficient solutions for developing complex reservoir management strategies (Cheng et al., 2008). Instead of solving the large problem directly, this approach consists of solving a sequence of small subproblems. Each subproblem is associated with a specific time period of the scheduling horizon and a possible state of the dynamic system (Carpentier et al., 2012). The size of dynamic problems grows exponentially with the number of state variables.

Another commonly used approach for solving multistage stochastic hydropower scheduling problems is by approximating the underlying stochastic process of the uncertain parameters to be discrete. The process can then be represented by a discrete scenario tree which ramifies at all points when new random data becomes known (Rocha and Kuhn, 2012). According to Kaut and Wallace (2007), the ability to generate good scenario trees is highly dependent on the knowledge of the underlying process. As the probability distribution of the uncertain parameters are rarely known, this approach may rely on unrealistic simplifying assumptions in order to achieve tractability (Guslitser, 2002). The size of these problems grows exponentially with the number of time stages, and do often suffer from the curse of dimensionality. According to Shapiro and Nemirovski (2005), multistage problems are computationally intractable even when medium accuracy solutions are sought. These findings show that it is important to focus on developing tractable methodologies, that can reasonably approximate the stochastic programs.

Stochastic programs needs to undergo some simplification in order to gain computational tractability (Kuhn et al., 2011). The Linear Decision Rules (LDR) approximation consists of restricting the recourse decisions associated with the stochastic program to be functions of the realisations of the uncertain parameters. According to Ben-Tal et al. (2003), the uncertain parameters are defined within an interval around their expected values, in which the size of the interval is given by the level of uncertainty. By applying the LDR approach, the original stochastic program is converted into a seminfinite program. In the case of fixed recourse, provided that the uncertainty set itself is computationally tractable, this program is computationally tractable. In the case of a polyhedral[1] uncertainty set, the fixed recourse program is equivalent to an explicit linear programming program. Although the LDR approach is very effective at reducing computational complexity, it may incur a considerable loss of optimality (Kuhn et al. 2011). By applying the approximation to both the primal version and the dual version of the original problem, this loss of optimality can be estimated by the gap between the optimal objective values of the two models.

The LDR approach was used in reservoir management as early as in 1969 by Revelle et al. (1969). After a long period of neglect, Ben-Tal et al. (2003) rediscovered the approach within the framework of robust optimization. LDR has successfully been used to solve supply chain problems with more than 70 decision stages (Ben-Tal et al., 2005). Tandberg and Vefring (2012) showed that the LDR approach can beneficially be applied to the generation planning problem. Network design problems involving hundreds of random variables (Atamturk and Zhang, 2007), and robust control problems involving 12 state variables and 20 time stages have also been successfully solved (Goulart and Kerrigan, 2005). Other application areas for LDR based robust optimization include capacity expansion of networks (Ordóñez and Zaho, 2007) and project scheduling (Ang et al., 2008).

The contribution of this thesis is the development of a multistage stochastic hydropower scheduling model based on the LDR approximation. Currently, there are few studies on this field. To evaluate the applicability of the approximation

[1] A set $P \subseteq R^n$ is a polyhedron if there is a system of finitely many inequalities $Ax \leq b$ such that $P = \{x \in R^n | Ax \leq b\}$.

to the long term scheduling problem, the LDR model will be demonstrated on four Norwegian hydropower plants. The trade-off between the accuracy and the tractability of the method will be investigated. Focus will also be on how uncertainty in price and inflow affects the problem and how the flexibility of the hydropower plants relates to the reservoir management strategies given by the model.

The thesis is divided into ten sections. Section 2 gives a presentation of the hydropower scheduling problem and the main challenges associated with it, while information about the four hydropower plants and electricity data is presented in Section 3. Assumptions and simplifications made throughout the thesis are presented in the end of this section. Section 4 presents the stochastic models developed to forecast price and inflow, while Section 5 presents the methods used to estimate the model parameters and the results from the estimations. The primal LDR model is presented in Section 6, while the dual version is presented in Section 7. The analysis and the conclusion is presented in Sections 8 and 9, respectively, while suggestions for further work are presented in Section 10.

2 Hydropower scheduling

In this section, a presentation of the hydropower scheduling problem and the main challenges associated with it is provided.

2.1 Reservoir management

The objective of long term hydropower scheduling is to utilise the available water resources in a way that maximizes the expected market value of production. This task is complicated by the presence of uncertainty in electricity price and inflow. The availability of limited amounts of water in the reservoirs, in combination with the uncertainty in the future amounts of inflow, makes the optimization problem more difficult because it creates a link between an operating decision in a given stage and the future consequences of this decision (Terry et al., 1986).

The average annual hydropower production in Norway is 125 TWh (Ministry of Petroleum and Energy, 2013), while the actual production may vary with a magnitude of 40 TWh from a dry year to a wet year (Kristiansen, 2004). The electricity demand is connected to heating requirements, which for obvious reasons are much higher in the winter season compared to the other seasons (Kjærland and Larsen, 2010). Inflow, on the other hand, is lowest during the winter when precipitation mainly comes as snow and highest during the spring when the snow melting starts, which can be seen in Figure 2.1.1. This implies that prices are highly influenced by the seasonal variations in inflow.

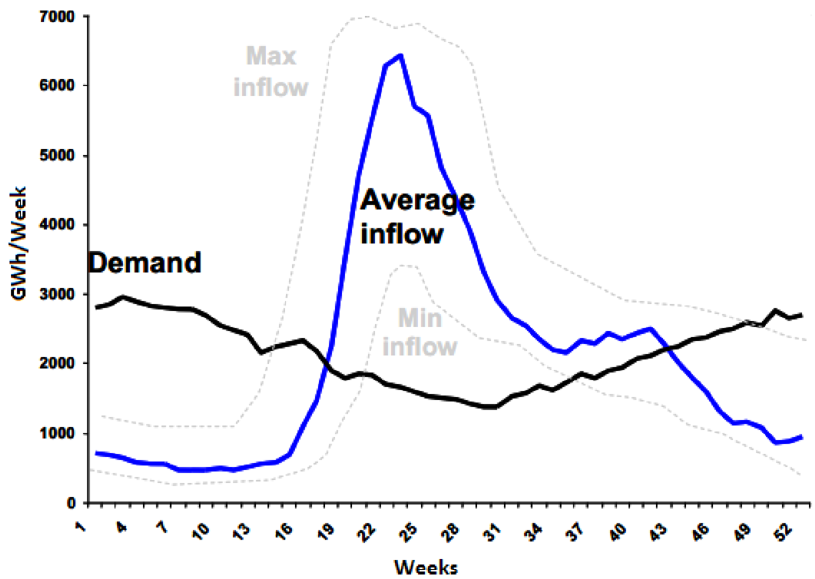

Figure 2.1.1: Weekly average, minimum and maximum inflow and demand in Norway (Doorman, 2012).

Due to the seasonal variations in inflow the year can be divided into three different periods (Doorman, 2012). In period 1 (week 1-17) precipitation mainly comes as snow. Period 2 (week 18-40) is the filling season as precipitation will come directly as inflow into the reservoirs and the accumulated snow will melt. Period 3 (week 41-52) is statistically the period with most precipitation and the highest inflow levels.

2.2 The concept of water values

Water is a free resource and the production costs are low and often neglected. However, the amounts of available water is limited and uncertain. Producing one unit of water today means that it cannot be produced in the future. This implies that the water has an opportunity cost, which is called the water value. The water value refers to the marginal value of having one additional unit of water available (Doorman, 2012).

Water at the bottom of the reservoir is more valuable than water at the top. When the reservoir is filled to its limit, the water value is equal to zero. More inflow will, in this situation, result in spillage. Hence, the extra water has no value to the producer. When the reservoir is nearly empty the water value is high, and a situation in which the producer is not be able to meet demand at high prices may occur. Hence, management of the reservoir at the top and bottom reservoir levels is crucial to avoid a situation of either spillage or shortage.

2.3 Flexibility of a hydropower reservoir

The term flexibility refers to the ability to allocate energy production to certain time periods in order to maximize profit(Crona, 2009). High flexibility gives the producer a larger possibility space to decide when and how much water to discharge for production, while low flexibility limits this option. The flexibility depends on the size of the reservoir, the amount and distribution of inflow into the reservoir and the production capacity. This will be elaborated in Section 3.1. Restrictions like time varying reservoir limits, maximum and minimum production requirements and maintenance periods reduces the flexibility of a hydropower plant.

Hydropower reservoirs are normally categorized within two different types; ”run of rivers” and ”reservoirs” (Rondeel, 2012). Run of rivers is a type of reservoir where little or no water storage is provided. They are characterized by a low degree of control on water discharge and thereby limited possibilities to adjust production to changes in price and inflow. Reservoirs, on the other hand, allows for water storage. The opportunity to store water creates an operational flexibility through which hydropower producers can adapt to price and inflow signals (Kjærland and Larsen, 2010). This gives hydropower plants with reservoirs an option to postpone production and wait for higher prices or more information about conditions affecting the market value of future production. Hence, the possibility to store water in the reservoirs can be viewed as a real option on future energy production where the water value represents the exercise price.

According to real option theory a reservoir with flexibility is more valuable than a reservoir without flexibility (Dixit and Pindyck, 1993). A similar conclusion is reached within optimization theory. For a maximization problem the objective value is non-increasing when imposing tighter constraints on the problem, while the opposite is true for a minimization problem (Lundgren et al., 2010). The water balance constraint is less strict for a reservoir with storage capacity than for a plant without. Reservoirs with storage capacity are therefore more valuable to the producer than those without, i.e. run of rivers.

2.4 Decomposed hydropower scheduling

Hydropower scheduling is a complex task, and is normally decomposed into three parts characterized by the scheduling horizon and the level of detail included. These levels are long term, seasonal term and short term scheduling (Wallace and Fleten, 2003). Long term scheduling represents the strategic management of the water resources. The objective is to obtain optimal use of the water resources with a time horizon of one to five years, depending on the characteristics of the system. A more detailed description of the hydropower system is included in seasonal term scheduling and the time horizon typically varies between 3 and 18 months. Short term scheduling represents the detailed physical operation of the hydropower plant within a time horizon of a day to a week, and with a time resolution of an hour or shorter. Stochastic models are used for long term and normally for seasonal term scheduling, while deterministic models are used for short term scheduling.

For hydropower systems with reservoirs the short term scheduling problem is a part of the long term scheduling problem in which the question is whether to release water now or store it for the future (Fleten et al., 2011). Hence, the long term scheduling problem imposes boundary conditions on the more detailed seasonal and short term scheduling. The most common principles for coupling between a longer term and a shorter term scheduling model are listed below:

- **Volume coupling**: The longer and shorter term scheduling models are coupled through a fixed reservoir level at a given point in time, i. e. the coupling time. This level is calculated in the long term model, and initialized as a boundary condition in the shorter term scheduling models. This procedure is rigid, and allows for little flexibility in the case of deviations from the original scheduling assumptions (Doorman, 2012).

- **Penalty functions**: The longer term and shorter term scheduling models are coupled through a fixed reservoir level at the coupling time. However, a deviation from the fixed volume is allowed, but will cause a penalty in the objective function. This penalty is not a real cost, but is used to allow for some flexibility with respect to deviations from the specified volume (Doorman, 2012).

- **Price coupling**: The longer and the shorter term scheduling models are coupled through a fixed water value at the coupling time. The water value corresponds to the dual value of the reservoir balance constraint in the long term model for the time period in which the coupling takes place (Doorman, 2012).

3 Data description

This section starts with a presentation of important factors describing the flexibility of a hydropower plant. A presentation of the hydropower plants studied in this thesis will then follow. Thereafter, a short description of the Nordic Power Market and the assumptions and simplifications made throughout the thesis is presented. An overview of electricity price properties will then follow, before a description of the correlation between the data series is presented at the end of the section.

3.1 Important factors

The relation between the production capacity of a hydropower plant, the size of the reservoir and the annual amount of inflow affects the flexibility of the hydropower plant, and can be described through various factors. These factor will be presented in this section, and Table 3.1.1 shows an overview of the factors for an average Norwegian producer[2].

Table 3.1.1: Factors for an average Norwegian hydropower producer.

Degree of regulation [year]	0.65
Utilization factor [%]	29.5
Load factor [%]	45

3.1.1 Degree of regulation

The degree of regulation is defined by the ratio between reservoir size and expected annual inflow, and describes the reservoir's ability to store water (Doorman, 2013). This factor states how many years it takes to fill the reservoir given average annual inflow and no generation, and can be used as a tool when determining the scheduling horizon of a hydropower plant. For plants with a high degree of regulation, decisions regarding water discharge may affect the state of the reservoir far into the future. Hence, a longer scheduling horizon needs to be considered for plants with a high degree of regulation than for plants with a lower one (Jain and Singh, 2003).

Inflow prediction will normally be of most significance to systems with a low degree of regulation because these reservoirs more often reach their maximum and minimum limits. A plant with a low degree of regulation is forced to produce more evenly distributed over the scheduling period in order to avoid spillage, while a plant with a high degree of regulation have more flexibility in choosing when to produce, enabling the power station to produce more during periods with high prices.

[2]The total installed capacity in Norway is 31.7 GW, the total reservoir capacity is 81 888 GWh (Hagem, 2011) and the total mean average inflow to the Norwegian reservoirs is 125 TWh (Ministry of Petroleum and Energy, 2013).

3.1.2 Utilization time

The utilization time of a hydropower plant measures the size of the reservoir compared to the power capacity (Ackermann, 2012). This factor describes how long time it takes to empty a full reservoir when running the generators at maximum capacity. High utilization time gives the plant little flexibility in choosing when to produce, while low utilization time enables the power station to produce more during periods with high prices.

3.1.3 Load factor

The load factor is defined by the ratio between the average annual inflow and the power capacity. The factor describes how long time it takes to produce an amount of water corresponding to one year of average inflow when running the generators at maximum capacity (Doorman, 2012). A high load factor allows for less flexibility than a lower one.

3.1.4 Energy coefficient

The amount of electricity generated by a hydropower plant is affected by the energy coefficient of that particular plant (Doorman, 2012). The larger the energy coefficient, the more energy per volume of water is generated. The energy coefficient is defined as:

$$e = \frac{1}{3.6 \cdot 10^6} \, \gamma \; g \; H \; \eta, \quad [{}^{kWh}/_{m^3}] \tag{3.1.1}$$

where γ is the water density $[{}^{kg}/_{m^3}]$, g is the gravity acceleration $[{}^{m}/_{s^2}]$, H is the plant head $[m]$ and η is the plant efficiency. Given the energy coefficient and the discharge capacity, Q $[{}^{m^3}/_{s}]$, the power capacity can be defined as:

$$P = 3.6 \; Q \; e, \quad [MW] \tag{3.1.2}$$

3.2 Presentation of the Hydropower Plants

The empirical analysis in this thesis is based on data from four Norwegian hydropower producers. This section presents technical and historical data and properties for these plants. Figure 3.2.1 shows where the hydropower plants are located. Figures showing historical and average inflow and reservoir levels are presented for all plants. In order not to reveal the identity of the hydropower producers, relative numbers are used, where 1 corresponds to the highest inflow observation.

3.2.1 Data preparation

The historical inflow series for the four hydropower plants show some degree of measurement error, as they contain some negative values for all of the hydropower plants. All these negative values are set equal to zero. Since these values constitute only a small proportion of the total time series, setting them equal to zero has a marginal impact on the inflow forecasts.

The inflow data series for Plant 1 is given as weekly energy flow $[^{MWh}/_{week}]$, while the inflow for Plants 2, 3 and 4 is measured daily and given in volume flow $[^{m^3}/_{s}]$. The LDR model requires the input data to have the unit energy flow per week $[^{MWh}/_{week}]$. Daily values for Plants 2, 3 and 4 are therefore aggregated into weekly values, and multiplied by the energy coefficient of the relevant plant.

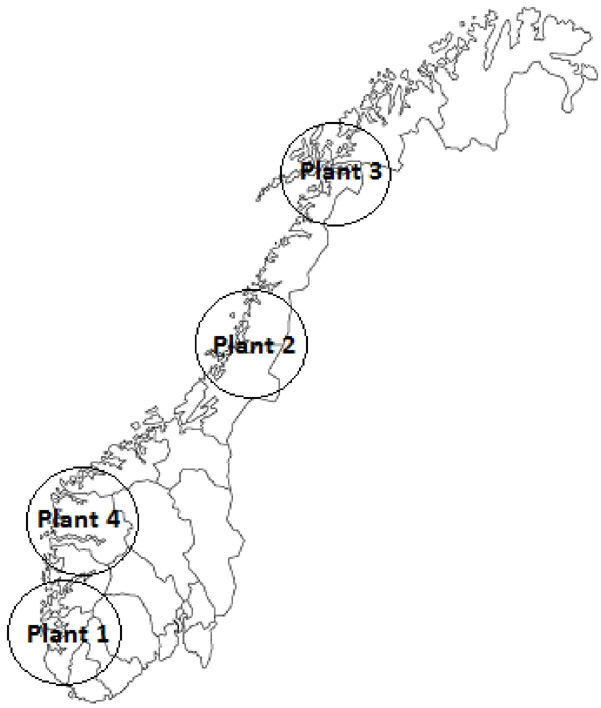

Figure 3.2.1: The map shows in were in Norway the four hydropower plants are located.

3.2.2 Hydropower Plant 1

Hydropower Plant 1 consists of one power station and five reservoirs, of which the lowest is considerably larger than the four others. The topology of this plant is presented in Figure 3.2.2. Only aggregated inflow series are available for this plant, and the reservoirs are therefore aggregated into one reservoir in the long term scheduling models.

The historical inflow series for Plant 1 consists of weekly observations in the period from January 1998 to August 2012. Before 2010 inflow were measured manually. This might have caused too high values in some weeks and too low in other weeks. From 2010 remote measurement has been used to measure inflow. The inflow data for Plant 1 show a lower degree of seasonality, and have higher

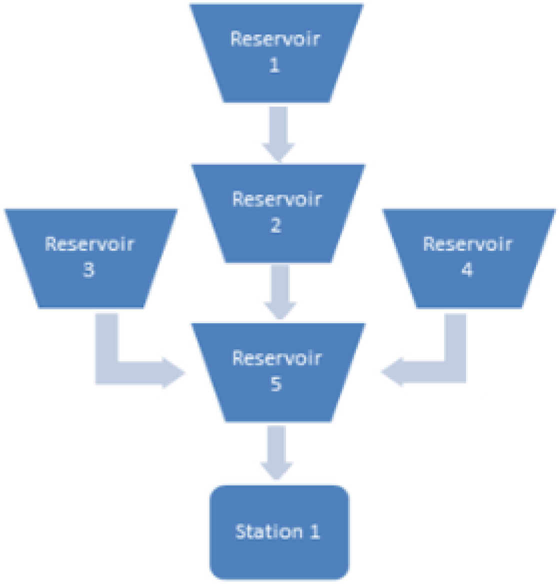

Figure 3.2.2: Topology of Plant 1.

inflow levels during the winter compared to the other plants studied in this thesis, see Figure 3.2.3. This is due to the location in Southern Norway, where the temperatures in the winter are normally higher than in the north of the country.

The plant has a degree of regulation of 0.55. The utilization factor of the aggregated reservoir is 23 %, while the load factor is 42 %. These factors are all lower than for an average Norwegian producer, see Table 3.1.1. The low degree of regulation means that Plant 1 has a lower ability to store inflow than an average plant. However the low utilization factor and load factor means that the production capacity is high compared to reservoir size and inflow, respectively. This implies that the short time it takes to fill the reservoir is compensated for by the relatively high production capacity. Due to the degree of regulation, a scheduling horizon of one year is chosen for Plant 1.

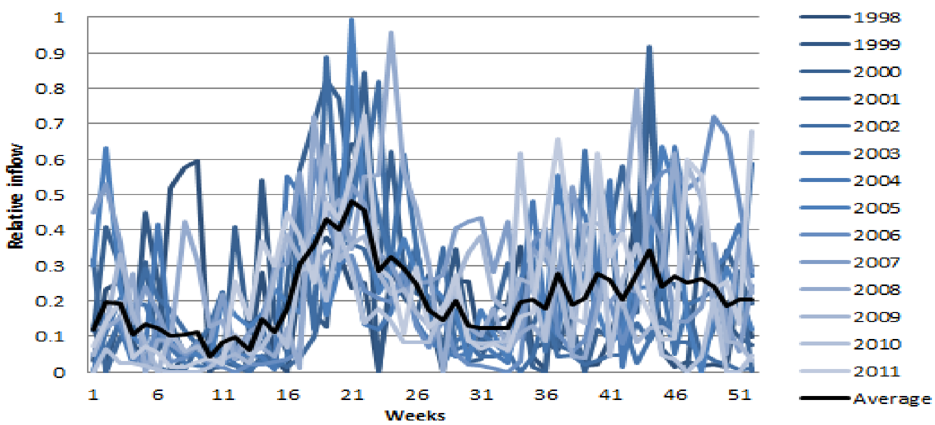

Figure 3.2.3: Historical and average inflow levels for Plant 1.

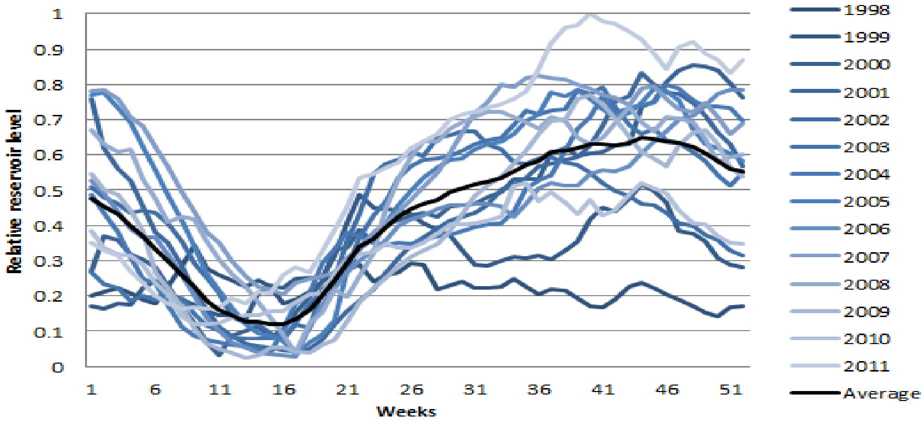

Figure 3.2.4: Historical and average reservoir levels for Plant 1.

3.2.3 Hydropower Plant 2

Hydropower Plant 2 consists of one power station and three reservoirs, of which the lowest is considerably larger than the two others. The topology of this plant is presented in Figure 3.2.5. Only aggregated inflow series are available for the plant, and the reservoirs are therefore aggregated into one reservoir in the long term scheduling models.

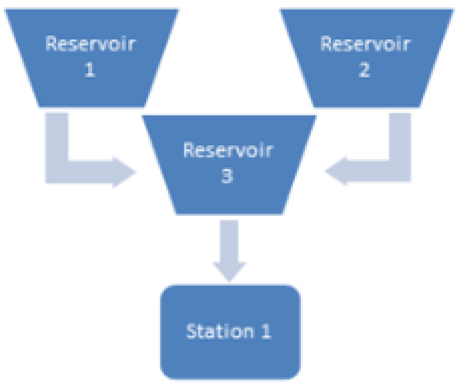

Figure 3.2.5: Topology of Plant 2.

The historical inflow series of Plant 2 consists of daily observations in the time period January 1998 to December 2008, and measurements are made at 12 a.m. each day. The time series shows a predictable seasonal pattern, with high inflow during the summer season and low inflow during the winter season, see Figure 3.2.6.

The plant has a degree of regulation of 0.37, which implies that the plant is less regulated than an average Norwegian plant, see Table 3.1.1. The utilization factor for the aggregated reservoir is 20 % while the load factor is 53 %. The low degree of regulation and the high load factor means that the reservoir is filled fast given average annual inflow, and that it takes long time to produce the average annual inflow at maximum capacity. This implies that the reservoir allows for little flexibility in choosing when to produce, and that the risk of spillage is high. Due to the degree of regulation, a scheduling horizon of one year is chosen for Plant 2.

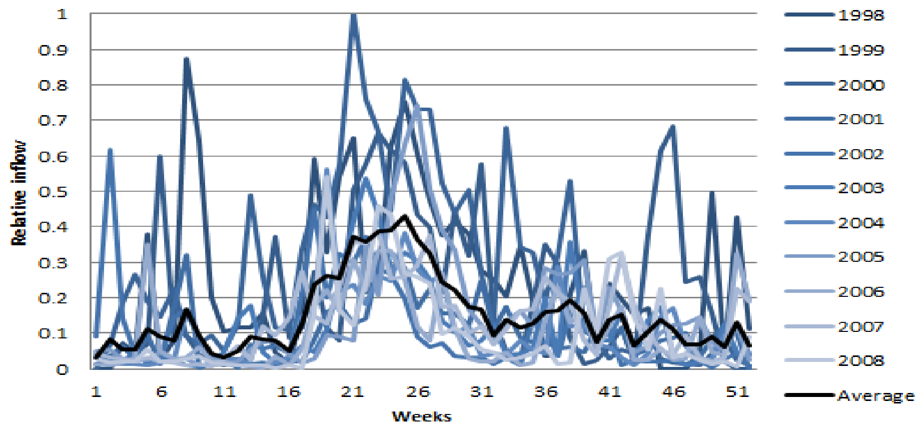

Figure 3.2.6: Historical and average inflow levels for Plant 2.

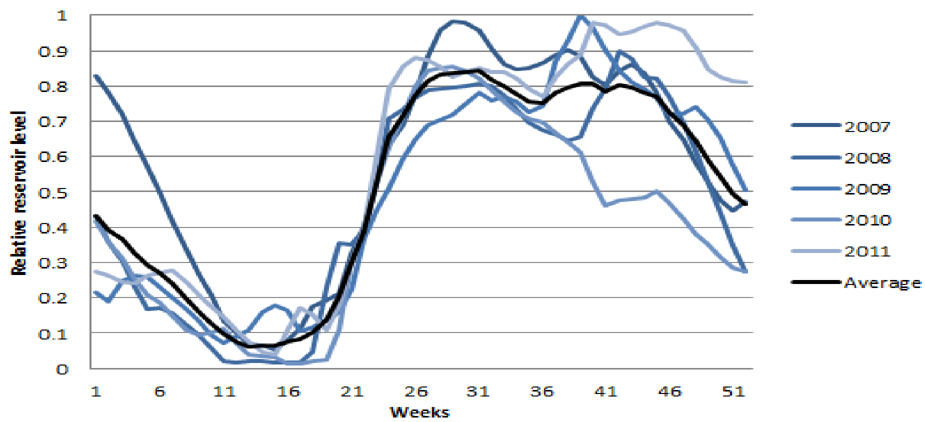

Figure 3.2.7: Historical and average reservoir levels for Plant 2.

3.2.4 Hydropower Plant 3

Hydropower Plant 3 consists of two reservoirs and four power stations, see Figure 3.2.8. The reservoirs associated with Stations 3 and 4 have limited amount of storage capacity and can be defined as run of rivers.

The historical inflow series of Plant 3 consist of daily observations in the period January 2007 to September 2012, and the measurements are made at 12 a.m. each day. The inflow series shows high variations during the year, with extremely low inflow in the winter season, see Figure 3.2.9. This is due to the location in Northern Norway, where the temperatures in the winter are normally low. The historical reservoir levels for Reservoir 1 are shown in Figure 3.2.10. The reservoir

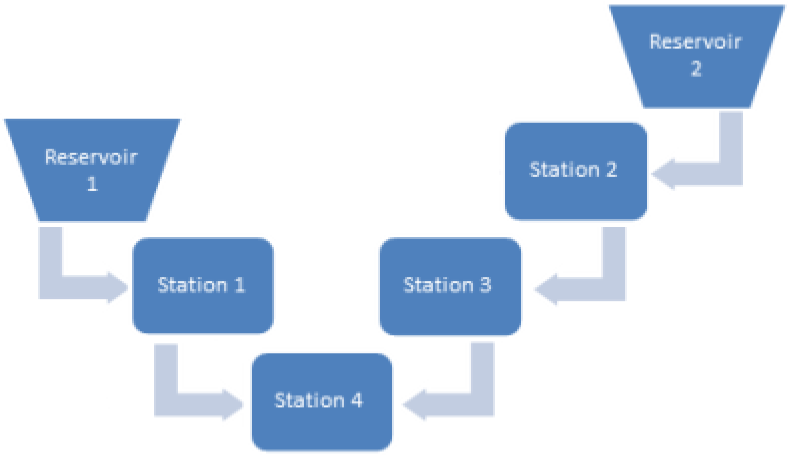

Figure 3.2.8: Topology of Plant 3.

patterns are similar for the two reservoirs, and a figure is therefore only provided for the largest reservoir of this plant.

The high degree of regulation and the low load factor of Power Station 1 indicates a high flexibility of this power station compared to the three others, see Table 3.2.1. The size of the reservoir and the capacity associated with this power station is large compared to the other stations, and due to the high degree of regulation of this station, a scheduling horizon of two years is used for Plant 3.

Table 3.2.1: Parameters for Hydropower Plant 3.

Power station	1	2	3	4
Degree of regulation	1.9	0.7	0.02	0.0
Utilization factor [%]	51.9	45.6	0.03	0.04
Load factor [%]	31.3	61.9	1.4	14.1

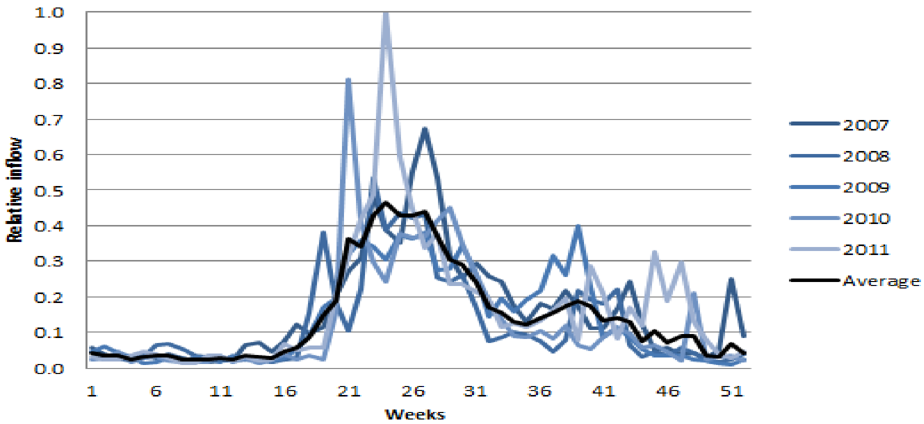

Figure 3.2.9: Historical and average inflow levels for Plant 3, Station 1.

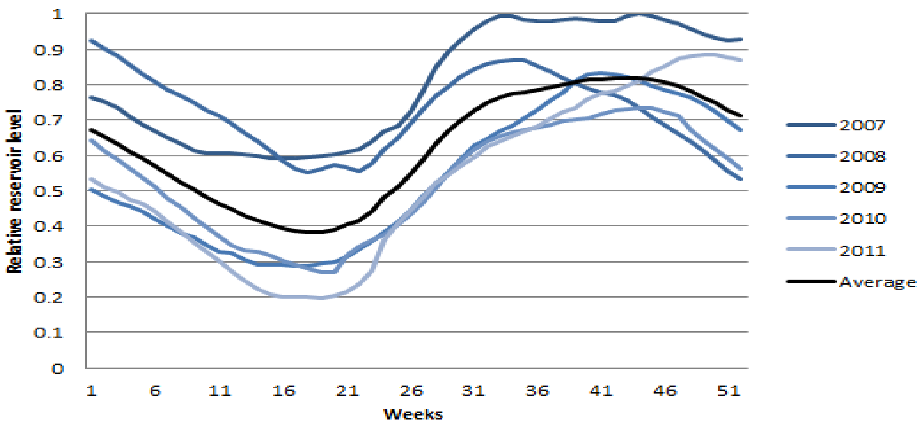

Figure 3.2.10: Historical and average reservoir levels for Plant 3, Reservoir 1.

3.2.5 Hydropower Plant 4

Hydropower Plant 4 consists of two reservoirs and four power stations, see Figure 3.2.11. The reservoirs associated with Stations 3 and 4 have limited amount of storage capacity and can be defined as run of rivers.

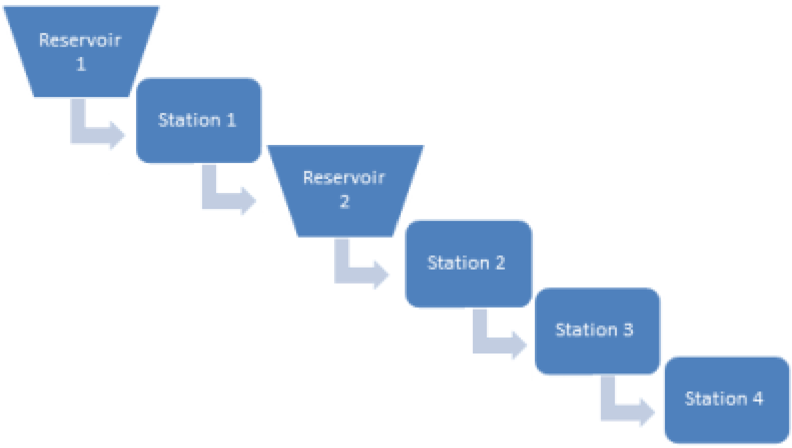

Figure 3.2.11: Topology of Plant 4.

The historical inflow series consists of weekly observations in the period January 1998 to December 2009, developed by NVE for reference reservoirs[3]. The reference reservoirs are located close to the reservoirs of Plant 4, and the geographic and climatic conditions are assumed to be representative. The inflow data for the reference reservoirs are adjusted to coincide with the mean annual inflow of the reservoirs of Plant 4 in the period of January 1998 to December 2009. This adjustment is done by multiplying the observations by the ratio between the mean annual inflow of the reservoir of interest and the mean annual inflow of the corresponding reference reservoir. The inflow series show a predictable seasonal

[3]An overview on how the time series is developed can be found in Holmqvist and Engen (2008) and Holmqvist (2012).

pattern, with large amounts of inflow during most of the year, see in Figure 3.2.12. This is due to the location south west in Norway. The historical reservoir levels for Reservoir 1 are presented in Figure 3.2.13.

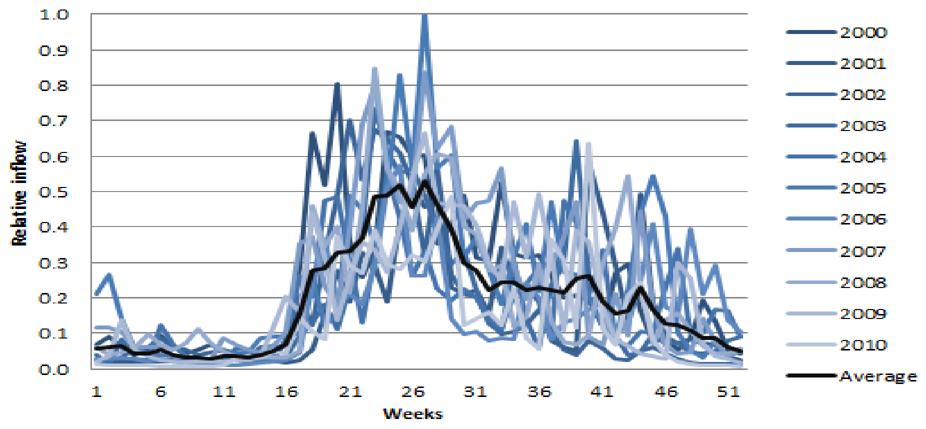

Figure 3.2.12: Historical and average inflow levels for Plant 4, Station 1.

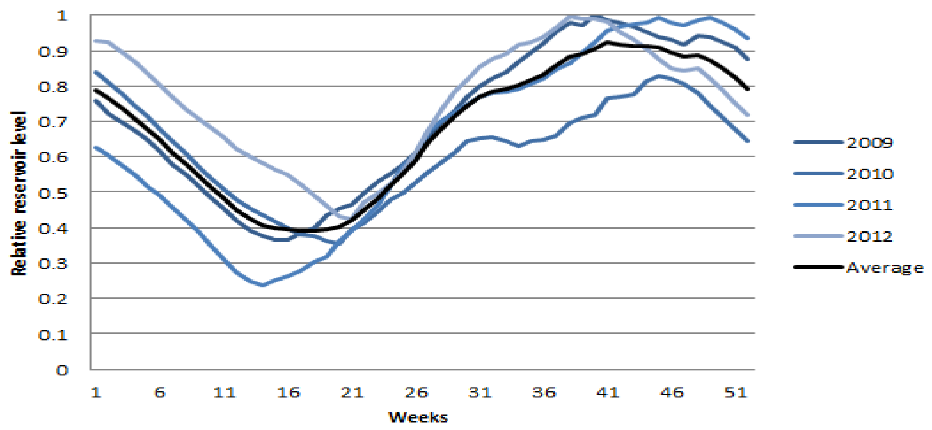

Figure 3.2.13: Historical and average reservoir levels for Plant 4, Reservoir 1.

The degree of regulation, utilization factor and load factor for the four power stations of Plant 4 can be found in Table 3.2.2. A scheduling horizon of one year is used for this plant.

Table 3.2.2: Parameters for Hydropower Plant 4.

Power station	1	2	3	4
Degree of regulation	1.1	0.5	0.04	0.0
Utilization factor [%]	47.4	16.3	0.3	0.1
Load factor [%]	41.4	35.5	7.0	11.6

3.3 The Nordic Power Market

Nord Pool Spot ASA is the Nordic power exchange market and consists of both a physical and a financial market. In the physical market, contracts are traded on day-ahead and intra-day basis. The bids to buy and sell electricity for each hour are aggregated into a demand curve and a supply curve, respectively. The system price is determined by the intersection of these two curves. Price areas are introduced due to grid congestions within Norway and between the Nordic countries. When the transmission capacity between price areas gets constrained, spot prices will generally rise above the system price in deficit areas and fall below the system price in surplus areas.

Financial power derivatives such as forward and futures, and options with forward and futures as underlying, are traded in the financial market. Forward and futures are used for trading and risk management, and as these derivate markets mature they will serve an important role in giving economic signals to operations scheduling (Kristiansen, 2004). The forward and futures prices at Nord Pool Spot reflect the value of electricity exchange at different times and are therefore necessary for the optimal use of hydropower during different periods of time (Nord Pool Spot, 2013).

3.3.1 Assumptions and Simplifications

The following assumptions and simplifications regarding the power market are made throughout this thesis:

- **Market power:** It is assumed that the production decisions taken by the four hydropower producers evaluated in this thesis do not affect the electricity price. Note that none of the hydropower plants in this thesis represent more than 0.83 % of the total domestic market share.

- **Area prices:** Local prices are not taken into account in this thesis. This simplification is done because longer time series are available for system prices than for area prices. Hence, the system price is used for each of the hydropower plants analyzed, and the same price model can be used for all of the plants. It is assumed that this will not have a significant impact on the results since the weekly average area prices tend to be similar to the weekly average system price, see Figure 3.3.1.

- **Completeness and no-arbitrage:** Risk adjusted prices are used because expected spot prices in future periods are generally different from forward prices for the same future periods due to the risk premium. By making decisions based on risk adjusted prices, the market value of production is maximized (Wallace and Fleten, 2003).

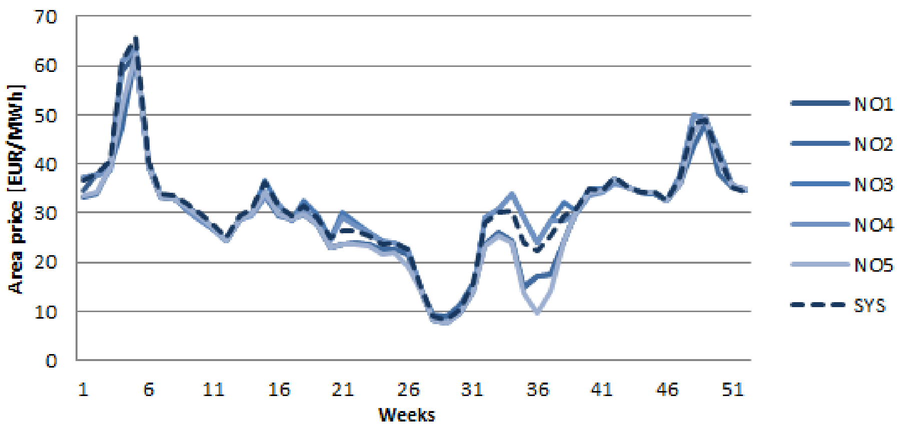

Figure 3.3.1: Weekly observed area prices and the system price in Norway during 2012 (Nord Pool Spot, 2013).

3.3.2 Electricity price properties

To analyze the behavior of spot prices, the Elspot data set is obtained from Nord Pool Spot's FTP server files (Nord Pool Spot, 2013). The data set consists of weekly system prices for an eleven year period beginning in the 1st week of 2002 and ending in the 52th week of 2012, containing a total of 572 observations. The times series of the spot prices are separated into two; cold seasons (week 1-17 and 41-52) and warm seasons (week 18-40).

Table 3.3.1: Descriptive Statistics for the Daily System Price time series (2002-2012).

Descriptive Statistics	Seasons All	Seasons Cold	Seasons Warm
Number of observations	571	319	253
Standard deviation [Euro/ MWh]	14.3	14.6	13.0
Min [Euro/ MWh]	8.4	16.2	8.4
Max [Euro/ MWh]	103.7	103.7	76.2
Skewness	1.1	1.3	0.8
Kurtosis	1.8	2.1	0.5

The statistics presented in Figure 3.3.2 reveals an erratic behavior of the system price. Prices are controlled by supply and demand and show seasonal and weekly variations. As can be seen in Table 3.3.2, the prices have maximum and minimum values of 103.7 $^{EUR}/_{MWh}$ and 8.4 $^{EUR}/_{MWh}$, respectively, and have a mean value of 37.2 $^{EUR}/_{MWh}$ during the sample period. The highest prices were reached during the two first weeks in 2003 and 2011 and last three weeks in 2002 and 2010. This is consistent with the fact that in the Nordic market prices are usually higher during the winter when the electricity demand is high.

Electricity prices are highly volatile, as measured by standard volatility measures.

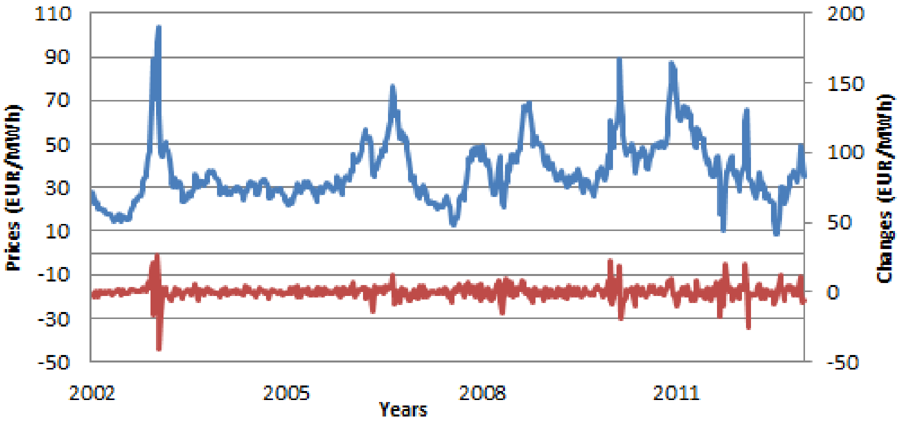

Figure 3.3.2: Daily system price time series in the period 2002-2012 (Nord Pool Spot, 2013). The daily system price series is plotted above and its daily changes below.

According to Fleten et al. (2001) the reason for this is that electricity has to be consumed once it is produced, and since demand is not particularly price elastic in the short term. The standard deviation of the spot prices is 14.6 for cold seasons and 13.0 for warm seasons. This indicates a higher stability of the mean price for warm seasons. The standard deviation for price changes is also higher for the cold seasons.

Extreme electricity prices are relatively frequent in Elspot. This is reflected in the sample kurtosis coefficients. For the whole period the kurtosis estimate is 1.8 and the excess kurtosis estimate is 3.8, which means that the distribution has heavier tails than a normal distribution with the same variance. This indicates that extremely low and high prices have a higher probability of occurrence. The positive sign of the skewness estimates reveals that high extreme values for the price are more likely than low extreme values. These characteristics indicate the existence of unsymmetrical fat tails in the Nordic electricity spot prices.

As discussed in Geman and Roncoroni (2006) the electricity prices show well-known qualitative features. An implication of these features is that, in contrast to other commodities, electricity prices are much more likely to be driven by demand and supply considerations, with demand in the short term market being inelastic. Some of these essential features are presented below:

- **Price spikes:** Electricity prices are highly volatile, and sudden price changes can occur. Many of the larger price jumps are followed by quick reversion, causing price spikes (Lucia and Schwartz, 2001). An explanation for these price spikes is large variations in demand and low elasticity of supply. The low elasticity follows from the limited storeability and transportability for electricity. In this thesis weekly prices are used, which will result in a loss of price spikes.

- **Mean reversion:** While, in the short run, the price of electricity might fluctuate up and down in response to different factors, it ought to be drawn back towards the marginal cost of producing electricity in the long run (Dixit and Pindyck, 1994). This level can be constant or periodic, where the latter can incorporate the seasonal trend (Geman and Rocoroni, 2006). In addition to general mean reversion towards a constant or seasonal dependent level, spot prices show a faster mean reversion after spikes.

- **Seasonality:** Spot prices have a seasonal variation throughout the year. According to Lucia and Schwartz (2001) this follows from the nature of electricity demand in the Nordic countries. The demand is highly dependent on the climate and is therefore also seasonal.

3.4 Correlation between data series

In this thesis covariance matrices for price and inflow are computed to be used as input to the LDR model. Inflow in week t is assumed to be correlated with inflow in period $t-1$ and with inflow in period $t+1$. This is consistent with the choice of an AR(1)-model for inflow, as described in Section 4.1.1. Correspondingly, the spot price in week t is assumed to be correlated with the spot price in week $t-1$ and the spot price in week $t+1$.

Since hydropower contributes to a great amount of the total power production in Norway, the spot price is strongly affected by the aggregated inflow. Limited inflow leads to lower reservoir levels and subsequently higher system prices. The spot price is therefore assumed to be negatively correlated with the inflow on a national level. Because scarce inflows often occurs nationally and locally at the same time, the spot price is also assumed to be negatively correlated with local inflow. According to Aas (2007) an aggregation of inflow over a longer period is suggested when modeling the relationship between inflow and price, due to the storage capacity of the reservoirs. In this thesis, it is therefore assumed that the spot price is correlated with inflow 20 weeks back in time.

The matrices are developed based on the residuals from the price and inflow models. Due to the short historical data set, the method is sensitive to outliers. To reduce the impact of outliers the residuals for each week t are adjusted, so that they represent the weighted average of the residuals in week $t-1$, t and $t+1$ for the same year. Weights of 0.25, 0.5 and 0.25 are put on the residuals from period $t-1$, t and $t+1$, respectively. To evaluate the accuracy of the matrices, the results should have been tested. However, testing is not done as correlation modeling is not the main focus of the thesis.

4 Stochastic models

Due to the stochastic behavior of price and inflow, stochastic models play a central role when evaluating future spot prices and inflow. This section presents the stochastic models used in order to estimate future expected spot prices and inflow.

4.1 Modeling inflow

Inflow variations cause uncertainty in power systems with a large share of hydropower. The inflow model needs to be versatile enough to capture seasonal variations and inflow dynamics. The model should also be as simple as possible to reduce computational complexity (Gjelsvik et. al, 2010). In order to meet these requirements a discrete time autoregressive and a continuous time one factor model are fitted to the available historical data set. These models are similar, but have different time steps and capture seasonality in different ways.

4.1.1 Autoregressive model

Even though inflow varies continuously, it is normally measured at particular points in time. Due to uncertainty in the inflow measurement, discrete time intervals of one day or one week are normally used. Since these intervals are quite long, a discrete time stochastic process as the autoregressive process of order p, AR(p), can be used to model the inflow, Ψ_t, in period t, where Ψ_t can be presented as:

$$\Psi_t = \delta + \sum_{i=1}^{p} \rho_i \, X_{t-i} + \zeta_t \qquad (4.1.1)$$

where δ and ρ_i are constants, with $-1 < \rho_i < 1$ and ζ_t is a normally distributed random variable with zero mean (Gjelsvik et. al, 2010). The first order autoregressive process, AR(1), is stationary and the long run expected value is identical for all values of t. The AR(1) model describes a mean reverting process, because Ψ_t tends to revert back to the long run expected value.

Since the historical inflow data sets contain weekly values, and weekly time steps are relatively long, it is accurate to only use the inflow in period $t-1$ when estimating inflow in period t. This corresponds to an AR(1) process. The order of the AR process is also tested using statistical hypothesis testing, and is found to be one. If daily time steps had been used it would probably been necessary to use a model with lags of higher order than one.

To incorporate the seasonal effects in the inflow patterns into the forecasting method, a seasonal factor is used to adjust the time series (Hiller and Lieberman, 2001). The seasonal factor measures how a single period compares to the overall average for an entire year. Using historical data, this formula is:

$$\text{Seasonal factor} = \frac{\text{Average for the period}}{\text{Overall average}} \tag{4.1.2}$$

According to Hillier and Lieberman (2001) it is easier to analyze the time series and detect new trends if the data sets first are adjusted to remove the effect of seasonal patterns. Thus, this formula is:

$$\text{Seasonally adjusted value} = \frac{\text{Actual value}}{\text{Seasonal factor}} \tag{4.1.3}$$

The seasonally adjusted values are used when estimating the parameters for the AR(1) model. This implies that Ψ_t is seasonally adjusted and need to be multiplied with the seasonal factor to take the seasonal pattern into account.

4.1.2 One factor model

A one factor model represents future expectation and uncertainty (Lucia and Schwartz, 2001). The behavior of inflow can be described in terms of two types of components. The first term is a totally predictable deterministic component that accounts for regularities in the evolution of inflow, such as a deterministic trend and any genuine periodic behavior (Seim and Thorsnes, 2007). The second component is stochastic and will be assumed to follow a particular continuous time diffusion process. The stochastic inflow parameter, Ψ_t, can be presented as:

$$\Psi_t = f(t) + A_t \tag{4.1.4}$$

The predictable components such as the level and the seasonality of the inflow is modeled by the deterministic function:

$$f(t) = \alpha + \gamma \cos((t+\tau)\frac{2\pi}{52}) \tag{4.1.5}$$

where the cosine function tries to capture annual seasonality. It is assumed that the stochastic part, A_t, follows a mean reverting Ornstein-Uhlenbeck process with zero long-run mean and a speed of adjustment for inflow of κ_Ψ:

$$dA_t = -\kappa_\Psi A_t dt + \sigma dZ \tag{4.1.6}$$

where dZ represents an increment to a standard Brownian motion Z_t. To show the mean reverting nature of the process Eq. 4.1.4 and 4.1.6 are rewritten as:

$$d(\Psi_t - f(t)) = \kappa_{\Psi_t}(f(t) - \Psi_t)dt + \sigma dZ \tag{4.1.7}$$

which shows that when Ψ_t deviates from the deterministic term, $f(t)$, it is pulled back to it at a rate that is proportional to the deviation. The distribution of Ψ_t conditional on A_0, where $A_0 = P_0 - f(0)$, is normal with mean and variance:

$$E_0(\Psi_t) = E(\Psi_t|A_0) = f(t) + (P_0 - f(0))e^{-\kappa_\Psi t} \tag{4.1.8}$$

$$Var_0(\Psi_t) = Var(\Psi_t|A_0) = \frac{\sigma^2}{2\kappa_\Psi}(1 - e^{-2\kappa_\Psi t}) \tag{4.1.9}$$

4.2 Modeling spot price

Electricity can be considered as a flow commodity because of the limited opportunity to store electricity and the limited transportability (Lucia and Schwartz, 2001). In electricity markets, arbitrage across time and space is limited. This limitation is crucial in explaining the behavior of electricity spot prices and derivate prices as compared to other commodities, because electricity prices are strongly dependent on the demand and their determinants like buisniess activity and temporal weather conditions in every moment.

4.2.1 Two factor model

Schwartz and Smith (2000) and Lucia and Schwartz (2001) discuss factor models for spot price dynamics and valuations of spot price derivatives. One of the limitations of the one factor models is that all future returns are perfectly correlated (Cortazar and Schwartz, 2003). This means that these prices always move in the same direction, a fact that is clearly contradicted by the data. Models with more factors avoid these limitations and have been shown to perform better than models with fewer factors. To account for a more realistic stochastic behavior, a two factor model for modeling the spot price is assumed to be adequate in this thesis.

The stochastic process followed by the spot price is represented by Π_t:

$$\Pi_t = f(t) + Y_t \tag{4.2.1}$$

The deterministic function $f(t)$ is the same as in Eq. 4.1.5. The stochastic part, Y_t, is decomposed into two factors:

$$Y_t = \chi_t + \xi_t \tag{4.2.2}$$

where χ_t captures short-term deviations and ξ_t represents the long term equilibrium level. Changes in the short run deviations are temporary changes in prices, while the changes in the equilibrium level represents fundamental market changes that are expected to persist (Schwartz and Smith, 2000). The mean reverting Ornstein-Uhlenbeck process with zero long run mean is used to model the short run deviations:

$$d\chi_t = -\kappa_P \chi_t dt + \sigma_\chi dz_\chi \tag{4.2.3}$$

where κ_P is the speed of reversion for price. The long term equilibrium level is assumed to follow a Brownian motion process:

$$d\xi_t = \mu_\xi dt + \sigma_\xi dz_\xi \tag{4.2.4}$$

where the two Wiener processes dz_χ and dz_ξ are correlated through:

$$dz_\chi dz_\xi = \rho_{\chi\xi} dt \tag{4.2.5}$$

Applying theory of risk neutral valuation, future prices are equal to the expected future spot price under the risk-adjusted process (Wallace and Fleten, 2003). The risk adjusted process for the stochastic part, Y_t, is obtained from standard arbitrage arguments with two derivative assets taking into account the non tradeable nature of Y_t. The risk adjusted processes for the state variables are:

$$d\chi_t = \kappa_\Pi(\alpha^* - \chi_t)dt + \sigma_\chi dz_\chi \tag{4.2.6}$$

$$d\xi_t = \mu_\xi^* dt + \sigma_\xi dz_\xi \tag{4.2.7}$$

where:

$$\alpha^* = -\frac{\lambda_\chi \sigma_\chi}{\kappa_\Pi} \tag{4.2.8}$$

$$\mu_\xi^* = \mu_\xi - \lambda_\xi \sigma_\xi \tag{4.2.9}$$

$$dz_\chi^* dz_\xi^* = \rho_{\chi\xi} dt \tag{4.2.10}$$

λ_χ and λ_ξ are the market prices of risk. It can be proven that a forecast of the future prices can be represented as:

$$F_0(\Pi_0, T) = E_0^*(\Pi_T) = f(T) + e^{-\kappa_P T}\chi_0 + \xi_0 + (1 - e^{-\kappa_\Pi T})\alpha^* + \mu_\xi^* T \tag{4.2.11}$$

and the variance as:

$$Var^*(\Pi_T) = (1 - e^{-2\kappa_\Pi T})\frac{\sigma_\chi^2}{2\kappa_\Pi} + \sigma_\xi^2 T + 2(1 - e^{-\kappa_\Pi T})\frac{\rho_{\chi\xi}\sigma_\chi\sigma_\xi}{\kappa_\Pi} \tag{4.2.12}$$

5 Parameter estimation

The stochastic models presented in Section 4 need accurate parameters in order to give useful forecasting values for inflow and price. The necessary parameters for the inflow models are estimated by fitting the inflow models to the historical inflow data provided by the hydropower producers presented in Section 3.2. The price models use historical spot prices and futures and forward data from the Nordic power market to estimate parameters. Sections 5.1 and 5.2 briefly describe the procedures used to estimate parameters, while Sections 5.3 and 5.4 present the results from the inflow and price parameter estimations, respectively.

Price and inflow models are developed for the purpose of providing input to the LDR model. However this is not the main focus of this thesis. The data available for the estimations are limited compared to the data most producers have available. Moreover most hydropower producers have access to good inflow and price models, such as the EMPS model (Wolfgang et al., 2009).

5.1 The numerical nonlinear least squares method

The numerical nonlinear least squares method is presented in Cortazar and Schwartz (2003) and Lucia and Schwartz (2002). This method is based on the idea of finding the parameters that minimize the sum of the squared errors between the observed value, Z_n, and the calculated value, $\hat{Z}_n$, in the data set:

$$\text{Sum of squared errors} = \sum_{i=1}^{N} (\hat{Z}_n - Z_n)^2 \qquad (5.1.1)$$

To calibrate the price model, spot prices and futures and forwards for N number of dates, t_i, where $i = 1, ..., N$ are used. For each date, t_i, there are M_i contracts with different maturities. For a given initial set of parameters the state variables[4] that minimize the sum of the squared errors between the values forecasted by the model and the the spot prices and futures and forward prices that particular day, are estimated. The estimated state variables and the observed futures and forwards are used to estimate the volatilities and correlation parameters. Given the implied state variables and parameters, the remaining parameters are estimated by minimizing the sum of the squared errors for the whole spot and derivative contracts sample. This procedure is repeated with the new set of parameters until convergence.

5.2 The Kalman filter

The state variables in the two factor model presented in Section 4.2.1 are not directly observable and can be estimated using information contained in futures

[4]A state variable is a variable in the set of variables that are used to describe the mathematical "state" of a dynamical system.

and forward prices (Schwartz and Smith, 2000). The Kalman filter is a recursive algorithm that produces estimates of these state variables, using related, observable time series of the variables, and a set of mathematical equations estimates the state variables in a way that minimizes the total sum of squared error (Welch and Bishop, 2001). Detailed descriptions of the Kalman filter are given in Harvey (1989) and West and Harrison (1996). Schwartz (1997) and Schwartz and Smith (2000) do also make use of this method.

5.3 Inflow model estimations

The autoregressive model (Inflow model 1) and the one factor model (Inflow model 2 and 3), presented in Section 4.1.2, are used for inflow modeling. In Inflow model 1, time periods of one month are used when estimating the seasonal factors. For long time series, shorter periods could have been used for estimating the seasonal factors in order to obtain a more accurate estimate. However, for plants with short time series, spikes may have affected the estimates to much if shorter time periods were used. The seasonally adjusted data are used to estimate the constants δ and ρ_i for the AR(1) model using ordinary least squares regression in Excel.

As described in Section 2.1, the year can be divided into three sub periods of different inflow pattern. This is done for Inflow model 2, and parameters are estimated using the nonlinear least squared method and the standard Solver of Excel. The parameters for Inflow model 3 are estimated using the same method as for Inflow model 2, but here only one period is used to represent the whole year. This is done to test if dividing the year leads to a better description of the realized inflow, compared to using just one period.

Data from the years 1998 to 2011 for Plant 1, 1998 to 2008 for Plant 2 and 1998 to 2009 for Plant 4 are used to estimate the parameters. The years 2009 to 2011 (Plant 1), 2006 to 2008 (Plant 2) and 2007 to 2009 (Plant 4) are used to run out of sample tests to measure the accuracy of the three inflow models. For Plant 3 the data series for inflow are too short (2007-2011) to run out of sample tests. Since Plant 2 and 3 have similar inflow patterns and are located in the same geographical area, the most accurate inflow model for Plant 2 is assumed to also be the most accurate inflow model for Plant 3. Plant 4 is a multi-reservoir system, and the testing is done for the largest reservoir. Since the inflow patterns are similar for all reservoirs, it is assumed that the most accurate inflow model is the same for all of them.

Table 5.3.1 summarises measures of accuracy for the hydropower plants[5]. The results presented in this table indicates that Inflow model 2 gives the least de-

[5]These error measures are commonly used when comparing different models to realised data. Cuthbertson and Nitzsche (2001) describes the different error measures used here and the reader is referred there for future details.

viation between realized inflow and forecasted inflow for the tested years for all hydropower plants. Figures 5.3.1 to 5.3.3 show graphically out of sample plots for Inflow model 2, including relative realised inflow for the tested years compared to the relative simulated inflow based on the estimated parameters[6]. Corresponding figures for Inflow model 1 and 3 are presented in Appendix A.1. Comparing the figures for Inflow model 2 with the figures for Inflow model 1 and 3 verifies that Inflow model 2 gives the least deviation. For Plant 2 the error measurements are quite large. An explanation for this is that the inflow levels are lower than average in two of the tested years (2006 and 2007). The figures for Plant 2 also vertify that the difference between the realised and the forecasted inflow is larger than for the two other plants.

Table 5.3.1: Error measures for out of sample tests for the inflow models.

	Mean error	Mean absolute error	Mean square error	Mean percentage error	Mean absolute percentage error	Root mean square error
Plant 1						
Model 1	0.3	2.8	12.5	98.0 %	127.7 %	3.5
Model 2	0.2	2.7	12.4	84.0 %	113.4 %	3.5
Model 3	0.3	3.0	14.4	112.0 %	141.9 %	3.8
Plant 2						
Model 1	3.3	7.5	87.1	217.1 %	233.4 %	9.3
Model 2	2.1	7.1	91.0	158.9 %	181.7 %	9.5
Model 3	6.3	10.2	182.8	347.7 %	363.6 %	13.5
Plant 4						
Model 1	0.3	2.8	12.5	98.0 %	127.7 %	3.5
Model 2	-0.4	1.6	4.5	52.4 %	92.5 %	2.1
Model 3	0.2	1.8	5.2	91.3 %	123.8 %	2.3

Figures 5.3.4 to 5.3.6 show weekly expected inflow values from the three inflow models compared to the average inflow for all plants. As described in Section 2.1, there are large inflow variations throughout a year. Intuitively, inflow models dividing the year into several periods will thus be able to capture this inflow pattern better than models using just one period. For this reason the results from Inflow model 1 and Inflow model 2 are assumed to adapt better to the seasonal variations of inflow than the results from Inflow model 3. This can also be verified from Figures 5.3.4 to 5.3.6, which show that Inflow model 3 is less fitted to the historical average inflow data than the two other models. Based on these findings and the results from the out of sample testing, Inflow model 2 is used in the further analysis, i.e. to provide input for the long term scheduling models.

[6]Relative values are calculated by dividing the inflow levels on the maximum inflow level to anonymize the identity of the hydropower producers.

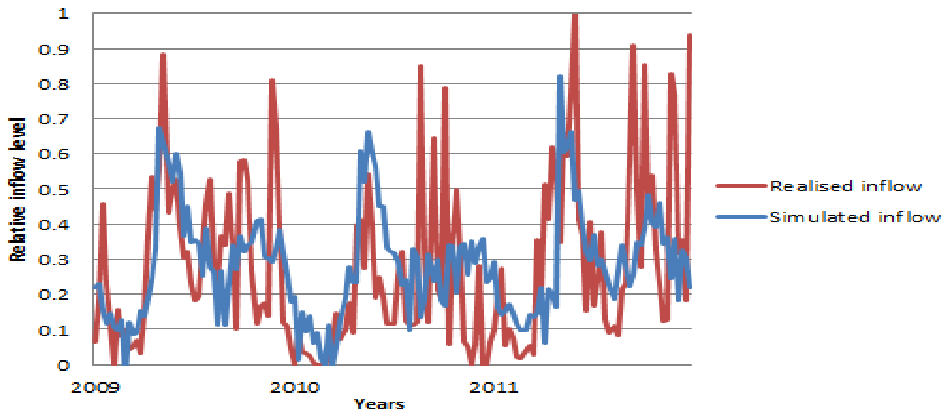

Figure 5.3.1: Inflow model 2 for Plant 1 (2009-2011).

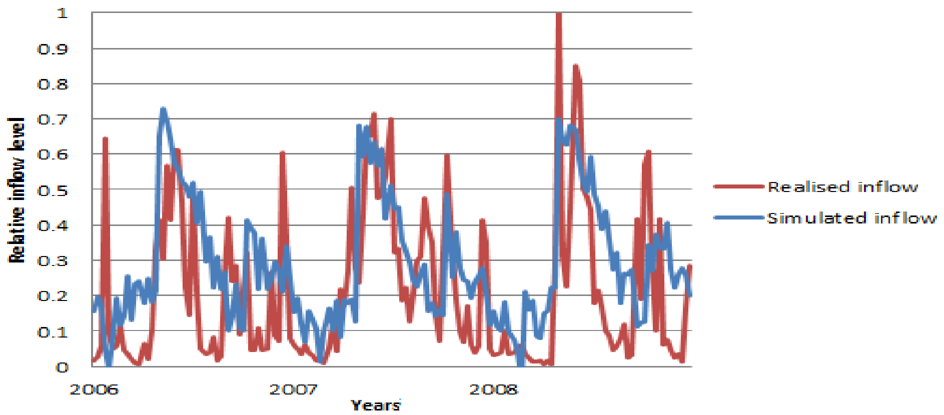

Figure 5.3.2: Inflow model 2 for Plant 2 (2006-2008).

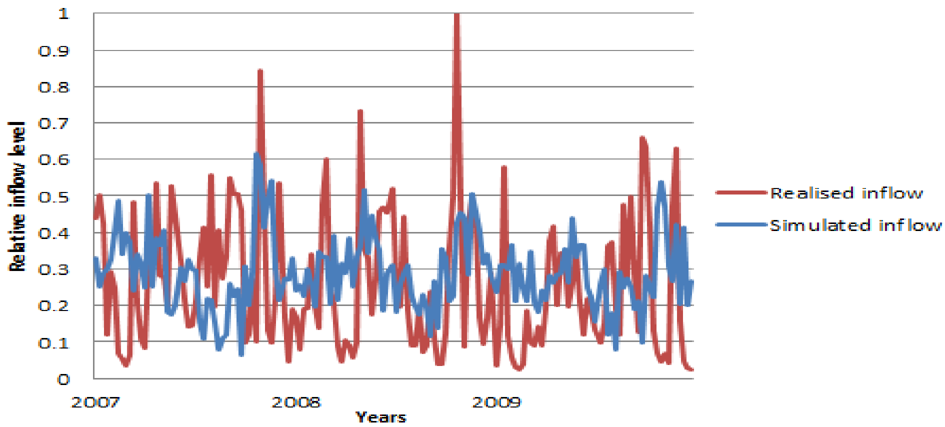

Figure 5.3.3: Inflow model 2 for Plant 4 (2007-2009).

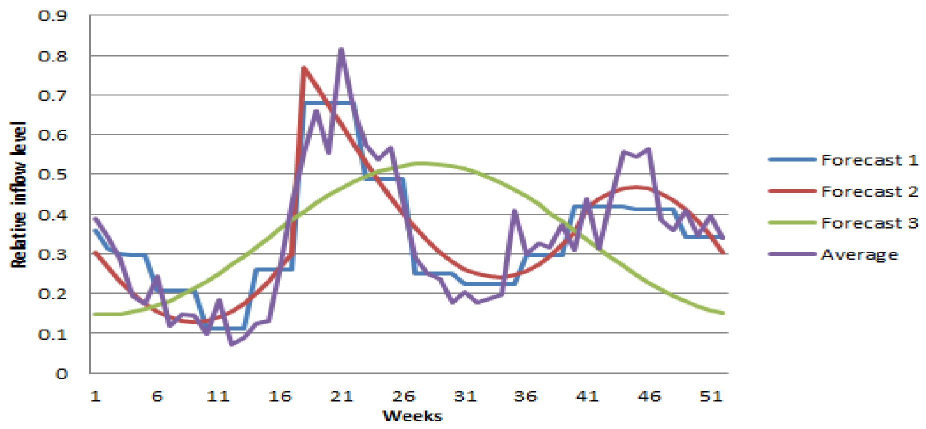

Figure 5.3.4: Forecasted and average inflow for Plant 1.

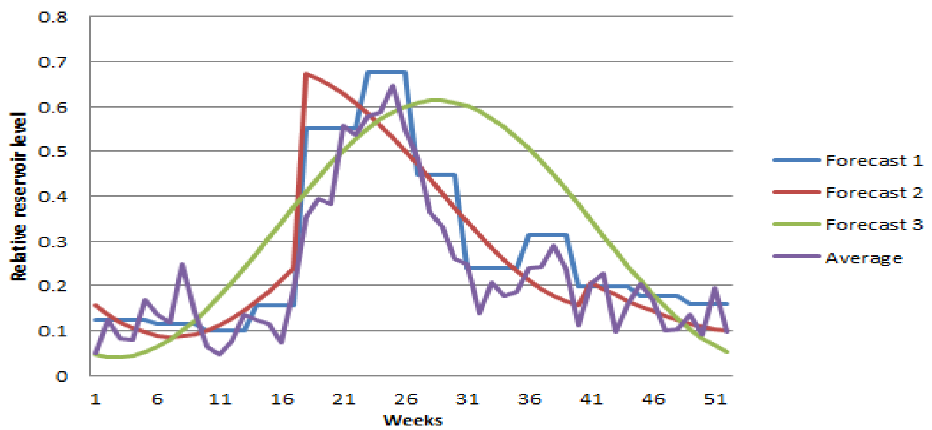

Figure 5.3.5: Forecasted and average inflow for Plant 2.

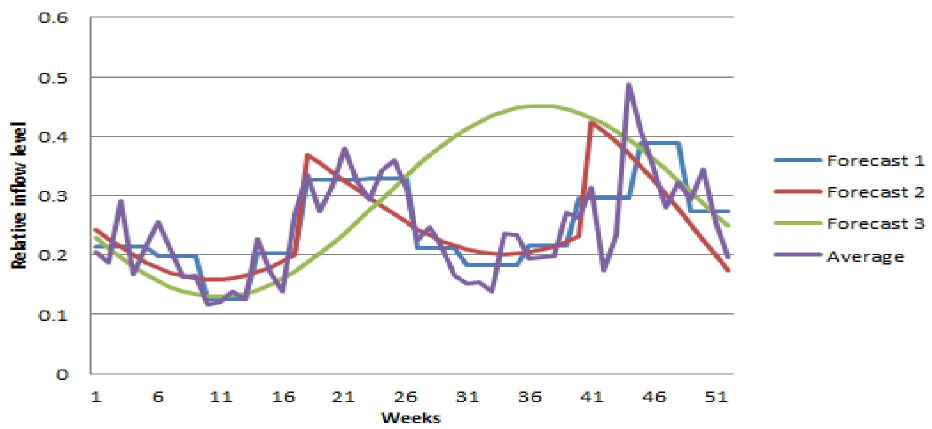

Figure 5.3.6: Forecasted and average inflow for Plant 4.

5.4 Price model estimations

The two-factor model presented in Section 4.2.1 is used for modeling the spot price. The parameters are estimated using the numerical nonlinear least squares method (Price model 1 and 2) and the Kalman filter (Price model 3).

The parameters used in Price model 1 are estimated by Lucia and Schwartz (2001), and the reader is referred there for future details. Some adjustments are made on the original parameters, and the adjusted parameters can be found in Appendix A.2. μ_ξ^* is set to zero, because the intention is to look at an average situation for price with an incentive neutral price curve. A negative μ_ξ^* will motivate to discharge water for production today instead of waiting. $\rho_{\chi\xi}$ is also set to zero according to Pilipovic (2007). In order to get a reasonable price level on the price curve, α^*, χ_0 and ξ_0 are all set to zero, while α is set equal to the average spot price for the last ten years (2003-2012), which is 309 $^{NOK}/_{MWh}$.

For Price model 2, parameters are estimated using data about spot prices and futures and forward from 2004 to 2012. The spreadsheet that is used is developed by Seim and Thorsnes (2007), and the futures and forward data are from NASDAQ (2012)[7]. The Kalman filter used to estimate the parameters for Price model 3 is developed by Bjørnsgard and Hauge (2007)[8]. Spot prices and yearly contracts from 2007-2012 are used for estimating the parameters. The short data set is due to limited futures and forward data. Ideally a longer data set should have been used. The use of contracts with different maturities, would also improved the data set. The estimated parameters can be found in Appendix A.2.

In order to measure the accuracy of the three models, the years 2010 to 2012 are used to run out of sample tests. Price model 1 is based on data from the years 1993 to 1999. However, the model is adjusted to the average price level of the years 2003 to 2012. It is therefore assumed as acceptable to test this model for the years 2010 to 2012, even though these years are not part of the data set used for parameter estimation. Price model 1 specify prices in $^{NOK}/_{MWh}$, while the two other models specify prices in $^{EUR}/_{MWh}$ since the futures and forward data available are given in $^{EUR}/_{MWh}$. In order to make the results comparable, the forecasted prices from Price model 1 are converted into $^{EUR}/_{MWh}$ by using daily exchange rates from DNB (2013)[9].

Table 5.4.1 summarizes measures of accuracy for the three price models. The results from this table verify that Price model 1 gives the least deviation between realized prices and forecasted prices in the years 2010 to 2012.

[7]The futures and forwards data have been collected by Benterud et al. (2012).

[8]Development of a spreadsheet and a Kalman filter is out the scope of this thesis.

[9]Forward exchange rates could alternatively have been used since futures and forward prices are used for estimation. However, this will only have a marginal impact on the calculated prices.

Table 5.4.1: Error measures for out of sample tests for the price models.

Price model	Mean error	Mean absolute error	Mean square error	Mean percentage error	Mean absolute percentage error	Root mean square error
1	-1.9	11.2	211.3	13.7%	36.4%	14.5
2	-0.1	11.3	179.7	17.7%	37.8%	13.4
3	0.2	11.8	210.4	21.1%	40.6%	14.5

The expected prices from the price models and the average weekly system prices in the period from 2004 to 2012 are shown in Figure 5.4.1. The results from the price models capture the seasonal variations in the spot prices, and give a fairly good estimate of the average weekly prices. The largest deviation is about 5.7 $^{EUR}/_{MWh}$ for Price model 1, 7.8 $^{EUR}/_{MWh}$ for Price model 2 and 6.4 $^{EUR}/_{MWh}$ for Price model 3. The results from Price model 1 is used in the further analysis since this model has the lowest errors.

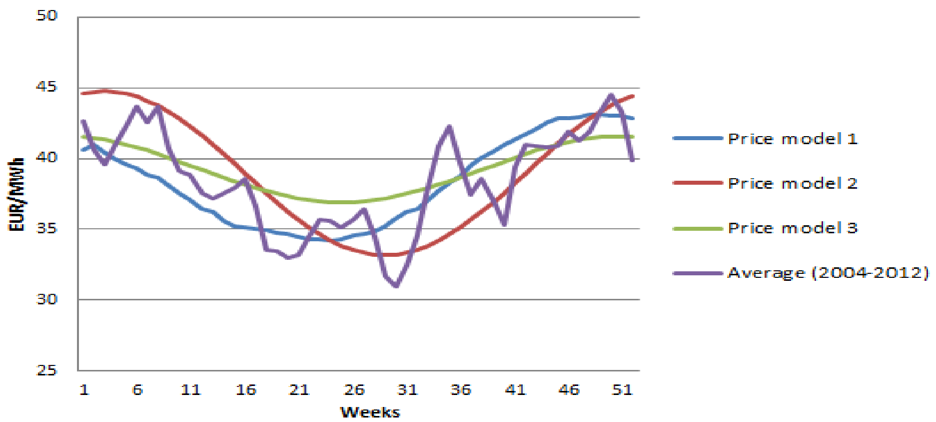

Figure 5.4.1: The result from the three price models compared to the average spot price (2004-2012).

6 Linear Decision Rules model

This section starts with a presentation of the methodology on which the LDR model is based. Model assumptions are explained, followed by a presentation of the deterministic, the stochastic and the LDR model. The problem sizes for the deterministic and the LDR models are then presented in the following section. The LDR model is intended to be coupled to a shorter term model through a fixed water value at the coupling stage. Section 6.4 describes how these water values can be found, while Section 6.5 presents an approximate method for taking a variable head of water into account.

6.1 Methodology

Optimization belongs to the field of applied mathematics and encompasses the use of mathematical models and methods to find the best alternative in decision making situations (Lundgren et al., 2010). An optimization model finds the value(s) of one or more decision variables that maximizes or minimizes a specified objective function, while at the same time satisfying one or more constraints. Depending on how the functions and variables used to describe the underlying problem are specified, optimization models are divided into different classes. This thesis considers Linear Programming (LP), which is a class of problems where all functions are linearly dependent on the decision variables and all variables are continuous.

For deterministic problems, all parameters are fully known when the decision variables are determined. However, most real-life problems include some uncertain parameters. When some of the parameters in a linear program are most appropriately described using random variables, a Stochastic Linear Program (SLP) results (Higle, 2005). Before a stochastic model can be developed, the timing of the decisions, relative to the resolution of uncertainty, must be specified. Decisions taken after information about the uncertain parameters is available offer an opportunity to adapt to the received information. These decisions are referred to as recourse decisions or adjustable variables. On the contrary, non adjustable variables correspond to variables that must be completely specified before the true values of the uncertain data become known. Consequently, the vector $\mathbf{x}$ of variables can be partitioned as $\mathbf{x} = (u^t, v^t)^T$, where the sub-vector u represents the non adjustable and v represents the adjustable variables.

In a Multistage Stochastic Linear Program (MSLP) an initial decision is followed by a sequence of uncertain parameters being revealed, and associated recourse decisions being made. In these models nonanticipativity constraints are included in order to ensure that the decisions taken at a specific stage[10] only rely on information that is available at this stage. According to Shapiro and Nemirovski (2005), MSLP's are computationally intractable even when medium

[10] A stage is a point in time where new information is available.

accuracy solutions are sought.

A tractable approximation of a MSLP can be found by restricting the recourse decisions, v, to be affine functions, i.e. linear plus a constant, of the uncertain parameters, Π (Ben-Tal et al., 2003). The history of observations up to time t is denoted $\Pi^t := (\Pi_1, ..., \Pi_t)$. Considering a sequential decision process in which the decision $v_t(\Pi^t)$ is selected at time t after the outcome of history Π^t has been observed, but before the future outcomes $\{\Pi^s\}_{s>t}$ have been revealed, the objective is to find a sequence of decision rules, v_t, $\forall t \in T$, that maps available decisions to observations and minimize or maximize the objective function subject to certain linear constraints. This gives the following decision rules:

$$v_t = v_t^0 + \sum_{r \in I_t} v_r^r \cdot \Pi_r, \qquad \forall t \in T \tag{6.1.1}$$

where v_t^0 and v_r^r are new non adjustable variables and I_t is a subset of $\{1, ..., t\}$. Requiring that v^t depends solely on Π^t reflects the nonanticipative nature of the problem (Kuhn et al., 2011). The uncertain parameters are defined within an interval around their nominal values in each time period t, Π_t^*. The size of the interval is given by the uncertainty level, θ. This interval is represented by the uncertainty set, Ξ, where:

$$\Xi := [\Pi_t^* \cdot (1 - \theta), \Pi_t^* \cdot (1 + \theta)], \qquad \forall t \in T \tag{6.1.2}$$

In the context of robust optimization the solutions must remain feasible for all realizations of the uncertain data within a given uncertainty set. Under this constraint, the objective function optimizes the guaranteed (worst case) value of the (uncertain) objective function. Replacing the objective function by a function minimizing or maximizing the expected value instead of the worst case value transforms the program into a stochastic program (Kuhn et al., 2011). In the case of fixed recourse, provided that the uncertainty set itself is computationally tractable, this program is computationally tractable. In the case of a polyhedral uncertainty set[11], the fixed recourse program is equivalent to an explicit LP program.

6.2 Hydropower scheduling models

An aggregated reservoir model and a multi-reservoir model are developed in this thesis. The aggregated reservoir model considers a hydropower plant with one aggregated power station and one aggregated reservoir. This means that the production capacity of all power stations and the potential energy level of all reservoirs are merged into one power station and one reservoir whose operation will be optimized. When using aggregated reservoir models, detailed reservoir drawdown methods are normally used to distribute production between power

[11] A set $P \subseteq R^n$ is a polyhedron if there is a system of finitely many inequalities $Ax \leq b$ such that $P = \{x \in R^n | Ax \leq b\}$ (Kuhn et al., 2011).

stations and allocate water between reservoirs[12]. However, this is considered out of the scope of this thesis.

In the multi-reservoir model the interaction between the reservoirs and power stations is taken into account. This model does also take into account that the water discharged from an upstream reservoir will enter a downstream reservoir, i.e. that the same water can be used for power generation at several power station. Moreover, the model includes the opportunity to discharge water from an upstream reservoir to a reservoir downstream without using the water for power generation. This may be beneficial in high price periods if the upstream power station has less production capacity than the downstream power station. For plants with one reservoir and one power station the two models will provide the same solution. For this reason, only the multi-reservoir models will be presented in this section. The aggregated reservoir model can be found in Appendix B.1.

6.2.1 Model assumptions

The model is run forward in time, assuming that present time, $t = 0$, is the period in which the reservoirs historically have been at their lowest water level. This corresponds to week 17, 16, 18 and 15 for Plant 1, 2, 3 and 4, respectively. For Plant 1, 2 and 4 a scheduling horizon of one year is used, while a two year horizon is used for Plant 3 due to its high degree of regulation. The objective function is discounted at a yearly risk free rate of 3 %, corresponding to a weekly risk free rate of 0.057 %[13]. This is appropriate due to the risk adjusted prices used in the stochastic models presented in Section 4.

Water stored in the reservoir at the end of the scheduling horizon is disregarded in this thesis, i.e. this water is assumed to have zero value. It is assumed that this simplification will not have any significant influence on the results since the end of the scheduling horizon is the point in time in which the reservoirs historically have reached their lowest levels. Another assumption is that 100 % of the water discharged from the upstream reservoir can be reused in the downstream reservoir.

6.2.2 Deterministic Model

The deterministic hydropower scheduling model assumes that future inflow and prices are fully known during the whole scheduling period. Using a deterministic hydropower scheduling model leads to scheduling strategies that essentially allocate water to the periods with the highest prices. (Wallace and Fleten, 2003). The risk of spillage will be underestimated, and the profit will be overestimated. Because all parameters are assumed to be fully known, there will be no extra discharge during the fall in case of more inflow than expected at near maximum

[12]The reader is referred to Doorman (2012) for a more thorough description of the reservoir draw down methods.

[13]The weekly risk free rate is calculated by: $\sqrt[52]{0.03} = 0.00057 = 0.057\%$ where 3 % is the yearly risk free rate.

reservoir levels. Moreover, there will be no holding back extra water during the winter in case the snow melting starts late and prices will be higher than expected. For this reason the deterministic model is assumed to give an optimistic upper bound on the optimal objective value, i.e. the expected market value of production. The deterministic model is defined as:

Index
t: Index for time periods.
i: Index for hydropower reservoirs.

Set
T: Set of time periods, $t = \{1, 2, ..., T\}$.
I: Set of hydropower reservoirs, $i = \{1, 2, ..., I\}$.

Parameters
R: Weekly interest rate.
Π_t: Electricity price in time period t $[^{NOK}/_{MWh}]$.
$\Psi_{t,i}$: Inflow to reservoir i in time period t $[MWh]$.
$M_{max,i}$: Maximum reservoir level for reservoir i $[MWh]$.
$M_{min,i}$: Minimum reservoir level for reservoir i $[MWh]$.
$M_{0,i}$: Initial reservoir level for reservoir i at time period t=0 $[MWh]$.
$Q_{max,i}$: Maximum amount of production from reservoir i $[MWh]$.
$Q_{min,i}$: Minimum amount of production from reservoir i $[MWh]$.

$$\sigma_{i,j}: \begin{cases} 1 \text{ if water from reservoir } i \text{ can be discharged into reservoir } j. \\ 0 \text{ otherwise.} \end{cases}.$$

Variables
V_0: Discounted market value of total production $[NOK]$.
$m_{t,i}$: Reservoir level in reservoir i in time period t $[MWh]$.
$q_{t,i}$: Production from reservoir i in time period t $[MWh]$.
$h_{t,i,j}$: Water discharged without production from reservoir i to reservoir j in time period t $[MWh]$.
$s_{t,i}$: Spillage from reservoir i in time period t $[MWh]$.

Mathematical formulation

$$V_0 = max \sum_{t=1}^{T} \sum_{i=1}^{I} \left[\frac{1}{(1+R)^t} (\Pi_t \cdot q_{t,i}) \right] \tag{6.2.1}$$

s.t.

$$q_{t,i} \geq Q_{min,i}, \quad \forall i \in I, \ \forall t \in T \tag{6.2.2}$$

$$q_{t,i} \leq Q_{max,i}, \quad \forall i \in I, \ \forall t \in T \tag{6.2.3}$$

$$m_{t,i} = M_{0,i}, \quad \forall i \in I, \ t = 0 \tag{6.2.4}$$

$$m_{t,i} \geq M_{min,i}, \quad \forall i \in I, \ \forall t \in T \tag{6.2.5}$$

$$m_{t,i} \leq M_{max,i}, \quad \forall i \in I, \ \forall t \in T \tag{6.2.6}$$

$$\begin{aligned} m_{t,i} = m_{t-1,i} + \Psi_{t,i} + \sum_{j=1}^{I} \sigma_{j,i} \cdot q_{t,j} + \sum_{j=1}^{I} \sigma_{j,i} \cdot h_{t,j,i} \\ -q_{t,i} - \sum_{j=1}^{I} \sigma_{i,j} \cdot h_{t,i,j} - s_{t,i}, \qquad \forall i \in I, \ \forall t \in T \end{aligned} \tag{6.2.7}$$

$$q_{t,i}, s_{t,i}, m_{t,i} \geq 0, \quad \forall i \in I, \ \forall t \in T \tag{6.2.8}$$

The objective function, Eq. (6.2.1), represents the discounted market value of total production from all reservoirs over the whole scheduling horizon. Lower and upper limits on production are stated by Eq. (6.2.2) and (6.2.3), while the initial reservoir levels are given by Eq. (6.2.4). The reservoir levels at the end of each period t have to be larger than a given minimum level and less than a given maximum level in each time period, stated by Eq. (6.2.5) and (6.2.6). Eq. (6.2.7) represents the reservoir balance, and states the relationship between the reservoir level at the end of time period $t-1$ and at the end of period t. Eq. (6.2.8) states that all decision variables have to be nonnegative.

6.2.3 Stochastic model

The stochastic hydropower scheduling model takes uncertainty in future prices and inflow into account. The variables for production, discharge and spillage are rewritten as:

$q_{t,i}^{(\Pi_t, \Psi_{t,i})}$: Production depends on price, Π_t, and inflow, $\Psi_{t,i}$.
$h_{t,i,j}^{(\Psi_{t,i})}$: Discharge from reservoir i to reservoir j depends on inflow, $\Psi_{t,i}$.
$s_{t,i}^{(\Psi_{t,i})}$: The loss of water due to spillage depends on inflow, $\Psi_{t,i}$.

This gives the following stochastic problem:

$$V_0 = max \ \mathbb{E} \left[\sum_{t=1}^{T} \sum_{i=1}^{I} \frac{1}{(1+R)^t} \left(\Pi_t \cdot q_{t,i}^{(\Pi_t, \Psi_{t,i})} \right) \right] \tag{6.2.9}$$

$$Q_{min,i} \leq q_{t,i}^{(\Pi_t, \Psi_{i,t})} \leq Q_{max,i}, \quad \forall i \in I, \ \forall t \in T \tag{6.2.10}$$

$$M_{min,i} \leq M_{0,i} + \sum_{s=1}^{t} \Psi_{s,i} + \sum_{s=1}^{t}\sum_{j=1}^{I} \sigma_{j,i} \cdot q_{s,j}^{(\Pi_r,\Psi_{s,j})}$$

$$+ \sum_{s=1}^{t}\sum_{j=1}^{I} \sigma_{j,i} \cdot h_{s,j,i}^{(\Psi_{s,j})} - \sum_{s=1}^{t} q_{s,i}^{(\Pi_s,\Psi_{s,i})} - \sum_{s=1}^{t}\sum_{j=1}^{I} \sigma_{i,j} \cdot h_{s,i,j}^{(\Psi_{s,i})} \tag{6.2.11}$$

$$- \sum_{s=1}^{t} s_{s,i}^{(\Psi_{s,i})} \leq M_{max,i}, \quad \forall i \in I, \ \forall t \in T$$

$$q_{t,i}^{(\Pi_t,\Psi_{t,i})}, \ s_{i,t}^{(\Psi_{t,i})} \geq 0, \quad \forall i \in I, \ \forall t \in T \tag{6.2.12}$$

$$h_{t,i,j}^{(\Psi_{t,i})} \geq 0, \quad \forall t \in T, \ \forall i \in I, \ \forall j \in I \tag{6.2.13}$$

The objective function, Eq. (6.2.9), represents the expected discounted market value of total production from all reservoirs over the whole scheduling horizon. Eq. (6.2.10) gives the upper and lower boundaries for production from reservoir i in time period t. Eq. (6.2.11) gives the upper and lower boundaries for the reservoir level, while Eq. (6.2.12) and (6.2.13) states that all variables have to be nonnegative.

6.2.4 LDR model

In the LDR model, the decision variables for production, discharge and spillage are adjustable, and allowed to depend on the observed data $(d_\tau : \tau \epsilon I_t\ )$. It is assumed that the production decision, $q_{t,i}$, is made at the beginning of period t. This decision is made on the basis of the realisations of price, Π_r, and inflow, Ψ_r, observed in the periods $r \in I_t$, where I_t is the set $\{1, ..., t\}$. Correspondingly, the discharge decision is made on the basis of the realisations of inflow, Ψ_r, observed in the periods $r \in I_t$. The variable for spillage, $s_{t,i}$, is auxiliary. This variable do not correspond to an actual decision, an can adjust itself to the realisations of inflow, Ψ_r, observed in the periods $r \in I_t$. Applying the methodology described in Section 6.1, the decision making policies are restricted to *affine decision rules*:

$$q_{t,i}^{(\Pi_t,\Psi_t)} = \delta_{t,i}^0 + \sum_{r\epsilon I_t} (\delta_{t,i}^r \cdot \Pi_r + \gamma_{t,i}^r \cdot \Psi_{r,i}), \quad \forall t \in T, \ \forall i \in I \tag{6.2.14}$$

$$h_{t,i,j}^{(\Psi_t)} = \rho_{t,i,j}^0 + \sum_{r\epsilon I_t} (\rho_{t,i,j}^r \cdot \Psi_{r,i}), \quad \forall t \in T, \ \forall i \in I, \ \forall j \in I \tag{6.2.15}$$

$$s_{t,i}^{(\Psi_t)} = \kappa_{t,i}^0 + \sum_{r\epsilon I_t} (\kappa_{t,i}^r \cdot \Psi_{r,i}), \quad \forall t \in T, \ \forall i \in I \tag{6.2.16}$$

where the variables ($\delta_{t,i}^0, \delta_{t,i}^r, \gamma_{t,i}^r, \rho_{t,i,j}^0, \rho_{t,i,j}^r, \kappa_{t,i}^0$ and $\kappa_{t,i}^r$) are the new non adjustable variables. When specifying these policies both future price and inflow are uncertain. However, both these parameters are assumed to be within the following uncertainty sets:

$$\Xi_{\Pi} := [\Pi_t^* \cdot (1-\theta^{\Pi}), \Pi_t^* \cdot (1+\theta^{\Pi})], \qquad \forall t \in T \tag{6.2.17}$$

$$\Xi_{\Psi} := [\Psi_{t,i}^* \cdot (1-\theta^{\Psi}), \Psi_{t,i}^* \cdot (1+\theta^{\Psi})], \qquad \forall i \in I, \forall t \in T \tag{6.2.18}$$

where θ^{Π} and θ^{Ψ} are nonnegative, and represent the uncertainty levels of price and inflow, respectively. Π_t^* represents the expected price, while $\Psi_{t,i}^*$ represents the expected inflow.

Figures 6.2.1 and 6.2.2 illustrates how price and inflow can vary between the upper and lower limit of their respective uncertainty sets. In these figures the uncertainty levels for both price, θ^{Π}, and inflow, θ^{Ψ}, are equal to 20 %, i.e. $\Pi_t \in [0.8 \cdot \Pi_t^*, 1.2 \cdot \Pi_t^*]$ and $\Psi_{t,i} \in [0.8 \cdot \Psi_{t,i}^*, 1.2 \cdot \Psi_{t,i}^*]$. The dotted lines in Figures 6.2.1 and 6.2.2 represent the lower limits, expected values and upper limits, while the bold line represents a random sample realisation for price and inflow, respectively.

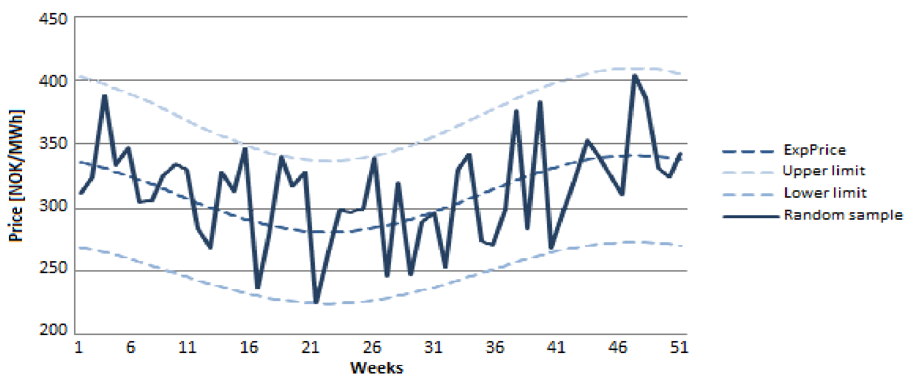

Figure 6.2.1: Random sample realisation of price, with expected values and upper and lower limits.

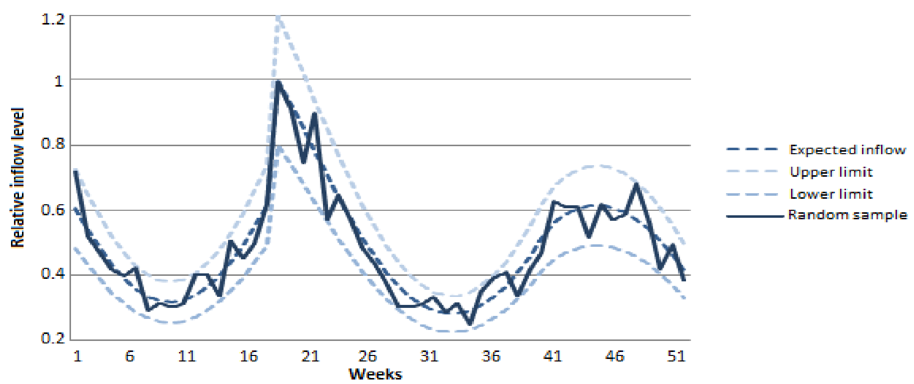

Figure 6.2.2: Random sample realization of inflow, with expected values and upper and lower limits.

The stochastic model is rewritten into an LDR model based on the procedure described in Appendix B. This gives the following model:

$$V_0 = max \ \left[\sum_{t=1}^{T}\sum_{i=1}^{I}\frac{1}{(1+R)^t}\left(\Pi_t^* \cdot \delta_{t,i}^0 + \sum_{r\epsilon I_t}\delta_{t,i}^r \cdot \Pi_t^* \cdot \Pi_r^* \right.\right.$$
$$\left.\left. + \sum_{r\epsilon I_t}\delta_{t,i}^r \cdot C_{t,r}^{\Pi,\Pi} + \sum_{r\epsilon I_t}\gamma_{t,i}^r \cdot \Pi_t^* \cdot \Psi_r + \sum_{r\epsilon I_t}\gamma_{t,i}^r \cdot C_{t,r}^{\Pi,\Psi}\right)\right] \tag{6.2.19}$$

$$\begin{aligned}
M_{0,i} + \sum_{s=1}^{t}\Psi_{s,i} - \theta^{\Psi} \cdot \sum_{r=1}^{t}\Psi_{s,i} + \sum_{s=1}^{t}\sum_{j=1}^{I}\sigma_{j,i} \cdot \delta_{s,j}^0 \\
+ \sum_{s=1}^{t}\sum_{j=1}^{I}\sum_{r\epsilon I_s}\sigma_{j,i} \cdot \delta_{s,j}^r \cdot \Pi_r - \theta^{\Pi} \cdot \sum_{s=1}^{t}\sum_{j=1}^{I}\sum_{r\epsilon I_s}\sigma_{j,i} \cdot d_{s,j}^r \cdot \Pi_r \\
+ \sum_{s=1}^{t}\sum_{j=1}^{I}\sum_{r\epsilon I_s}\sigma_{j,i} \cdot \gamma_{s,j}^r \cdot \Psi_{r,j} - \theta^{\Psi} \cdot \sum_{s=1}^{t}\sum_{j=1}^{I}\sum_{r\epsilon I_s}\sigma_{j,i} \cdot y_{s,j}^r \cdot \Psi_{r,j} \\
+ \sum_{s=1}^{t}\sum_{j=1}^{I}\sigma_{j,i} \cdot \rho_{s,j,i}^0 + \sum_{s=1}^{t}\sum_{j=1}^{I}\sum_{r\epsilon I_s}\sigma_{j,i} \cdot \rho_{s,j,i}^r \cdot \Psi_{r,j} \\
-\theta^{\Psi} \cdot \sum_{s=1}^{t}\sum_{j=1}^{I}\sum_{r\epsilon I_s}\sigma_{j,i} \cdot p_{s,j,i}^r \cdot \Psi_{r,j} - \sum_{s=1}^{t}\delta_{s,i}^0 - \sum_{s=1}^{t}\sum_{r\epsilon I_s}\delta_{s,i}^r \cdot \Pi_r \\
-\theta^{\Pi} \cdot d_{s,i}^r \cdot \Pi_r - \sum_{s=1}^{t}\sum_{r\epsilon I_s}\gamma_{s,i}^r \cdot \Psi_{r,i} - \theta^{\Psi} \cdot \sum_{s=1}^{t}\sum_{r\epsilon I_s}y_{s,i}^r \cdot \Psi_{r,i} \\
- \sum_{s=1}^{t}\sum_{j=1}^{I}\sigma_{i,j} \cdot \rho_{s,i,j}^0 - \sum_{s=1}^{t}\sum_{j=1}^{I}\sum_{r\epsilon I_s}\sigma_{i,j} \cdot \rho_{s,i,j}^r \cdot \Psi_{r,i} \\
-\theta^{\Psi} \cdot \sum_{s=1}^{t}\sum_{j=1}^{I}\sum_{r\epsilon I_s}\sigma_{i,j} \cdot p_{s,i,j}^r \cdot \Psi_{r,i} - \sum_{s=1}^{t}\kappa_{s,i}^0 - \sum_{s=1}^{t}\sum_{r\epsilon I_s}\kappa_{s,i}^r \cdot \Psi_{r,i} \\
-\theta^{\Psi} \cdot \sum_{s=1}^{t}\sum_{r\epsilon I_s}k_{s,i}^r \cdot \Psi_{r,i} \geq M_{min,i}, \quad \forall i \in I, \ \forall t \in T
\end{aligned} \tag{6.2.20}$$

$$
\begin{aligned}
M_{0,i} + \sum_{s=1}^{t} \Psi_{s,i} + \theta^{\Psi} \cdot \sum_{r=1}^{t} \Psi_{s,i} + \sum_{s=1}^{t}\sum_{j=1}^{I} \sigma_{j,i} \cdot \delta^{0}_{s,j} \\
+ \sum_{s=1}^{t}\sum_{j=1}^{I}\sum_{r\epsilon I_s} \sigma_{j,i} \cdot \delta^{r}_{s,j} \cdot \Pi_r + \theta^{\Pi} \cdot \sum_{s=1}^{t}\sum_{j=1}^{I}\sum_{r\epsilon I_s} \sigma_{j,i} \cdot d^{r}_{s,j} \cdot \Pi_r \\
+ \sum_{s=1}^{t}\sum_{j=1}^{I}\sum_{r\epsilon I_s} \sigma_{j,i} \cdot \gamma^{r}_{s,j} \cdot \Psi_{r,j} + \theta^{\Psi} \cdot \sum_{s=1}^{t}\sum_{j=1}^{I}\sum_{r\epsilon I_s} \sigma_{j,i} \cdot \\
y^{r}_{s,j} \cdot \Psi_{r,j} + \sum_{s=1}^{t}\sum_{j=1}^{I} \sigma_{j,i} \cdot \rho^{0}_{s,j,i} + \sum_{s=1}^{t}\sum_{j=1}^{I}\sum_{r\epsilon I_s} \sigma_{j,i} \cdot \rho^{r}_{s,j,i} \cdot \Psi_{r,j} \\
+\theta^{\Psi} \cdot \sum_{s=1}^{t}\sum_{j=1}^{I}\sum_{r\epsilon I_s} \sigma_{j,i} \cdot p^{r}_{s,j,i} \cdot \Psi_{r,j} - \sum_{s=1}^{t} \delta^{0}_{s,i} - \sum_{s=1}^{t}\sum_{r\epsilon I_s} \delta^{r}_{s,i} \cdot \Pi_r \\
+\theta^{\Pi} \cdot d^{r}_{s,i} \cdot \Pi_r - \sum_{s=1}^{t}\sum_{r\epsilon I_s} \gamma^{r}_{s,i} \cdot \Psi_{r,i} + \theta^{\Psi} \cdot \sum_{s=1}^{t}\sum_{r\epsilon I_s} y^{r}_{s,i} \cdot \Psi_{r,i} \\
- \sum_{s=1}^{t}\sum_{j=1}^{I} \sigma_{i,j} \cdot \rho^{0}_{s,i,j} - \sum_{s=1}^{t}\sum_{j=1}^{I}\sum_{r\epsilon I_s} \sigma_{i,j} \cdot \rho^{r}_{s,i,j} \cdot \Psi_{r,i} + \theta^{\Psi} \cdot \sum_{s=1}^{t}\sum_{j=1}^{I}\sum_{r\epsilon I_s} \sigma_{i,j} \cdot \\
p^{r}_{s,i,j} \cdot \Psi_{r,i} - \sum_{s=1}^{t} \kappa^{0}_{s,i} - \sum_{s=1}^{t}\sum_{r\epsilon I_s} \kappa^{r}_{s,i} \cdot \Psi_{r,i} + \theta^{\Psi} \cdot \sum_{s=1}^{t}\sum_{r\epsilon I_s} k^{r}_{s,i} \cdot \Psi_{r,i} \\
\leq M_{max,i}, \quad \forall i \in I, \ \forall t \in T
\end{aligned}
\tag{6.2.21}
$$

$$
\begin{aligned}
\delta^{0}_{t,i} + \sum_{r\epsilon I_t} \delta^{r}_{t,i} \cdot \Pi_r - \theta^{\Pi} \cdot \sum_{r\epsilon I_t} d^{r}_{t,i} \cdot \Pi_r \\
+ \sum_{r\epsilon I_t} \gamma^{r}_{t,i} \cdot \Psi_{r,i} - \theta^{\Psi} \cdot \sum_{r\epsilon I_t} y^{r}_{t,i} \cdot \Psi_{r,i} \geq Q_{min,i}, \quad \forall i \in I, \ \forall t \in T
\end{aligned}
\tag{6.2.22}
$$

$$
\begin{aligned}
\delta^{0}_{t,i} + \sum_{r\epsilon I_t} \delta^{r}_{t,i} \cdot \Pi_r + \theta^{\Pi} \cdot \sum_{r\epsilon I_t} d^{r}_{t,i} \cdot \Pi_r \\
+ \sum_{r\epsilon I_t} \gamma^{r}_{t,i} \cdot \Psi_{r,i} + \theta^{\Psi} \cdot \sum_{r\epsilon I_t} y^{r}_{t,i} \cdot \Psi_{r,i} \leq Q_{max,i}, \quad \forall i \in I, \ \forall t \in T
\end{aligned}
\tag{6.2.23}
$$

$$
\begin{aligned}
\rho^{0}_{t,i,j} + \sum_{r\epsilon I_t} \rho^{r}_{t,i,j} \cdot \Psi_{r,i} - \theta^{\Psi} \cdot \sum_{r\epsilon I_t} p^{r}_{t,i,j} \cdot \Psi_{r,i} \\
\geq 0, \quad \forall t \in T, \ \forall i \in I, \ \forall j \in I
\end{aligned}
\tag{6.2.24}
$$

$$
\kappa^{0}_{t,i} + \sum_{r\epsilon I_t} \kappa^{r}_{t,i} \cdot \Psi_{r,i} - \theta^{\Psi} \cdot \sum_{r\epsilon I_t} \kappa^{r}_{t,i} \cdot \Psi_{r,i} \geq 0, \quad \forall i \in I, \ \forall t \in T
\tag{6.2.25}
$$

$$-d^r_{t,i} \leq \delta^r_{t,i} \leq d^r_{t,i}, \quad 1 \leq r \leq t \leq T,\ \forall i \in I \tag{6.2.26}$$

$$-y^r_{t,i} \leq \gamma^r_{t,i} \leq y^r_{t,i}, \quad 1 \leq r \leq t \leq T,\ \forall i \in I \tag{6.2.27}$$

$$-p^r_{t,i,j} \leq \rho^r_{t,i,j} \leq p^r_{t,i,j}, \quad 1 \leq r \leq t \leq T,\ \forall i \in I,\ \forall j \in I \tag{6.2.28}$$

$$-k^r_{t,i} \leq \kappa^r_{t,i} \leq k^r_{t,i}, \quad 1 \leq r \leq t \leq T,\ \forall i \in I \tag{6.2.29}$$

The objective function, Eq. (6.2.19), represents the expected discounted market value of total production from all reservoirs over the whole scheduling horizon. The upper and lower production levels are stated by Eq. (6.2.23) and (6.2.22), while Eq. (6.2.21) and (6.2.20) state that the reservoir levels have to be less than a given maximum level and larger than a given minimum level. Eq. (6.2.24) and (6.2.25) states that spillage and discharge have to be nonnegative, while Eq. (6.2.26) to (6.2.29) give the absolute values for the new variables.

All constraints are defined to hold for all possible realizations of price and inflow within the specified uncertainty sets. This means that the highest possible production, i.e. the production corresponding to the highest inflow outcome[14] and highest price outcome[15], can not exceed the production capacity in any time period. At the same time the lowest possible production, i.e. the production corresponding to the lowest inflow outcome[16] and lowest price outcome[17], has to be greater than or equal to the minimum production requirement in all time periods.

The constraint requiring that the reservoir levels have to be greater than or equal to a given minimum level has to hold for the case in which the lowest possible inflow, the lowest possible production and discharge from upstream reservoirs and the highest possible production, the highest possible discharge and the highest possible spillage occur in all time periods. At the same time the constraint requiring that the reservoir levels have to be less than or equal to a given maximum level has to hold for the opposite case. The reservoir levels given by these two extreme cases will hereafter be referred to as the highest possible and lowest possible reservoir levels. These reservoir levels are unlikely to occur. However, due to the equivalences presented in Appendix B.1.4, these bounds are

[14] A situation in which the realization of inflow is equal to its upper bound in all time periods, i.e. $\Psi_{t,i} = \Psi^*_{t,i} + \theta^\Psi \cdot \Psi^*_{t,i}$, $\forall t \in T$.

[15] A situation in which the realization of price is equal to its upper bound in all time periods, i.e. $\Pi_t = \Pi^*_t + \theta^\Pi \cdot \Pi^*_t$, $\forall t \in T$.

[16] A situation in which the realization of inflow is equal to its lower bound in all time periods, i.e. $\Psi_{t,i} = \Psi^*_{t,i} - \theta^\Psi \cdot \Psi^*_{t,i}$, $\forall t \in T$.

[17] A situation in which the realization of price is equal to its lower bound in all time periods, i.e. $\Pi_t = \Pi^*_t - \theta^\Pi \cdot \Pi^*_t$, $\forall t \in T$.

necessary in order to guarantee that no reservoir levels higher or lower than the reservoir limits can possibly occur.

6.3 Problem size

The deterministic model and the LDR model presented in Sections 6.2.2 and 6.2.4, respectively, are implemented and solved in Xpress MP. In this section, the problem sizes of these models are presented.

The deterministic model has three decision variables for each reservoir i and time period t, and one decision variable for each reservoir i, reservoir j and time period t. The topology parameter is defined such that water can only be discharged downstream in the topology, meaning that $i \leq j,\ \forall i, j \in I$. This gives a total of $3 \times T \times I + 0.5 \times T \times I \times I$ variables. The model has five constraints for each reservoir i in time period t, which gives a total of $5 \times T \times I$ constraints. Plant 1, 2 and 4 are run for $T = 52$ time periods, while Plant 3 is run for $T = 104$ time periods. Plant 1 and 2 do both have $I = 1$ reservoirs, while Plant 3 and Plant 4 have $I = 4$ reservoirs. The problem size for each plant is presented in Table 6.3.2.

Table 6.3.1: Problem sizes for the deterministic model.

Plant	# Variables	# Constraints
Plant 1 and 2	182	260
Plant 3	1460	2080
Plant 4	732	1040

When applying the LDR approach, the problem sizes increases. The LDR model has two decision variables with dimension $I \times T$, six with dimension $0.5 \times T \times T \times I$, one with dimension $0.5 \times T \times I \times I$ and one with dimension $0.25 \times T \times T \times I \times I$. The model has five constraints with dimension $T \times I$, one with dimension $0.5 \times T \times I \times I$, one with dimension $1.5 \times T \times T \times I$ and one with dimension $0.25 \times T \times T \times I \times I$. The problem size for each plant is presented in Table 6.3.2.

Table 6.3.2: Problem sizes for the LDR model.

Plant	# Variables	# Constraints
Plant 1 and 2	8216	4316
Plant 3	195 520	111 072
Plant 4	49 088	28 496

6.4 Water values

The LDR model is intended to be coupled to a shorter term scheduling model with a scheduling horizon of one week. The coupling is assumed to take place through a fixed water value at the end of the first period of the scheduling horizon of the long term scheduling model. Considering a plant with one power station and one reservoir, the water value will correspond to the dual value of the following constraint:

$$m_t + q_t + s_t, = M_{t-1} + \Psi_t, \quad \forall t \in T \tag{6.4.1}$$

Eq. (6.4.1) states that the reservoir level in week $t-1$ must equal the reservoir level in week t plus inflow minus discharge and spillage in week t. The dual value of this constraint for $t = 1$ corresponds to the water value at the end of the first week, and expresses how much the profit increases when one extra unit of water is available in the initial reservoir.

The reservoir level constraints, Eq. (B.1.46) and (B.1.47) in Appendix B.1.6, ensure that the reservoir level at the end of each week is within its limits. However, these constraints do not link one time period to the preceding one such as Eq. (6.4.1) does. For this reason, the dual variables of these constraints do not correspond to the water values at the end of each time period. To make it possible to extract the water value at the end of the first period from the model results, Eq. (6.4.2) can be added to the LDR model. This constraint is obtained by inserting the affine decision rules into Eq. (6.4.1). In order to get an inequality constraint, the spillage variable, s_t, is removed, and the inequality constraint is rewritten based on the equivalences presented in Appendix B.1.4. The new constraint for the LDR model is defined as:

$$\begin{aligned}
M_0 + \sum_{s=1}^{t} \Psi_s + \theta^{\Psi} \cdot \sum_{s=1}^{t} \Psi_s - \sum_{s=1}^{t} \delta_s^0 - \sum_{s=1}^{t} \sum_{r \in I_s} \delta_s^r \cdot \Pi_r \\
+\theta^{\Pi} \cdot \sum_{s=1}^{t} \sum_{r \in I_s} d_s^r \cdot \Pi_r - \sum_{s=1}^{t} \sum_{r \in I_s} \gamma_s^r \cdot \Psi_r + \theta^{\Psi} \cdot \sum_{s=1}^{t} \sum_{r \in I_s} y_s^r \cdot \Psi_r \\
- \sum_{s=1}^{t} \kappa_s^0 - \sum_{s}^{t} \sum_{r \in I_s} \kappa_s^r \cdot \Psi_r + \theta^{\Psi} \cdot \sum_{s=1}^{t} \sum_{r \in I_s} k_s^r \cdot \Psi_r + \delta_t^0 \\
+ \sum_{r \in I_t} \delta_t^r \cdot \Pi_r + \theta^{\Pi} \cdot \sum_{r \in I_t} d_t^r \cdot \Pi_r + \sum_{r \in I_t} \gamma_t^r \cdot \Psi_r + \theta^{\Psi} \cdot \sum_{r \in I_t} y_t^r \cdot \Psi_r \\
\leq M_0 + \sum_{s=1}^{t} \Psi_s - \theta^{\Psi} \cdot \sum_{s=1}^{t} \Psi_s, \quad \forall t = 1
\end{aligned} \tag{6.4.2}$$

The dual value of this constraint is equivalent to the water value at the end of the first period[18]. This constraint is weakly dominated by Eq. (B.1.46) and (B.1.47), and will therefore not affect the solution.

[18]The dual value of Eq. (6.4.2) corresponds to the *expected* water value, because it states how much the *expected* profit increases by having one additional unit of water available. The word water value will hereafter refer to *expected* water value.

6.5 Head variations

Production varies with both water discharge from the reservoir and the head of water, as can be seen from Eq. (3.1.1) and (3.1.2) in Section 3.1. The head of water varies with the reservoir volume, indicating that production will be higher at high reservoir volumes due to a higher head of water. The LDR model can not directly deal with a variable head of water as this will make the problem nonlinear and non convex. By assuming a constant average head of water the model will set too high energy levels at low reservoir volumes and too low energy levels at at high reservoir volumes.

One way of accounting for a variable head of water is by penalizing low heads of water and rewarding high heads of water. This can be done by adding head sensitivities of economic gain with respect to small changes in the reservoir volumes to the objective function. This approach is used in Gjelsvik and Wallace (1996) and Gjelsvik and Haugstad (2005), and will be described below.

For a hydropower system with I reservoirs, where $i = 1, ..., I$, V_t^i denotes the reservoir volume at the end of week t, while h_t^i denotes the water surface elevation referred to sea level. It is assumed that there is a power station with output P_t^i immediately downstream reservoir i. h is the index of an upstream reservoir, while j is the index of a downstream reservoir. The outlet of power station i is assumed to be submerged into reservoir j. If a situation in which the volume V_t^i is changed by a small amount, ΔV_t^i, without changing the discharge q_t^i, then the influence of ΔV_t^i on production in power station i downstream reservoir i and power station h upstream reservoir i can be expressed as:

$$\frac{\delta P_t^i}{\delta V_t^i} = \frac{\delta P_t^i}{\delta h_t^i} \cdot \frac{\delta h_t^i}{\delta V_t^i} = \frac{1}{A_t^i} \cdot \frac{P_t^i}{h_t^i - h_t^j} \tag{6.5.1}$$

$$\frac{\delta P_t^h}{\delta V_t^i} = \frac{\delta P_t^h}{\delta h_t^i} \cdot \frac{\delta h_t^i}{\delta V_t^i} = \frac{1}{A_t^i} \cdot \frac{P_t^i}{h_t^h - h_t^i} \tag{6.5.2}$$

where:

$$A_t^i = (\frac{\delta h_t^i}{\delta V_t^i})^{-1} \tag{6.5.3}$$

is the surface area of reservoir i. The spot price in time period t, Π_t, is used as the marginal value of the generation change. The change in profit due to variable head can then be approximated by adding the following head sensitivity terms to the objective function

$$\sum_{t=1}^{T} \sum_{i=1}^{n} \tilde{c_t^i} \, \Delta \, V_t^i \tag{6.5.4}$$

where:

$$\tilde{c_t^i} = \frac{\Pi_t}{A_t^I} \left[\frac{P_t^i}{h_t^i - h_t^j} - \frac{P_t^i}{h_t^h - h_t^i} \right] \tag{6.5.5}$$

The $\tilde{c}$-coefficients can be positive or negative. An increase in the volume of reservoir i increases the profit associated with the downstream power station i because the head of water increases, while it decreases the profit associated with the upstream power station h because the head of water is decreased due to a higher backwater level. If there is no downstream reservoir or the outlet of the power station is not submerged, the second term of Eq. (6.5.5) is equal to zero.

By running the deterministic model for the expected values of price and inflow without any corrections for variable head, the nominal reservoir operations schedule with nominal values of P_t^i, V_t^i, h_t^i and A_t^i is found. From these values the $\tilde{c}$-coefficients can be derived. ΔV_t^i is defined to be the deviation of the optimal reservoirs volumes from the expected reservoir volumes in time t (Steinsbø, 2008). Eq. (6.5.4) is inserted into the objective function of the LDR model for all possible flows, and a schedule taking variable head of water into account is found.

7 Dual Linear Decision Rules models

Althrough the LDR approach is very effective at reducing the computational complexity of stochastic problems, it may result in a considerable loss of optimality. Kuhn et al. (2011) propose to apply the LDR approach not only on the primal stochastic problem, but also on the dual version of this problem. The approximation error introduced by the LDR approach can be estimated by the gap between the optimal objective values of the primal and the dual LDR models, i.e the duality gap.

This section starts with a presentation of basic duality theory, before the dual version of the stochastic model presented in Section 6 is presented. The LDR approximation is applied to the dual stochastic model in order to develop the dual LDR model, and this model is presented in Section 7.2.2. The dual versions of the aggregated reservoir stochastic model and the aggregated reservoir LDR model can be found in Appendix C.1. The final section presents the problem size of the dual LDR model.

7.1 Duality theory

Associated with every LP problem, there is a dual problem which is defined with exactly the same input data as the original primal problem (Lundgren et al., 2010). Let the primal problem (P) be defined as:

$$\max z = \mathbf{c}^T\mathbf{x} \tag{7.1.1}$$

$$\mathbf{A}\mathbf{x} \leq \mathbf{b} \tag{7.1.2}$$

$$\mathbf{x} \geq \mathbf{0} \tag{7.1.3}$$

When formulating the dual version of this problem one dual variable is created for every primal constraint, and one dual constraint is defined for every primal variable. Since the primal problem presented above is a maximization problem the dual problem (D) becomes a minimization problem, and can be defined as:

$$\min w = \mathbf{b}^T\mathbf{y} \tag{7.1.4}$$

$$\mathbf{A}^T\mathbf{y} \leq \mathbf{c} \tag{7.1.5}$$

$$\mathbf{y} \geq \mathbf{0} \tag{7.1.6}$$

The weak and strong duality theorems describe the relationship between the primal and the dual models. The weak duality theorem states that if $\mathbf{x}$ is a feasible solution for the primal problem with objective $\mathbf{c}$, and $\mathbf{y}$ is a feasible solution for its dual problem with objective $\mathbf{b}$, then:

$$\mathbf{c}^T\mathbf{x} \leq \mathbf{b}^T\mathbf{y} \tag{7.1.7}$$

The theorem implies that the value of the objective function for any feasible solution of the primal maximization problem is bounded from above by the value of the objective function for any feasible solution of the dual minimization problem. Similarly, the value of the objective function for the dual minimization problem is bounded from below by the value of the objective function for any feasible solution of the primal maximization problem.

The strong duality theorem states that if $\mathbf{x}$ is an optimal solution for the primal maximization problem with objective $\mathbf{c}$, and $\mathbf{y}$ is an optimal solution for the dual minimization problem with objective $\mathbf{b}$, then:

$$\mathbf{c}^T\mathbf{x} = \mathbf{b}^T\mathbf{y} \tag{7.1.8}$$

This theorem implies that there must exist a feasible solution to each respective problem with identical objective function values. Strong duality holds if and only if the duality gap is equal to zero.

Primal LDR leads to a pessimistic approximation of the original problem that underestimates the producer's flexibility (Kuhn et al., 2011). In contrast, the use of dual LDR results in an optimistic approximation that overestimates the producers flexibility. The duality gap, i.e. the difference between the optimal objective values of the primal and dual LDR models, can be used to estimate the approximation error incurred by the LDR approach. The objective value of the primal LDR model, P^L, is a lower bound on the optimal objective value of the exact problem, P, where the gap between P and P^L can be defined as:

$$\Delta^L = \max\ P - \max\ P^L \tag{7.1.9}$$

where Δ^L necessarily is nonnegative as P^L is a restriction of a maximization problem. The objective value of the dual LDR model, D^U, is an upper bound on the optimal objective value of the exact problem, D, where the gap between D^U and D can be defined as:

$$\Delta^U = \min\ D^U - \min\ D \tag{7.1.10}$$

where Δ^U necessarily is nonnegative as D^U is a restriction of a minimization problem. Neither Δ^L and Δ^U can be calculated, but the joint primal and dual approximation error will give an indication of the duality gap, defined as:

$$\Delta = \min\ D^U - \max\ P^L \tag{7.1.11}$$

The duality gap is illustrated in Figure 7.1.1 and can be found by solving the primal and dual LDR approximated problems:

$$\begin{gathered}
\Delta = \min\ D^U - \max\ P^L \\
\Delta = \min\ D^U - \min\ D + \min\ D - \max\ P + \max\ P - \max\ P^L \\
\Delta = \Delta^U + \min\ D - \max\ P + \Delta^L \\
\Delta \geq \Delta^U + \Delta^L
\end{gathered} \tag{7.1.12}$$

The last equality in Eq. (7.1.12) follows from weak duality and show that the duality gap, Δ, constitutes an upper bound on Δ^U and Δ^L. A large duality gap indicates the possibility for a large approximation error, and corresponding low accuracy. Similarly, a small duality gap indicates a small approximation error and high accuracy.

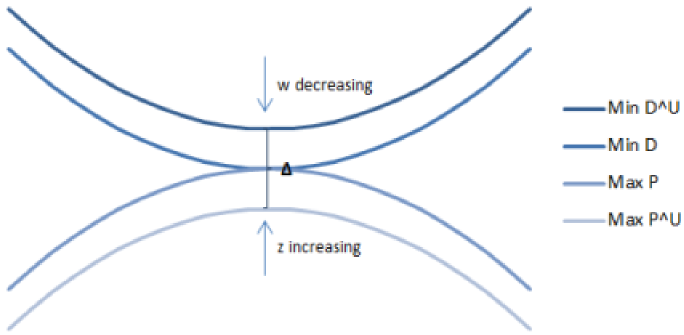

Figure 7.1.1: An illustration of the duality gap, Δ, between a primal maximization problem and a dual minimization problem.

7.2 Dual hydropower scheduling models

The same assumptions as were made for the primal models presented in Section 6.2.1 are made for the dual models presented in this section.

7.2.1 Stochastic model

The primal stochastic model presented in Section 6.2.3 has three sets of variables and four sets of constraints, which gives a dual problem with three sets of constraints and four sets of variables. The new sets of dual variables are defined as:

$$\iota_{t,i}^{(\Pi_t,\Psi_{t,i})}, \zeta_{t,i}^{(\Pi_t,\Psi_{t,i})}, \nu_{t,i}^{(\Pi_t,\Psi_{t,i})} \text{ and } \mu_{t,i}^{(\Pi_t,\Psi_{t,i})}, \ \forall t \in T \tag{7.2.1}$$

The stochastic dual model is developed based on Lundgren et al. (2010) and presented below:

$$\begin{aligned} Z_0 = min\ \mathbb{E}\ \Bigg[\sum_{t=1}^{T}\sum_{i=1}^{I} \Bigg(& -Q_{min,i} \cdot \iota_{t,i}^{(\Pi_t,\Psi_{t,i})} + Q_{max,i} \cdot \zeta_{t,i}^{(\Pi_t,\Psi_{t,i})} \\ & + \left(M_{max,i} - M_{0,i} - \sum_{s=1}^{t} \Psi_s \right) \cdot \nu_{t,i}^{(\Pi_t,\Psi_{t,i})} \\ & + \left(-M_{min,i} + M_{0,i} + \sum_{s=1}^{t} \Psi_s \right) \cdot \mu_{t,i}^{(\Pi_t,\Psi_{t,i})} \Bigg) \Bigg] \end{aligned} \tag{7.2.2}$$

$$-\iota_{t,i}^{(\Pi_t,\Psi_{t,i})} + \zeta_{t,i}^{(\Pi_t,\Psi_{t,i})} + \sum_{s=t}^{T}\sum_{j=i}^{I}\sigma_{j,i}\cdot\nu_{s,j}^{(\Pi_s,\Psi_{s,j})} - \sum_{s=t}^{T}\nu_{s,i}^{(\Pi_s,\Psi_{s,i})}$$
$$-\sum_{s=t}^{T}\sum_{j=i}^{I}\sigma_{j,i}\cdot\mu_{s,j}^{(\Pi_s,\Psi_{s,j})} + \sum_{s=t}^{T}\mu_{s,i}^{(\Pi_s,\Psi_{s,i})} \geq \frac{1}{(1+R)^t}\cdot\Pi_t, \qquad (7.2.3)$$
$$\forall t \in T,\ \forall i \in I$$

$$\sum_{s=t}^{T}\sum_{j=i}^{I}\sigma_{j,i}\cdot\nu_{s,j}^{(\Pi_s,\Psi_{s,j})} - \sum_{s=t}^{T}\sum_{j=1}^{I}\sigma_{i,j}\cdot\nu_{s,i}^{(\Pi_s,\Psi_{s,i})}$$
$$-\sum_{s=t}^{T}\sum_{j=i}^{I}\sigma_{j,i}\cdot\mu_{s,j}^{(\Pi_s,\Psi_{s,j})} + \sum_{s=t}^{T}\sum_{j=1}^{I}\sigma_{i,j}\cdot\mu_{s,i}^{(\Pi_s,\Psi_{s,i})} \geq 0, \qquad (7.2.4)$$
$$\forall t \in T,\ \forall i \in I,\ \forall j \in I$$

$$-\sum_{s=t}^{T}\nu_{s,i}^{(\Pi_s,\Psi_{s,i})} + \sum_{s=t}^{T}\mu_{s,i}^{(\Pi_s,\Psi_{s,i})} \geq 0, \quad \forall t \in T,\ \forall i \in I \qquad (7.2.5)$$

$$\iota_{t,i}^{(\Pi_t,\Psi_{t,i})}, \zeta_{t,i}^{(\Pi_t,\Psi_{t,i})}, \nu_{t,i}^{(\Pi_t,\Psi_{t,i})}, \mu_{t,i}^{(\Pi_t,\Psi_{t,i})} \geq 0, \quad \forall t \in T,\ \forall i \in I \qquad (7.2.6)$$

7.2.2 LDR model

As for the primal LDR model, the decision making policies are restricted to *affine decision rules*:

$$\iota_{t,i}^{(\Pi_t,\Psi_{t,i})} = \iota_{t,i}^{0} + \sum_{r\in I_t}(\iota_{1,t,i}^{r}\cdot\Pi_r + \iota_{2,t,i}^{r}\cdot\Psi_{r,i}), \quad \forall t \in T,\ \forall i \in I \qquad (7.2.7)$$

$$\zeta_{t,i}^{(\Pi_t,\Psi_{t,i})} = \zeta_{t,i}^{0} + \sum_{r\in I_t}(\zeta_{1,t,i}^{r}\cdot\Pi_r + \zeta_{2,t,i}^{r}\cdot\Psi_{r,i}), \quad \forall t \in T,\ \forall i \in I \qquad (7.2.8)$$

$$\nu_{t,i}^{(\Pi_t,\Psi_{t,i})} = \nu_{t,i}^{0} + \sum_{r\in I_t}(\nu_{1,t,i}^{r}\cdot\Pi_r + \nu_{2,t,i}^{r}\cdot\Psi_{r,i}), \quad \forall t \in T,\ \forall i \in I \qquad (7.2.9)$$

$$\mu_{t,i}^{(\Pi_t,\Psi_{t,i})} = \mu_{t,i}^{0} + \sum_{r\in I_t}(\mu_{1,t,i}^{r}\cdot\Pi_r + \mu_{2,t,i}^{r}\cdot\Psi_{r,i}), \quad \forall t \in T,\ \forall i \in I \qquad (7.2.10)$$

where the variables ($\iota_{t,i}^{0}, \iota_{1,t,i}^{r}, \iota_{2,t,i}^{r}, \zeta_{t,i}^{0}, \zeta_{1,t,i}^{r}, \zeta_{2,t,i}^{r}, \nu_{t,i}^{0}, \nu_{1,t,i}^{r}, \nu_{2,t,i}^{r}, \mu_{t,i}^{0}, \mu_{1,t,i}^{r}$ and $\mu_{2,t,i}^{r}$) are new nonadjustable variables. The uncertainty sets are defined in the same way as in Section 6.2.4. The stochastic dual model is rewritten based on the procedure described in Appendix C, which gives the following model:

$$\begin{aligned}
Z_0 = min \ \sum_{t=1}^{T}\sum_{i=1}^{I}\Bigg[& -Q_{min,i}\cdot\iota_{t,i}^0 - \sum_{r\in I_t} Q_{min,i}\cdot\iota_{1,t,i}^r\cdot\Pi_r^* \\
& -\sum_{r\in I_t} Q_{min,i}\cdot\iota_{2,t,i}^r\cdot\Psi_{r,i}^* + Q_{max,i}\cdot\zeta_{t,i}^0 + \sum_{r\in I_t} Q_{max,i}\cdot\zeta_{1,t,i}^r\cdot\Pi_r^* \\
& +\sum_{r\in I_t} Q_{max,i}\cdot\zeta_{2,t,i}^r\cdot\Psi_{r,i}^* + M_{max,i}\cdot\nu_{t,i}^0 \\
& +\sum_{r\in I_t} M_{max,i}\cdot\nu_{1,t,i}^r\cdot\Pi_r^* + \sum_{r\in I_t} M_{max,i}\cdot\nu_{2,t,i}^r\cdot\Psi_{r,i}^* - M_{0,i}\cdot\nu_{t,i}^0 \\
& -\sum_{r\in I_t} M_{0,i}\cdot\nu_{1,t,i}^r\cdot\Pi_r^* - \sum_{r\in I_t} M_{0,i}\cdot\nu_{2,t,i}^r\cdot\Psi_{r,i}^* \\
& -\sum_{s\in I_t}\Psi_{s,i}^*\cdot\nu_{t,i}^0 - \sum_{s\in I_t}\sum_{r\in I_t}\nu_{1,t,i}^r\cdot\Psi_{s,i}^*\cdot\Pi_r^* - \sum_{s\in I_t}\sum_{r\in I_t}\nu_{1,t,i}^r\cdot C_{s,r}^{\Pi,\Psi} \\
& -\sum_{s\in I_t}\sum_{r\in I_t}\nu_{2,t,i}^r\cdot\Psi_{s,i}^*\cdot\Psi_{r,i}^* - \sum_{s\in I_t}\sum_{r\in I_t}\nu_{2,t,i}^r\cdot C_{s,r}^{\Psi,\Psi} \\
& -M_{min,i}\cdot\mu_{t,i}^0 - \sum_{r\in I_t} M_{min,i}\cdot\mu_{1,t,i}^r\cdot\Pi_r^* - \sum_{r\in I_t} M_{min,i}\cdot\mu_{2,t,i}^r\cdot\Psi_{r,i}^* \\
& +M_{0,i}\cdot\mu_{t,i}^0 + \sum_{r\in I_t} M_{0,i}\cdot\mu_{1,t,i}^r\cdot\Pi_r^* + \sum_{r\in I_t} M_{0,i}\mu_{2,t,i}^r\cdot\Psi_{r,i}^* \\
& +\sum_{s\in I_t}\Psi_{s,i}^*\cdot\mu_{t,i}^0 + \sum_{s\in I_t}\sum_{r\in I_t}\mu_{1,t,i}^r\cdot\Psi_{s,i}^*\cdot\Pi_r^* + \sum_{s\in I_t}\sum_{r\in I_t}\mu_{1,t,i}^r\cdot C_{s,r}^{\Pi,\Psi} \\
& +\sum_{s\in I_t}\sum_{r\in I_t}\mu_{2,t,i}^r\cdot\Psi_{s,i}^*\cdot\Psi_{r,i}^* + \sum_{s\in I_t}\sum_{r\in I_t}\mu_{2,t,i}^r\cdot C_{s,r}^{\Psi,\Psi}\Bigg]
\end{aligned} \tag{7.2.11}$$

$$\begin{aligned}
\iota_{t,i}^0 + \sum_{r\in I_t}\iota_{1,t,i}^r\cdot\Pi_r - \theta^{\Pi}\cdot\sum_{r\in I_t} l_{1,t,i}^r\cdot\Pi_r + \sum_{r\in I_t}\iota_{2,t,i}^r\cdot\Psi_{r,i} \\
-\theta^{\Psi}\cdot\sum_{r\in I_t} l_{2,t,i}^r\cdot\Psi_{r,i} \geq 0, \quad \forall t\in T,\ \forall i\in I
\end{aligned} \tag{7.2.12}$$

$$\begin{aligned}
\zeta_{t,i}^0 + \sum_{r\in I_t}\zeta_{1,t,i}^r\cdot\Pi_r - \theta^{\Pi}\cdot\sum_{r\in I_t} c_{1,t,i}^r\cdot\Pi_r + \sum_{r\in I_t}\zeta_{2,t,i}^r\cdot\Psi_{r,i} \\
-\theta^{\Psi}\cdot\sum_{r\in I_t} c_{2,t,i}^r\cdot\Psi_{r,i} \geq 0, \quad \forall t\in T,\ \forall i\in I
\end{aligned} \tag{7.2.13}$$

$$\begin{aligned}
\nu_{t,i}^0 + \sum_{r\in I_t}\nu_{1,t,i}^r\cdot\Pi_r - \theta^{\Pi}\cdot\sum_{r\in I_t} \upsilon_{1,t,i}^r\cdot\Pi_r + \sum_{r\in I_t}\nu_{2,t,i}^r\cdot\Psi_{r,i} \\
-\theta^{\Psi}\cdot\sum_{r\in I_t} \upsilon_{2,t,i}^r\cdot\Psi_{r,i} \geq 0, \quad \forall t\in T,\ \forall i\in I
\end{aligned} \tag{7.2.14}$$

$$\mu^0_{t,i} + \sum_{r\in I_t} \mu^r_{1,t,i} \cdot \Pi_r - \theta^\Pi \cdot \sum_{r\in I_t} u^r_{1,t,i} \cdot \Pi_r + \sum_{r\in I_t} \mu^r_{2,t,i} \cdot \Psi_{r,i} - \theta^\Psi \cdot \sum_{r\in I_t} u^r_{2,t,i} \cdot \Psi_{r,i} \geq 0, \quad \forall t \in T,\ \forall i \in I \tag{7.2.15}$$

$$\begin{aligned}
&-\iota^0_{t,i} - \sum_{r\in I_t} \iota^r_{1,t,i} \cdot \Pi_r - \theta^\Pi \cdot \sum_{r\in I_t} l^r_{1,t,i} \cdot \Pi_r - \sum_{r\in I_t} \iota^r_{2,t,i} \cdot \Psi_{r,i} \\
&-\theta^\Psi \cdot \sum_{r\in I_t} l^r_{2,t,i} \cdot \Psi_{r,i} + \zeta^0_{t,i} + \sum_{r\in I_t} \zeta^r_{1,t,i} \cdot \Pi_r - \theta^\Pi \cdot \sum_{r\in I_t} c^r_{1,t,i} \cdot \Pi_r \\
&+\sum_{r\in I_t} \zeta^r_{2,t,i} \cdot \Psi_{r,i} - \theta^\Psi \cdot \sum_{r\in I_t} c^r_{2,t,i} \cdot \Psi_{r,i} + \sum_{s=t}^{T} \sum_{j=i}^{I} \sigma_{j,i} \cdot \nu^0_{s,j} \\
&+\sum_{s=t}^{T} \sum_{j=i}^{I} \sum_{r\in I_s} \sigma_{j,i} \cdot \nu^r_{1,s,j} \cdot \Pi_r - \theta^\Pi \sum_{s=t}^{T} \sum_{j=i}^{I} \sum_{r\in I_s} \sigma_{j,i} \cdot \upsilon^r_{1,s,j} \cdot \Pi_r \\
&+\sum_{s=t}^{T} \sum_{j=i}^{I} \sum_{r\in I_s} \sigma_{j,i} \cdot \nu^r_{2,s,j} \cdot \Psi_{r,j} - \theta^\Psi \cdot \sum_{s=t}^{T} \sum_{j=i}^{I} \sum_{r\in I_s} \sigma_{j,i} \cdot \upsilon^r_{2,s,j} \cdot \Psi_{r,j} \\
&-\sum_{s=t}^{T} \nu^0_{s,i} - \sum_{s=t}^{T} \sum_{r\in I_s} \nu^r_{1,s,i} \cdot \Pi_r - \theta^\Pi \cdot \sum_{s=t}^{T} \sum_{r\in I_s} \upsilon^r_{1,s,i} \cdot \Pi_r \\
&-\sum_{s=t}^{T} \sum_{r\in I_s} \nu^r_{2,s,i} \cdot \Psi_{r,i} - \theta^\Psi \cdot \sum_{s=t}^{T} \sum_{r\in I_s} \upsilon^r_{2,s,i} \cdot \Psi_{r,i} - \sum_{s=t}^{T} \sum_{j=i}^{I} \sigma_{j,i} \cdot \mu^0_{s,j} \\
&-\sum_{s=t}^{T} \sum_{j=i}^{I} \sum_{r\in I_s} \sigma_{j,i} \cdot \mu^r_{1,s,j} \cdot \Pi_r - \theta^\Pi \cdot \sum_{s=t}^{T} \sum_{j=1}^{I} \sum_{r\in I_s} \sigma_{j,i} \cdot u^r_{1,s,j} \cdot \Pi_r \\
&-\sum_{s=t}^{T} \sum_{j=i}^{I} \sum_{r\in I_s} \sigma_{j,i} \cdot \mu^r_{2,s,j} \cdot \Psi_{r,j} - \theta^\Psi \cdot \sum_{s=t}^{T} \sum_{j=1}^{I} \sum_{r\in I_s} \sigma_{j,i} \cdot u^r_{2,s,j} \cdot \Psi_{r,j} \\
&+\sum_{s=t}^{T} \mu^0_{s,i} + \sum_{s=t}^{T} \sum_{r\in I_s} \mu^r_{1,s,i} \cdot \Pi_r - \theta^\Pi \cdot \sum_{s=t}^{T} \mu^0_{s,i} + \sum_{s=t}^{T} \sum_{r\in I_s} u^r_{1,s,i} \cdot \Pi_r \\
&+\sum_{s=t}^{T} \sum_{r\in I_s} \mu^r_{2,s,i} \cdot \Psi_{r,i} - \theta^\Psi \cdot \sum_{s=t}^{T} \sum_{r\in I_s} u^r_{2,s,i} \cdot \Psi_{r,i} \\
&\geq \frac{1}{(1+R)^t} \cdot (\Pi^*_t + \theta^\Pi \cdot \Pi^*_t), \quad \forall t \in T,\ \forall i \in I
\end{aligned} \tag{7.2.16}$$

$$
\begin{aligned}
&\sum_{s=t}^{T}\sum_{j=i}^{I}\sigma_{j,i}\cdot\nu_{s,j}^{0}+\sum_{s=t}^{T}\sum_{j=i}^{I}\sum_{r\in I_s}\sigma_{j,i}\cdot\nu_{1,s,j}^{r}\cdot\Pi_r\\
&-\theta^{\Pi}\cdot\sum_{s=t}^{T}\sum_{j=i}^{I}\sum_{r\in I_s}\sigma_{j,i}\cdot v_{1,s,j}^{r}\cdot\Pi_r+\sum_{s=t}^{T}\sum_{j=i}^{I}\sum_{r\in I_s}\sigma_{j,i}\cdot\nu_{2,s,j}^{r}\cdot\Psi_{r,j}\\
&-\theta^{\Psi}\cdot\sum_{s=t}^{T}\sum_{j=i}^{I}\sum_{r\in I_s}\sigma_{j,i}\cdot v_{2,s,j}^{r}\cdot\Psi_{r,j}-\sum_{s=t}^{T}\sum_{j=1}^{i}\sigma_{i,j}\cdot\nu_{s,i}^{0}\\
&-\sum_{s=t}^{T}\sum_{j=1}^{i}\sum_{r\in I_s}\sigma_{i,j}\cdot\nu_{1,s,i}^{r}\cdot\Pi_r-\theta^{\Pi}\cdot\sum_{s=t}^{T}\sum_{j=1}^{i}\sum_{r\in I_s}\sigma_{i,j}\cdot v_{1,s,i}^{r}\cdot\Pi_r\\
&-\sum_{s=t}^{T}\sum_{j=1}^{i}\sum_{r\in I_s}\sigma_{i,j}\cdot\nu_{2,s,i}^{r}\cdot\Psi_{r,i}-\theta^{\Psi}\cdot\sum_{s=t}^{T}\sum_{j=1}^{i}\sum_{r\in I_s}\sigma_{i,j}\cdot v_{2,s,i}^{r}\cdot\Psi_{r,i}\\
&-\sum_{s=t}^{T}\sum_{j=i}^{I}\sigma_{j,i}\cdot\mu_{s,j}^{0}-\sum_{s=t}^{T}\sum_{j=i}^{I}\sum_{r\in I_s}\sigma_{j,i}\cdot\mu_{1,s,j}^{r}\cdot\Pi_r\\
&-\theta^{\Pi}\cdot\sum_{s=t}^{T}\sum_{j=i}^{I}\sum_{r\in I_s}\sigma_{j,i}\cdot u_{1,s,j}^{r}\cdot\Pi_r-\sum_{s=t}^{T}\sum_{j=i}^{I}\sum_{r\in I_s}\sigma_{j,i}\cdot\mu_{2,s,j}^{r}\cdot\Psi_{r,j}\\
&-\theta^{\Psi}\cdot\sum_{s=t}^{T}\sum_{j=i}^{I}\sum_{r\in I_s}\sigma_{j,i}\cdot u_{2,s,j}^{r}\cdot\Psi_{r,j}+\sum_{s=t}^{T}\sum_{j=1}^{i}\sigma_{i,j}\cdot\mu_{s,i}^{0}\\
&+\sum_{s=t}^{T}\sum_{j=1}^{i}\sum_{r\in I_s}\sigma_{i,j}\cdot\mu_{1,s,i}^{r}\cdot\Pi_r-\theta^{\Pi}\cdot\sum_{s=t}^{T}\sum_{j=1}^{i}\sum_{r\in I_s}\sigma_{i,j}\cdot u_{1,s,i}^{r}\cdot\Pi_r\\
&+\sum_{s=t}^{T}\sum_{j=1}^{i}\sum_{r\in I_s}\sigma_{i,j}\cdot\mu_{2,s,i}^{r}\cdot\Psi_{r,i}-\theta^{\Psi}\sum_{s=t}^{T}\sum_{j=1}^{i}\sum_{r\in I_s}\sigma_{i,j}\cdot u_{2,s,i}^{r}\cdot\Psi_{r,i}\\
&\geq 0,\quad \forall t\in T,\ \forall i\in I,\ \forall j\in I
\end{aligned}
\tag{7.2.17}
$$

$$
\begin{aligned}
&-\sum_{s=t}^{T}\nu_{s,i}^{0}-\sum_{s=t}^{T}\sum_{r\in I_s}\nu_{1,s,i}^{r}\cdot\Pi_r-\theta^{\Pi}\cdot\sum_{s=t}^{T}\sum_{r\in I_s}v_{1,s,i}^{r}\cdot\Pi_r\\
&-\sum_{s=t}^{T}\sum_{r\in I_s}\nu_{2,s,i}^{r}\cdot\Psi_{r,i}-\theta^{\Psi}\cdot\sum_{s=t}^{T}\sum_{r\in I_s}v_{2,s,i}^{r}\cdot\Psi_{r,i}+\sum_{s=t}^{T}\mu_{s,i}^{0}\\
&+\sum_{s=t}^{T}\sum_{r\in I_s}\mu_{1,s,i}^{r}\cdot\Pi_r-\theta^{\Pi}\cdot\sum_{s=t}^{T}\sum_{r\in I_s}u_{1,s,i}^{r}\cdot\Pi_r+\sum_{s=t}^{T}\sum_{r\in I_s}\mu_{2,s,i}^{r}\cdot\Psi_{r,i}\\
&-\theta^{\Psi}\cdot\sum_{s=t}^{T}\sum_{r\in I_s}u_{2,s,i}^{r}\cdot\Psi_{r,i}\geq 0,\quad \forall t\in T,\ \forall i\in I
\end{aligned}
\tag{7.2.18}
$$

$$
-l_{t,i}^{r}\leq\iota_{t,i}^{r}\leq l_{t,i}^{r},\quad l_{t,i}^{r}=|\iota_{t,i}^{r}|,\quad 1\leq r\leq t\leq T,\ \forall i\in I
\tag{7.2.19}
$$

$$-c^r_{t,i} \leq \zeta^r_{t,i} \leq c^r_{t,i}, \quad c^r_{t,i} = |\zeta^r_{t,i}|, \quad 1 \leq r \leq t \leq T, \ \forall i \in I \tag{7.2.20}$$

$$-v^r_{t,i} \leq \nu^r_{t,i} \leq v^r_{t,i}, \quad v^r_{t,i} = |\nu^r_{t,i}|, \quad 1 \leq r \leq t \leq T, \ \forall i \in I \tag{7.2.21}$$

$$-u^r_{t,i} \leq \mu^r_{t,i} \leq u^r_{t,i}, \quad u^r_{t,i} = |\mu^r_{t,i}|, \quad 1 \leq r \leq t \leq T, \ \forall i \in I \tag{7.2.22}$$

7.3 Problem size

The dual LDR model presented in Section 7.2 is implemented and solved in Xpress MP. This model has four decision variables with dimension $T \times I$ and 16 decision variables with dimension $0.5 \times T \times T \times I$. The model has six constraints with dimension $T \times I$, one constraint with dimension $T \times I \times I$ and four constraints with dimension $0.5 \times T \times T \times I$. The problem size of the dual LDR model is presented in Table 7.3.1.

Table 7.3.1: Problem sizes for the dual LDR model.

Plant	# Variables	# Constraints
Plant 1 and 2	21 840	5 720
Plant 4	87 360	23 712
Plant 3	347 776	90 688

8 Analysis

This section starts with a presentation of the results from the primal LDR model. The analysis of these results will focus on how the reservoirs are managed in order to maximize the expected market value of production, and how the proposed reservoir management strategies relates to the properties of the hydropower plants. The following section presents the computational times of both the primal and the dual LDR model. This section will also investigate the complexity reduction introduced by the LDR approach and present the duality gaps for all the four hydropower plants for different uncertainty levels.

In order to demonstrate how the LDR model is intended to be used by the hydropower producers, and to compare the performance of the LDR model and the deterministic model, a ten years series simulation is performed for Plant 1. The results from this simulations is presented in Section 8.3. The main objective of long term scheduling is to initialise boundary conditions for the shorter term scheduling models. To illustrate how this can be done, water values at the end of the first week, as a function of the initial reservoir level, are presented in the following section. An approximate method for taking a variable head of water into account is presented in Section 8.5, before the main shortcomings of the approach taken in this thesis are presented in Section 8.6.

8.1 Results from the primal models

The deterministic model and the LDR model presented in Section 6.2 is implemented and solved in Xpress MP. As described in Section 6.2.2 the deterministic model assumes that price and inflow are fully known and equal to their expected values, while the LDR model assumes that price and inflow can drift around their expected values, varying within a given uncertainty set. In Sections 8.1.2 and 8.1.3, it will be shown that this causes the LDR model to provide more restrictive reservoir management strategies than the deterministic model. As a result, the expected profit given by the deterministic model is higher than the expected profit given by the LDR model. This result verifies that the LDR model behaves like it is intended to, but does not provide an correct representation of how the two models perform in relation to each other. For this reason, the profits are only presented for Plant 1 and 2. In reality, the actual price and inflow deviate from their expected values, which will cause the LDR model to perform better than the deterministic model. This is verified through simulation, and will be elaborated in Section 8.3.

Figures depicting the reservoir management strategies given by the deterministic model and the LDR model are presented for all plants, while figures showing the corresponding production strategies can be found in Appendix D. All figures are operating with relative numbers, in which 1 corresponds to the maximum reservoir level. This is done in order not to reveal the identity of the hydropower producers.

For all plants the uncertainty levels of price and inflow are assumed to be equal and constant in all time periods. In reality, there is higher uncertainty related to some periods of the year than others, which could have been incorporated in the model. However, constant uncertainty levels are used because a thorough analysis of historical uncertainty levels has not been performed in this thesis. For this reason, there is lack of basis for determining neither how high the uncertainty levels for price and inflow are compared to each other, nor how the uncertainty relates to different time periods.

8.1.1 Reservoir management

Due to uncertainty in the future amount of inflow, hydropower producers faces the risk of spillage at high reservoir levels, and the risk of emptying the reservoir too early in the winter. Spillage will result in a loss of water, while emptying the reservoir too early may result in a lost opportunity to produce at high prices. Both situations will result in lost profits, and producers aim to avoid them when deciding their long term reservoir management strategy. As the uncertainty in the future amount of inflow increases, the risk that one or both of these situations will occur increases. This gives the producers an incentive to operate the reservoirs more restrictively when the uncertainty is high, i.e. to avoid filling or emptying the reservoirs to its boundaries. As a consequence, the producers flexibility in choosing when to produce will decrease with increasing uncertainty.

The realisations of price and inflow are uncertain when running the LDR model forward in time, and the constraints are defined to hold for all possible realisations of price and inflow within a given uncertainty set. Increasing the uncertainty level will cause the constraints to tighten as they have to hold for a larger range of outcomes. As a consequence, the feasible region for the production variables decreases. In other words, the flexibility in choosing a strategy that will keep the reservoir within its upper and lower limits regardless of which price and inflow outcome that occurs, decreases.

Due to the decision rule, Eq. (6.2.14) in Section 6.2.4, the LDR model allows for adjustment of production based on the realisations of price and inflow. The production variables can take values that allow for adjustment to a greater or lesser extent[19]. A high degree of adjustment will cause a larger difference between the highest possible and the lowest possible production than a low degree of adjustment[20]. This will in turn cause a larger gap between the highest

[19]If q_t represents production and $q_t = \delta_t^0 + \sum_{r=1}^{t} \Pi_r \cdot \delta_t^r + \sum_{r=1}^{t} \Psi_r \cdot \gamma_t^r$, high values on δ_t^r and γ_t^r compared to δ_t^0 will cause a high degree of adjustment, while the opposite will cause a low degree of adjustment. If both δ_t^r and γ_t^r equal zero, production will neither depend on realised price nor on realised inflow.

[20]For zero degree of adjustment, the highest possible production will equal the lowest possible production.

possible and the lowest possible reservoir level. This can be explained by the fact that the lowest possible reservoir level corresponds to the case of the highest possible production, while the highest possible reservoir level corresponds to the case of the lowest possible production, see Section 6.2.4. Moreover, a high degree of adjustment will cause the gap to increase more at increasing uncertainty level. As a result, a higher degree of adjustment is possible without causing infeasibility when the uncertainty level is low than when the uncertainty level is high.

At a certain uncertainty level there will only be one scheduling strategy that satisfies both the maximum and the minimum reservoir level constraints, Eq. (6.2.20) and (6.2.21) in Section 6.2.4. Production, discharge and spillage will thus be the same for all realisations of price and inflow, i.e. the decisions can not be adjusted based on the realisations of the two parameters. At this uncertainty level, a point at which the lowest possible reservoir level equals the minimum reservoir limit and the highest possible reservoir level equals the maximum reservoir limit, will be reached. If this uncertainty level is exceeded, either higher production, discharge or spillage must be scheduled in order for the maximum reservoir constraint to hold. However, if production, discharge or spillage increases, the minimum reservoir constraint will be violated.

The highest uncertainty level for which the model is still feasible depends on the flexibility of the hydropower plant and on the length of the scheduling horizon considered. As described in Section 3.1, high flexibility entails more options regarding when to discharge the available water than low flexibility. This means that water can be stored during the summer when prices are low, and produced during the winter when prices are high. At low flexibility there are few possible strategies making it possible to avoid both spillage and emptying the reservoir when prices are still high. This will make it necessary to produce at low prices instead of saving water for production in the high price periods. As mentioned in the above paragraphs, increasing the uncertainty level will reduce the flexibility in choosing when to produce further, and eventually make it impossible to find a reservoir management strategy that will hold for all realisations of price and inflow within the uncertainty set.

The difference between the total amounts of inflow in the highest and the lowest inflow outcomes increases for each time period of the scheduling horizon. When the length of the scheduling horizon increases, the feasible solution space will thus decrease. This will in turn lead to a decrease in the highest uncertainty level for which the model is still feasible. In reality, a situation in which either the highest or the lowest possible inflow outcome occurs in each period of the scheduling horizon is not realistic. In order to avoid these situations, restrictions on the total inflow from all time periods could have been introduced. This will be elaborated in Section 8.6.

8.1.2 Results from the aggregated reservoir models

As mentioned in Sections 3.2.2 and 3.2.3, only aggregated inflow data is available for Plant 1 and 2. For this reason, the aggregated reservoir model presented in Appendix B is used for these plants. Both of the plants have one power station and several reservoirs, of which the lowest reservoir is considerably lager than the others. Due to these topologies, the aggregated reservoir model is assumed to provide acceptable results for both plants. A scheduling horizon of 52 weeks is used for both plants.

Plant 2 is characterised by a low degree of regulation and a high load factor, i.e. the production capacity is low compared to both the size of the reservoir and the expected amount of inflow. This implies that the reservoir fills up quickly, and a large amount of the total production has to take place in low price periods in order to avoid the risk of spillage. In other words, the flexibility in choosing when to produce is low. Plant 1 has a higher degree of regulation and a lower load factor than Plant 2, which implies that this plant is more flexible in choosing when to produce.

The results from the LDR model show that the expected levels to which the reservoir of both plants are filled decreases at increasing uncertainty level, see Figures 8.1.1 and 8.1.2. This can be explained by the increased risk of spillage, and implies that the available water is discharged at lower prices when the uncertainty is high than when the uncertainty is low. As a result, the profit decreases at increasing uncertainty level, which can be seen in Table 8.1.1. Due to the low flexibility of Plant 2, the reservoir management strategies for the different uncertainty levels are relatively similar, which implies small differences in profit for this plant.

The reservoir management strategies given by the deterministic model causes the reservoirs of both plants to empty completely at the end of the scheduling horizon. However, none of the expected scheduling strategies given by the LDR model will cause the expected reservoir level to reach its lower limit at any point, see Figures 8.1.1 and 8.1.2. This is due to the fact that the minimum reservoir constraints have to hold for lowest possible reservoir level, shown in Figures 8.1.3 and 8.1.4[21]. Increasing production in the last scheduling periods will thus cause negative reservoir levels if the lowest possible reservoir level occurs, which is obviously not possible. The restrictive strategies given by the LDR model causes the expected profit to be lower than the profit given by the deterministic model, which can be seen in Table 8.1.1[22].

[21] Figures are only provided for Plant 1. Similar figures for Plant 2 can be found in Appendix D.

[22] As mentioned in Section 1, these profits apply for the case in which the realised price and inflow equals their expected values. In reality, the realisations will deviate from the expected values which will cause the LDR model to perform better than the deterministic model, see Section 8.3.

Table 8.1.1: Expected profits obtained from the LDR model in percentage of the profit given by the deterministic model.

Uncertainty level	5 %	10 %	15 %	20 %	30 %
Profit Plant 1 [%]	94	89	-	84.9	73.2
Profit Plant 2 [%]	83.04	83.02	82.51	-	-

In the case of 30 % and 15 % uncertainty for Plant 1 and 2, respectively, there is only one scheduling strategy that ensures feasibility regardless of the realisations of price and inflow within the uncertainty set. The maximum feasible uncertainty level of Plant 1 exceeds the maximum level of Plant 2 because this plant has higher flexibility in choosing when to produce.

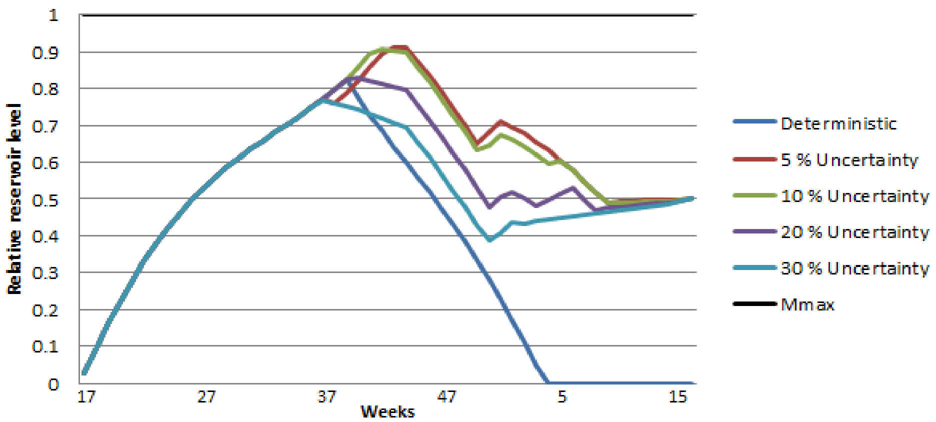

Figure 8.1.1: Relative expected reservoir levels for Plant 1.

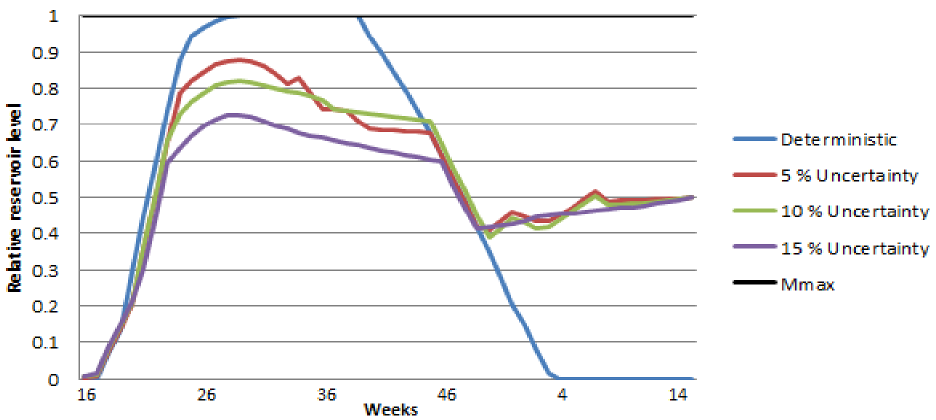

Figure 8.1.2: Relative expected reservoir levels for Plant 2.

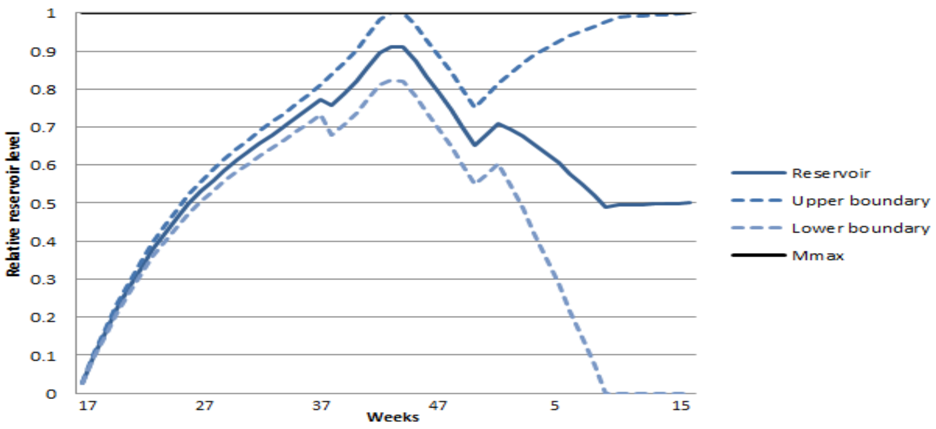

Figure 8.1.3: The figure show the lowest possible, the expected and the highest possible reservoir level for an uncertainty level of 5 % for Plant 1.

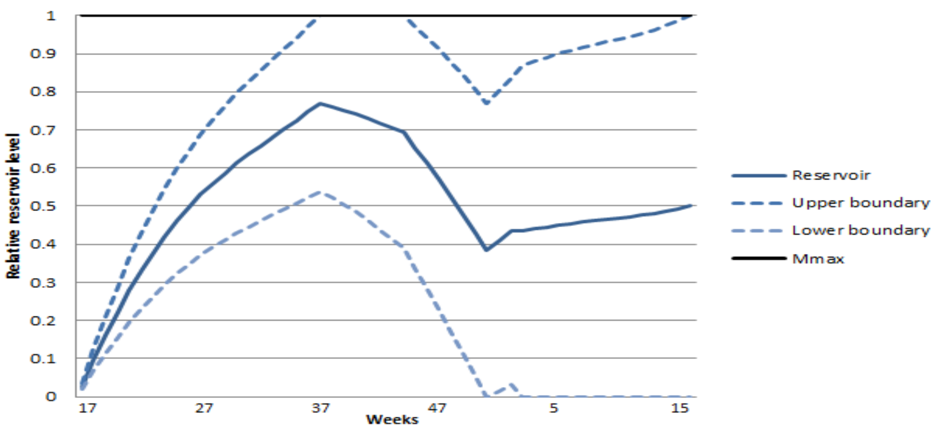

Figure 8.1.4: The figure show the lowest possible, the expected and the highest possible reservoir level for an uncertainty level of 30 % Plant 1.

8.1.3 Results from the multi-reservoir models

A scheduling horizon of 104 weeks is used for Plant 3, while 52 weeks is used for Plant 4. Power Station 1 in Plant 3 is characterised by a high degree of regulation, see Section 3.2.4. Regardless of the realisations of price and inflow, the storage capacity of the reservoir corresponding to this power station will never be fully utilised. The reservoir is filled to a level such that the minimum reservoir constraint will hold for all realisations of price and inflow in all time periods. As a result, the level to which the reservoir is filled increases with increasing uncertainty level, see Figure 8.1.5. Despite the fact that there is unused storage capacity, and more water potentially could have been stored for production in high price periods, the power station produces relatively evenly in all the other time periods, see Figure D.3.1 in Appendix D. The reason for this is that all the water used for power generation in Power Station 1 can be reused in Power Station 4. The reservoir associated with Power Station 4 is a run of river with no storage capacity and the power station has lower production capacity than Power Station 1. Spillage will therefore occur whenever the production at Power Station 1 is higher than the maximum capacity of Power Station 4.

Power Station 2 in Plant 3 has a relatively low degree of regulation and a high load factor compared to Power Station 1. This implies that the power station has to produce at maximum capacity during much of the year in order to avoid the risk of spillage. As can be seen from Figure 8.1.6, the level to which Reservoir 2 is filled decreases at increasing uncertainty level due to the increased risk of spillage. Since the reservoirs associated with Power Station 3 and 4 are run of rivers, they will produce the minimum of the amount of water that enters the power station and their production capacity in all weeks.

As can be seen from Figures 8.1.7 and 8.1.8, the reservoir management strategies for Power Stations 1 and 2 in Plant 4 are relatively similar to the strategies presented for Plant 3. All the water discharged from Reservoir 1 will enter Reservoir 2, and Reservoir 2 will therefore reach its highest level later than Reservoir 1. Due to the large amount of water that enters Reservoir 2, this power station produces at maximum capacity during most of the year, see Figure D.4.2 in Appendix D. The reservoirs associated with Power Station 3 and 4 are run of rivers, and will produce the minimum of the amount of water that enters the power station and their maximum production capacity in all weeks.

In the case of 15 % and 20 % uncertainty for Plant 1 and 2, respectively, there is only one scheduling strategy that will ensure feasibility regardless of the realisations of price and inflow. Due to the arguments provided in Section 8.1.1, it is assumed that the model would have remained feasible for a higher uncertainty level for Plant 3 if a scheduling horizon of one year had been used.

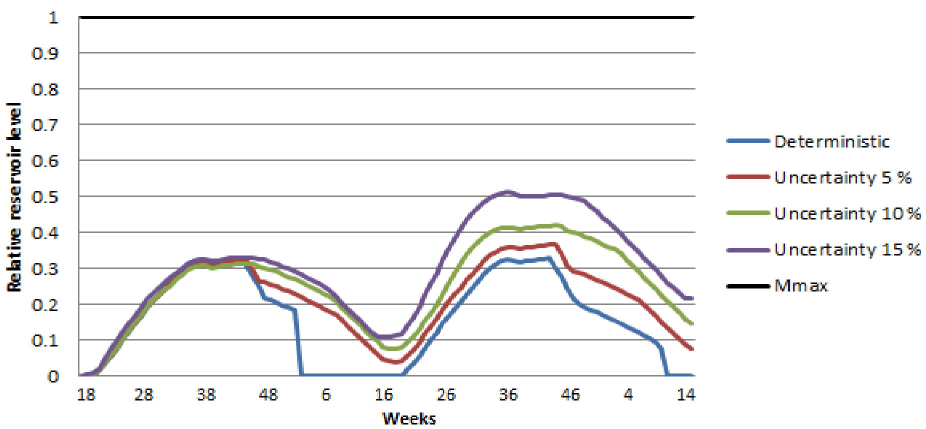

Figure 8.1.5: Relative expected reservoir levels for Reservoir 1 in Plant 3.

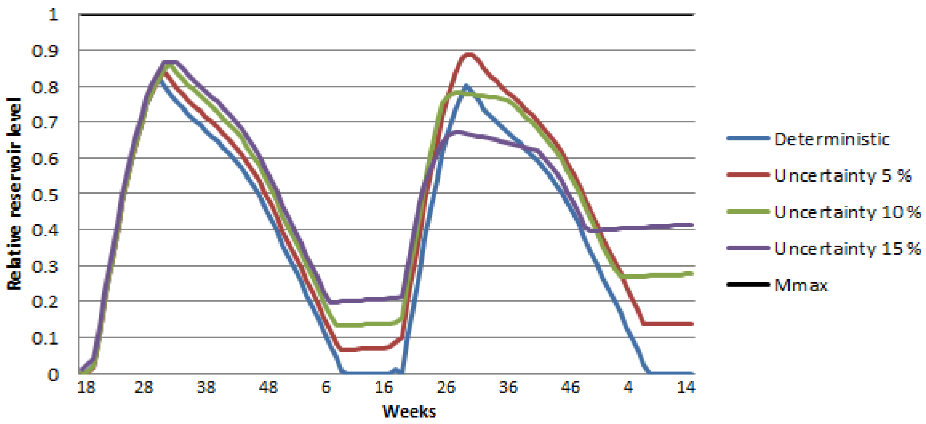

Figure 8.1.6: Relative expected reservoir levels for Reservoir 2 in Plant 3.

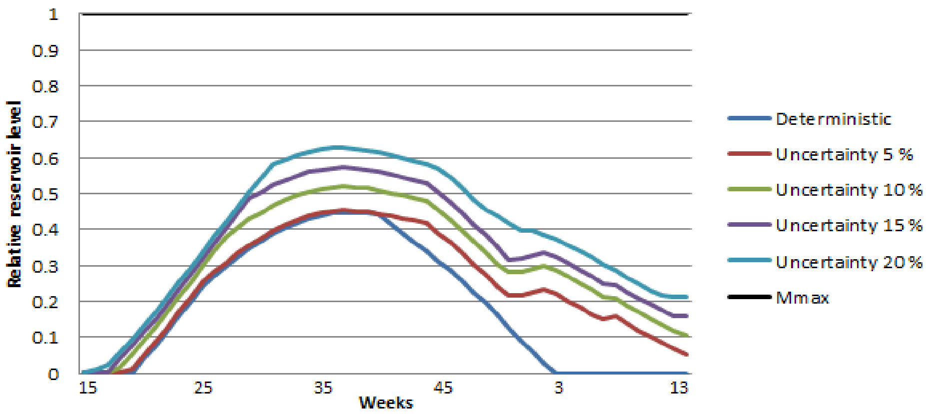

Figure 8.1.7: Relative expected reservoir levels for Reservoir 1 in Plant 4.

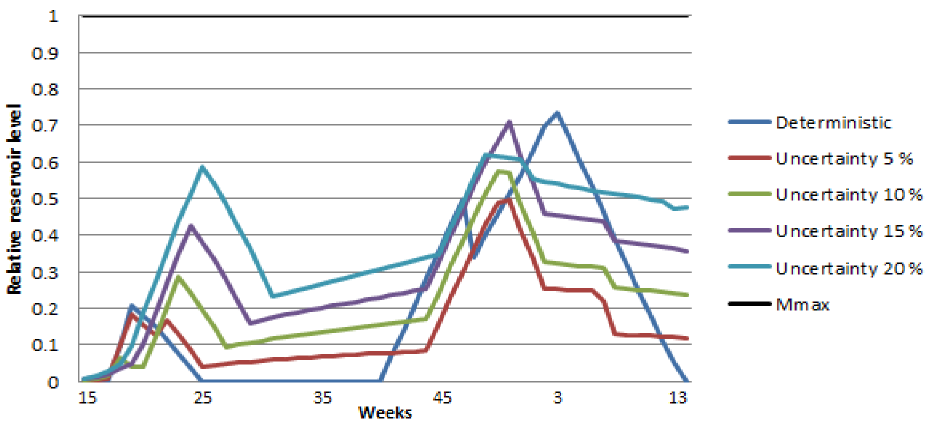

Figure 8.1.8: Relative expected reservoir levels for Reservoir 2 in Plant 4.

8.1.4 Uncertainty levels

Sections 8.1.2 and 8.1.3 present the maximum uncertainty levels for which the models are feasible. This level is limited by the uncertainty in inflow because the level of inflow affects the reservoir level directly, and will hence affect the feasibility of the maximum and minimum reservoir level constraints. The price determines which periods that are the most profitable for production, and will thus affect the reservoir levels indirectly. However, the price will only affect the scheduling strategy in situations in which the producer has flexibility in choosing when to produce. At low flexibility, the producer has little or no possibility to let the price affect the scheduling strategy. Increasing the uncertainty level of the price will therefore be of low or no significance for the feasibility of the model.

Looking at historical inflow data, there are several periods in which the realisations of price and inflow are not within the uncertainty sets defined by the maximum feasible uncertainty levels. However, none of the years in historical data sets have values that are either above or below the uncertainty set in all weeks. High values in some weeks tend to be balanced by low values in others. For this reason it is not considered as necessary to use an uncertainty level covering all historical realisations of price and inflow.

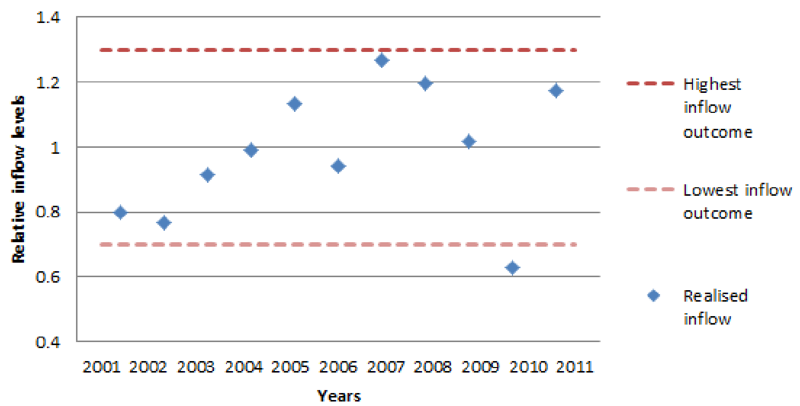

Figure 8.1.9: The scatter points corresponds to the total annual inflow for Plant 1 in the years 2001-2011. The dotted lines corresponds to the total annual inflow if the highest and the lowest inflow outcomes occur in all periods. The lines apply for an uncertainty level of 30 %.

When evaluating which uncertainty level to use, it is interesting to look at the range of the historical total annual inflow levels. Figure 8.1.9 shows that the realised total annual inflow for Plant 1 is between the total annual inflow corresponding to the lowest and highest inflow outcomes for an uncertainty level of 30 % in all the years 2001 to 2011, except for 2010. This is the maximum feasible uncertainty level for Plant 1. From Figure 8.1.10 it can also be seen that the average inflow for these years is between the highest and lowest inflow outcomes in almost all weeks. Similar results are found for the three other plants for their respective maximum feasible levels. Based on these findings, an uncertainty level of 30 % is considered necessary for Plant 1 in order for the uncertainty set to cover both wet years and dry years. However, taking into account that both these extremes may occur will cause extremely restrictive scheduling strategies. It will in Section 8.3 be proven that an uncertainty level of 10 % would have given the highest profits for Plant 1 in the years 2002 to 2012.

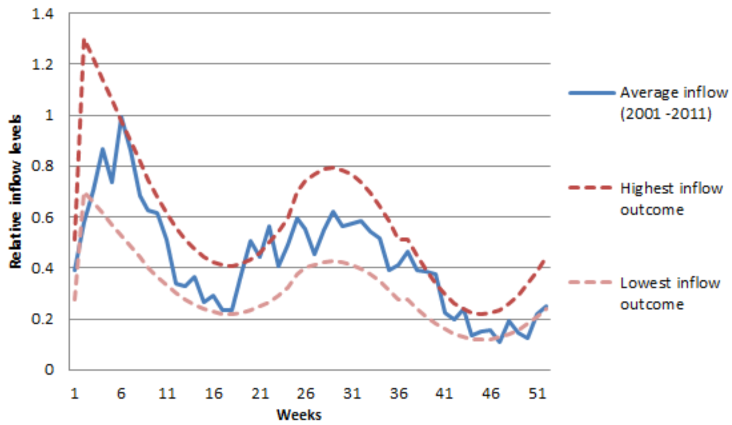

Figure 8.1.10: The solid line corresponds to average inflow for Plant 1 in the years 2001-2011, while the dotted lines corresponds to the highest and the lowest inflow outcomes in all periods. The lines apply for an uncertainty level of 30 %.

8.2 Computational times and complexity reduction

As described in Section 1, the size of the stochastic models often used to solve long term hydropower scheduling problems grow exponentially with the number of time stages or state variables, and the problems may become computationally intractable. The LDR model grows only polynomially with the number of time stages and enables scalability to multistage models.

Table 8.2.1: The table presents the computational times of the primal and dual LDR models.

Number of time stages	52	104
Primal model with I=1 [s]	4.0	119.4
Dual model with I=1 [s]	3.0	90.8
Primal model with I=4 [s]	10.7	268.1
Dual model with I=4 [s]	36.8	1428.1

The results presented in Table 8.2.1 shows that both the primal and the dual LDR models have short computational times. This is one of the most important properties of the LDR model, and an important argument for using this approach for long term hydropower scheduling. Due to the short computational times, the approach introduces the opportunity to rerun the model whenever new information is available. The long term scheduling model can, for instance, be rerun whenever a shorter term scheduling model is run, within an acceptable time frame. As a result the LDR model is able to provide updated boundary conditions to shorter term scheduling models more frequently than models with longer computational times.

As described in Section 1, LDR are very effective at reducing computational complexity, but may incur a considerable loss of optimality. Hence, the solution of the LDR model is expected to deviate somewhat from the solution of the exact problem. The duality gap, explained in Section 7.1, measures how large this loss of optimality is.

Table 8.2.2: Duality gaps for all the hydropower plants.

Uncertainty level	5 %	10 %	15 %	20 %	30 %
Plant 1 [%]	8	17	-	32	44
Plant 2 [%]	21	24	31	-	-
Plant 3 [%]	20	36	58	-	-
Plant 4 [%]	11	24	32	54	-

The results presented in Table 8.2.2 show that the duality gap increases with increasing uncertainty levels. The gaps for Plant 1, 2 and 4 are relatively similar, while Plant 3 stands out with higher duality gaps. The high gaps can be explained by the scheduling horizon of two years used for this plant. The gaps for all plants are relatively large, but taken into account that the uncertainty level for price and inflow applies in every time period and that these models are run once for T time periods, the results are considered as acceptable. If the models are rerun whenever new information is available, the duality gap is expected to decrease.

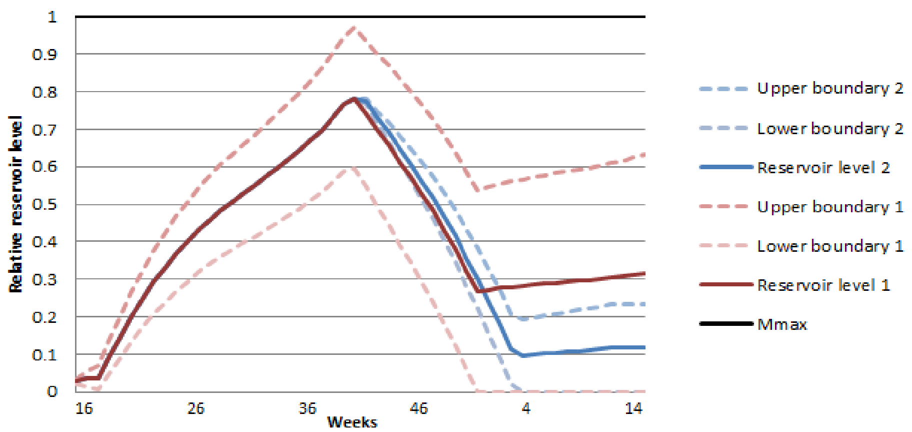

Figure 8.2.1: Illustration of a rerunning process.

Figure 8.2.1 illustrates a rerunning process where the LDR model is ran twice for Plant 2. The first run is at the start of week 16 and the second run is at the start of week 42. When the model is rerun, the reservoir level at the end of week 41 is used as input, and the model proposes a new reservoir management strategy for the rest of the scheduling period. As can be seen from this figure, the lowest possible and the highest possible reservoir levels for the second run lies between the corresponding reservoir levels for the first run. The gap at the end of the scheduling period is significantly smaller for second run than for the first run. This indicates that the rerunning process will lead to a more accurate solution for the scheduling problem. Rerunning the model every time new information is available is therefore assumed to cause lower duality gaps than those presented in Table 8.2.2. Based on the computational times and the duality gaps presented in this section the LDR approximation is considered to give an acceptable trade-off between tractability and accuracy for long term hydropower scheduling problems.

8.3 Simulations

In order to demonstrate how the hydropower producers can use the LDR model in practice, and to investigate how the LDR model performs compared to the deterministic model, simulations are performed[23]. A series of simulations over 10 years has been run for Plant 1, where the realisations of price and inflow equal the realised system prices and inflow to this plant from week 17 in 2002 to week 16 in 2012[24]. Plant 1 is arbitrarily chosen as the test plant for the simulations.

The models are run for 52 time periods, and rerun every fourth week, with a total of 130 runs. In reality, the model is intended to be rerun at least every week in order to be coupled to a shorter term model. However, it is assumed that rerunning the model every fourth week will provide a satisfactory basis for demonstrating how the LDR model is supposed to be used, and to compare the performance of the two models. At every rerun, the reservoir level at the end of the preceding four week period is used as the initial reservoir level for the next run. Expected price and inflow given by the price and inflow models presented in Section 4 are used as input[25]. The LDR model is run for uncertainty levels of 5 %, 10 % and 30 % in order to investigate which level that leads to the best performance.

Running the LDR model for the previously mentioned uncertainty levels will cause scheduling strategies that are feasible for all realisations of price and inflow within the defined uncertainty set. However, in some time periods the actual realisations of price and inflow are not within this uncertainty set. The simulation results show that this may cause an infeasible production strategy. In periods in which

[23]Ideally the LDR model should have been compared to a model that is currently used in practice instead of the deterministic model. A brief overview of these methods is given in Section 1. However, such a model has not been available for this thesis.

[24]System prices are used because local prices are not available on Nord Pool Spot for the entire simulation period.

[25]In order to get a more realistic forecast of the expected prices, forward prices could have been discounted and used as input. However, these data are not readily available, and have not been collected.

the actual realisations are higher than the upper limit of the uncertainty set, the calculated production may exceed the production capacity[26]. When the actual realisations are lower than the lower limit of the uncertainty set, production strategies resulting in negative reservoir levels may occur. In both cases the production has been adjusted manually in order to obtain a feasible strategy. It is assumed that this problem can be avoided or reduced by using better price and inflow forecasts, as this will cause less realisations of price and inflow outside the uncertainty set.

The profits obtained from the simulations are presented in Table 8.3.1. As can be seen from this table, the LDR model performs better than the deterministic model for all the uncertainty levels for which it is run. The highest profit is obtained at an uncertainty level of 10 %. The profits are therefore given in percentage of the profit for this uncertainty level. Table 8.3.2 presents the average prices obtained per produced and per released unit of water. The prices are obtained by dividing the total profit on the total production and on the sum of the total production and the total amount of spillage, respectively.

Table 8.3.1: Simulated profits given in percentage of the profit obtained at an uncertainty level of 10 %.

Uncertainty level	Deterministic	5 %	10 %	30 %
Profit [%]	96.1	99.6	100.0	98.0

Table 8.3.2: Average prices produced and released unit of water. The prices are given in $^{NOK}/_{MWh}$.

Uncertainty level	Deterministic	5 %	10 %	30 %
Av. price per produced MWh	323.1	334.9	333.7	323.9
Av. price per released MWh	317.4	327.4	328.9	320.0

The main reason why the LDR model performs better than the deterministic model is the ability to adjust production to the realisations of price and inflow. As explained in Section 8.1.1, the allowed degree of adjustment increases at decreasing uncertainty level. This implies that production is most adapted to the realisations of price and inflow at an uncertainty level of 5 %. This can be proven by the fact that the highest average price per produced unit of water is obtained at this uncertainty level, see Table 8.3.2. However, at this uncertainty level, the model does not take into account that the realised price and inflow can be more than 5 % higher or lower than expected. This causes more realisations outside the uncertainty set than for higher uncertainty levels, which leads to more periods of spillage and more periods at which the reservoir is empty at high prices. Taking spillage into account, the average price per released unit of water is lower for 5

[26] $q_t = \delta_t^0 + \sum_{r=1}^{t} \Pi_r \cdot \delta_t^r + \sum_{r=1}^{t} \Psi_r \cdot \gamma_t^r \nleq Q_{max}$, where q_t represents the calculated production and Π_r and Ψ_r represent realised price and inflow, respectively.

% than for 10 % uncertainty. At an uncertainty level of 10 % the production does not adapt to the realisations of price and inflow to the same extent as at uncertainty level of 5 %. However, the scheduling strategy for 10 % uncertainty causes less spillage and a higher total production. This gives a higher total profit and a higher average price per water unit released.

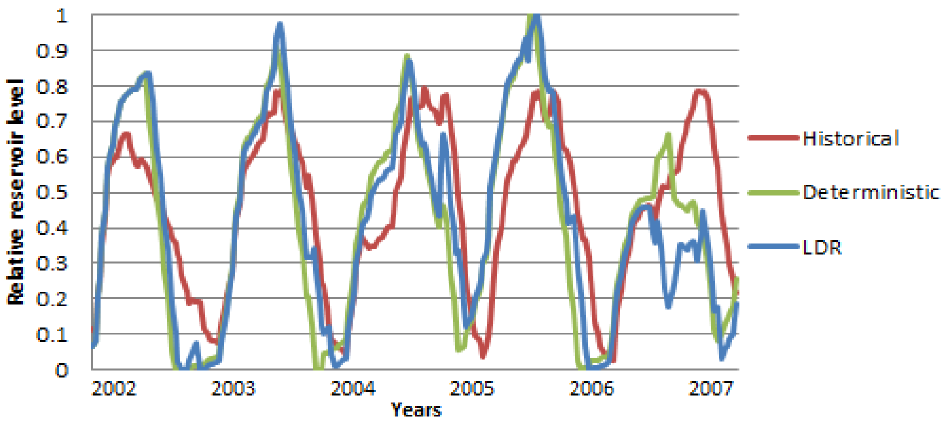

Figure 8.3.1: Relative reservoir levels for the years 2002-2007.

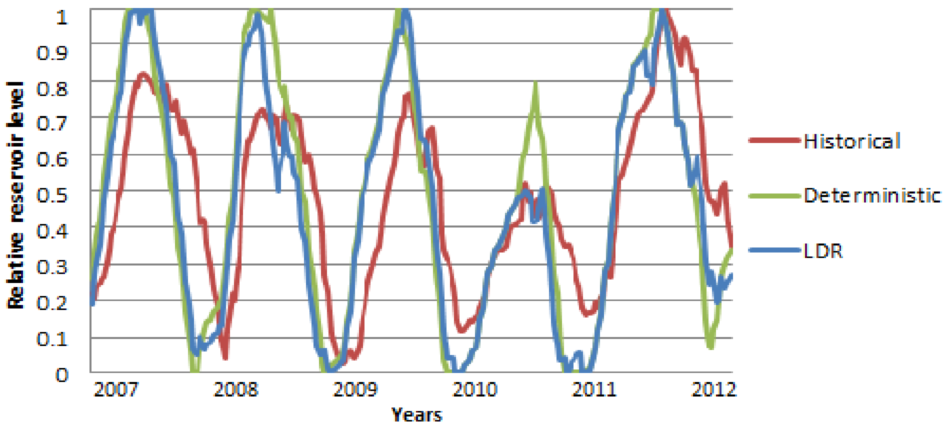

Figure 8.3.2: Relative reservoir levels for the years 2007-2012.

Figures 8.3.1 and 8.3.2 show the expected reservoir levels given by the LDR model for an uncertainty level of 10 %, the reservoir levels given by the deterministic model and the historical reservoir levels. As can be seen from these figures, the reservoir levels given by the LDR model fluctuate more from year to year and within the year than the reservoir levels given by the deterministic model. This is due to the fact that the LDR model adapts to variations in price and inflow, in contrast to the deterministic model. Moreover, since the LDR model takes into account that the realisations of price and inflow can be 10 % higher than expected, this model causes 24 % less spillage than the deterministic model.

The strategy given by the LDR model causes the reservoir to be filled and emptied closer to its boundaries compared to the historical reservoir levels. This leads to higher reservoir levels when the expected prices are high and potentially higher profits. However, this strategy involves a higher risk of spillage and of emptying the reservoir when prices are still high. Information about reserve requirements, maintenance and shutdowns during the simulation period is not available, and is not taken into account when comparing the reservoir levels.

8.4 Water values

The LDR model is intended to be coupled to a shorter term model. As explained in Section 2.4, this coupling may take place through a fixed water value. It is assumed that the coupling will take place at the end of the first week of the scheduling period. Water values for different initial reservoir levels are found for Plant 2 to demonstrate how the long term model can be coupled to a shorter term model. Plant 2 is arbitrarily chosen as the test plant for the water value calculations.

The water values are found from the dual values of Eq. 6.4.2 in Section 6.4. In order to verify the results, the water values are also found by first running the model for a set of initial reservoir levels, and then running the model again adding one extra unit of water to the initial reservoir levels. The differences in profits with and without the extra unit of water express the water values for the different initial reservoir levels.

As described in Section 2.2, the water value expresses how much the profit increases by having one extra unit of water available in the reservoir. As long as there is production capacity available, the extra unit of water will be produced in the period causing the largest increase in profit. The water value will therefore equal the expected price of one MWh in this period. When the initial reservoir level increases, the flexibility in choosing which period to produce the extra unit of water decreases since the maximum production level is reached in more of the periods. As a result, the water value is a non increasing function of the initial reservoir level. This can be seen in Figures 8.4.1 and 8.4.2, which show the water value at the end of the first week as a function of the initial reservoir level for uncertainty levels of 15 % and 5 %, respectively.

When the initial reservoir level reaches 73 000 MWh and 113 000 MWh, for uncertainty levels of 15 % and 5 % respectively, the water value equals zero. At these initial reservoir levels, spillage will occur during the scheduling period. Adding one extra unit of water will therefore increase the amount of spilled water, and not cause any increase in profit. At increasing uncertainty levels of price and inflow, the risk of reaching the upper reservoir limit increases, and hence the risk of spillage increases. This is why the water value reaches zero at a lower initial reservoir level for 15 % uncertainty compared to 5 % uncertainty.

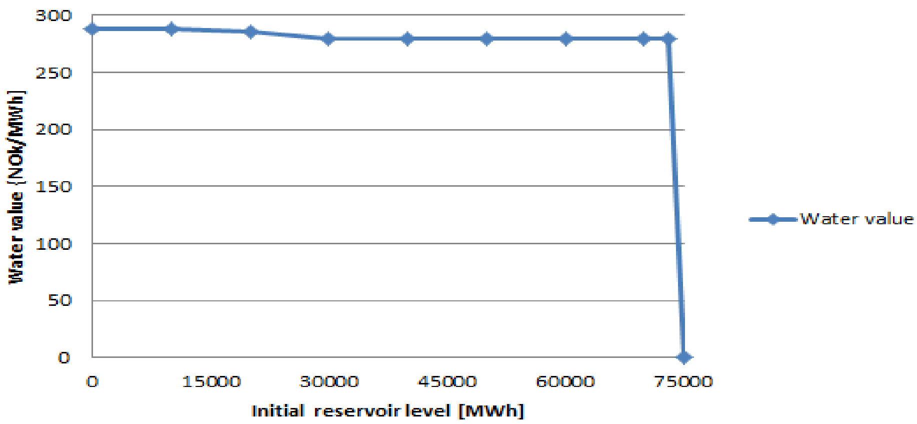

Figure 8.4.1: The water value at the end of week one as a function of the initial reservoir level for an uncertainty level of 15 %.

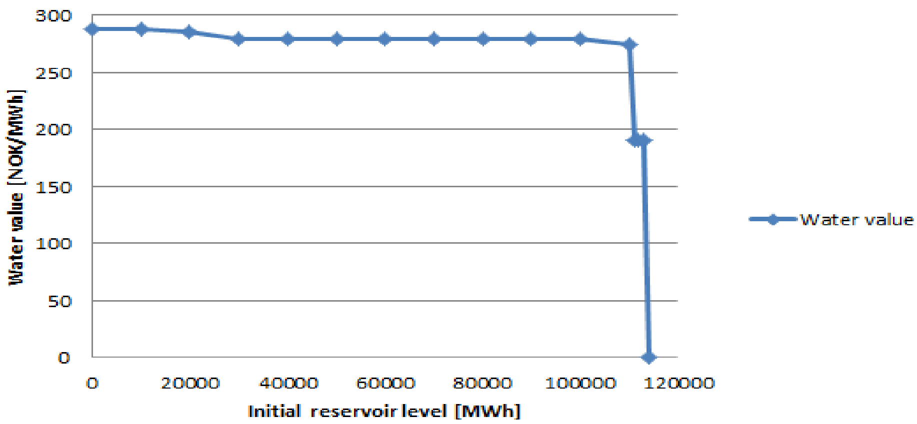

Figure 8.4.2: The water value at the end of week one as a function of the initial reservoir level for an uncertainty level of 5 %.

8.5 Head corrections

The models presented in this thesis can not deal with a variable head in an exact way, as the problem will become nonlinear and non convex. As a result the energy generated per amount of water is overestimated for low reservoir levels and underestimated for high reservoir levels. The approach outlined in Section 6.5 has been tested on one arbitrarily chosen plant, Plant 2, in order to see how corrections for a variable head will affect the reservoir management strategy. The reservoir of Plant 2 is assumed to be shaped like a cylinder.

Table 8.5.1: Increase in profit with head corrections.

Uncertainty level	5 %	10 %	15 %
Change in profit [%]	0.6	0.3	0.0

The percentage increase in profit when head corrections are included is presented in Table 8.5.1 for uncertainty levels of 5 %, 10 % and 15 %. Figures 8.5.1 and 8.5.2 show the expected reservoir levels with and without head corrections at uncertainty levels of 5 % and 10 %, respectively. For an uncertainty level of 15 % the graphs representing the reservoir level with and without head corrections overlap completely, and a figure is therefore not included for this uncertainty level.

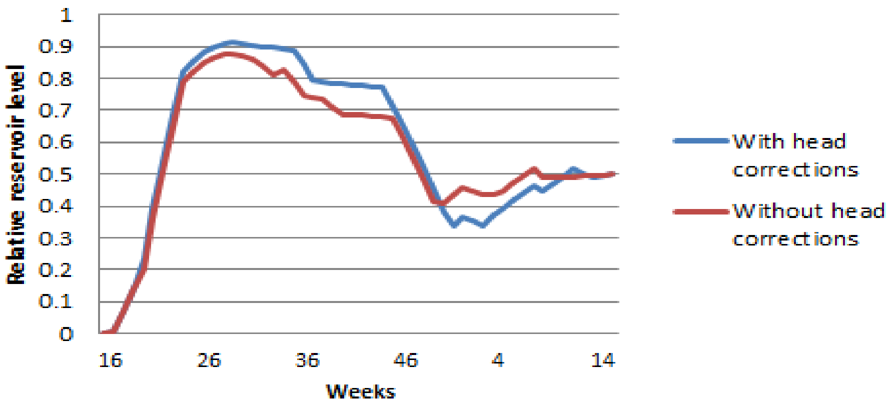

Figure 8.5.1: Expected relative reservoir levels with and without head corrections for an uncertainty level of 5 %.

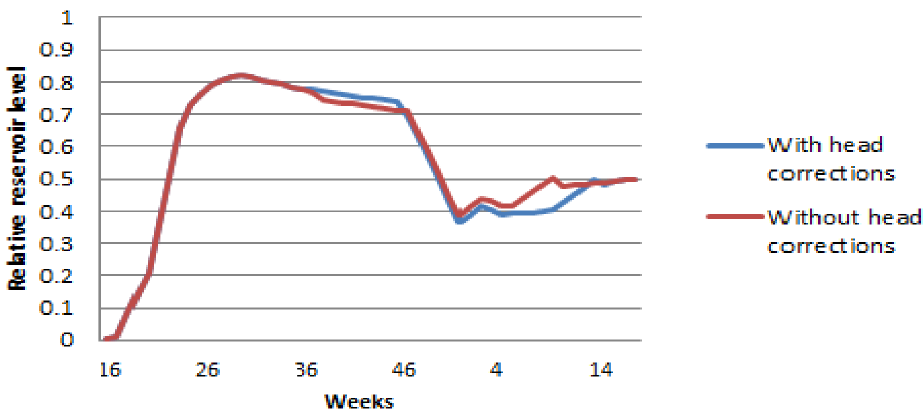

Figure 8.5.2: Expected relative reservoir levels with and without head corrections for an uncertainty level of 10 %.

When head corrections are included, the model will recognize an incentive to keep the reservoir level high, as this will give a higher head. Producing at a higher head causes a larger proportion of the potential energy in the discharged water to be converted into electrical energy. At uncertainty levels of 5 % and 10 % an increase in volume can be seen until week 46, which leads to increased profits. At 15 % uncertainty, there is only one feasible production strategy, which means that the model has no ability to adjust the reservoir level depending on the correction factors. This is the reason why the graphs representing the reservoir levels with and without head corrections overlap. It is assumed that deviation between the reservoir levels with and without head corrections will increase somewhat for plants with a higher flexibility than Plant 2.

8.6 Main shortcomings

The approach taken in this thesis has several shortcomings, which leaves room for future improvements. The main shortcomings are presented in this section.

The LDR model is quite sensitive to input data, and realistic input data for price and inflow is therefore of importance for the results. The stochastic price and inflow models developed in this thesis are based on short time series. As a result, extreme values affect the price and inflow forecasts too much. The covariance matrices used as input to the LDR models are derived from the residuals from the price and inflow models, and are thus based on the same time series. Longer time series would have provided a better basis for analysis, giving more realistic representations and better foundations for the parameter estimations. However, price and inflow modeling is not the main focus of this thesis and the results from the price and inflow models are therefore assumed to be acceptable for the purpose of the thesis. Most hydropower producers have access to better forecasting models, such as the EMPS model (Wolfgang et al., 2009), and may also have longer historical time series for price and inflow available. It is assumed that using input data from such models will give more realistic forecasts for the long term scheduling.

Weekly time steps are used in all models, and this results in a loss of price spikes. This means that weeks with large internal price variations will be smoothed out, which may result in too low or too high water allocations to these weeks. However, it is assumed that the this will be captured in the shorter term scheduling models.

As described in Section 8.1, the uncertainty levels for price and inflow are assumed to be equal and constant for all time periods. If longer time series were available, studies of how the historical uncertainty levels vary could have been performed. It is assumed that this would have resulted in a more realistic uncertainty representation, and is left for future studies.

The LDR model is defined to hold for both the lowest and highest price and inflow outcomes in all time periods. When the scheduling horizon is long and the uncertainty levels are high, the gap between the highest possible and the lowest possible reservoir level will be large at the end of the scheduling horizon. However, a situation in which either the highest or the lowest inflow outcome occurs in each time period is not realistic. As mentioned in Section 8.1.1 this could have been accounted for by restricting the total inflow from all periods. The gap between the two extreme reservoir levels would then decrease, leading to a higher solution space for production and presumably higher profits. It is also assumed that this would have caused the model to remain feasible for higher levels of uncertainty.

In practice the flexibility of a power station is often restricted by time varying constraints on reservoir level and/or dispatch volumes due to environmental reasons. These restrictions are not accounted for by the models developed in this thesis. This leads to an overestimation of the actual profit. In addition, information about maintenance and discharge restrictions could be incorporated to improve the analysis. However, these data were not available for the majority of the producers.

9 Conclusion

In this thesis a multistage stochastic hydropower scheduling problem, in which price and inflow are uncertain parameters, is studied. Based on historical spot prices and inflow data from four hydropower producers, stochastic price and inflow models are developed. The forecasts provided by these models are evaluated through out-of-sample testing, and a one factor model for inflow and a two factor model for price are proven to give the most accurate results.

A stochastic multistage scheduling model is developed based on the LDR approximation. The uncertain parameters are defined within an interval around their expected values, in which the size of the interval is given by the uncertainty levels of the parameters. Increasing the uncertainty levels is shown to cause more restrictive reservoir management strategies. It is also shown that more restrictive strategies are proposed for plants with a low flexibility than for plants with a higher one. The problem is proven to be feasible up to a certain uncertainty level, depending on the flexibility of the hydropower plants and on the length of the scheduling horizon.

To compare the performance of the LDR model and the corresponding deterministic model, a ten year series simulation is performed for one of the hydropower plants studied in this thesis. The simulation scenario corresponds to the realisations of price and inflow in the years 2002 to 2012, and both models are rerun every fourth week with updated initial reservoir levels. At an uncertainty level of 10 % the LDR model is shown to give an average price per released MWh that is 11.5 NOK higher than the price given by the deterministic model. The main reason for this result is the ability of the LDR model to adjust production to the realisations of price and inflow.

The LDR approximation is applied to both the primal version and the dual version of the original stochastic problem. The difference between the optimal objective values of the two problems defines the duality gap, which corresponds to the upper bound on the approximation error imposed by the LDR approach. It is found that the duality gap increases as the uncertainty levels of price and inflow increases. For a scheduling horizon of 52 time stages, the gaps are found to be in a range of 8 % to 44 % for uncertainty levels of 5 % to 30 %. This indicates that the LDR approximation causes potentially high duality gaps. However, the gaps are expected to decrease if the model is rerun whenever new information is available.

The complexity reduction caused by the LDR approximation leads to short computational times. When solved for 104 time stages, the primal LDR model has a run time of 268 seconds. This implies that the model can be rerun whenever new information about price and inflow is available. As a result, the model is able to provide updated boundary conditions to a shorter term model more frequently than models with longer computational times. In conclusion, the LDR approximation is considered to give an acceptable trade-off between tractability and accuracy for multistage stochastic hydropower scheduling problems.

10 Further Work

Many aspects of this thesis can be further developed, and some of them are presented in this section:

- A study of the historical price and inflow data will give a better understanding of the price and inflow uncertainty dynamics. Based on these results, different uncertainty levels for price and inflow can be used for different time periods.
- A situation where either the highest or lowest inflow outcome occurs in each time period is unrealistic. In order to account for this, restrictions on the total annual inflow could have been introduced in the LDR model.
- The LDR model grows polynomially with the number of time stages, and has a short computational time. This leads to an opportunity to use daily time steps instead for weekly, and daily prices can then be taken into account. Hence, the impact of weekdays and holidays could have been incorporated through dummy variables.
- The performance of the LDR model can be compared to the performance of a currently used method for long term hydropower scheduling through simulation.

References

Aas, K. (2007): *A Model for simulation of Nordic Electricity Spot Prices.* Energyforum conference on Nordic Modelling & Measuring Energy Risk, September 26. 2007.

Ackermann, T. (2012): *Wind Power in Power Systems.* 2nd edition, John Wiley & Sons Ltd.

Ang, M., Chou, M., Sim., and So, K. (2008): *A robust optimization framework for analyzing distribution systems with transshipments.* Working paper. National University of Singapore, Singapore.

Atamturk, A. and Zhang, M. (2007): *Two-stage robust network flow and design under demand uncertainty.* Mathematics of Operations Research 55 (4), 662-673.

Ben-Tal, A., Goryashko, A., Guslitzer, E. and Nemirovski, A. (2003): *Adjustable robust solutions of uncertain linear programs.* Mathematical Programming, 99, 351-376.

Ben-Tal A., Golany, B., Nemirovski, A. and Vial, J.P. (2005): *Supplier-retailer flexible commitments contracts: A robust optimization approach.* Manufacturing and Service Operations Management, 7(3), 248-273, 2005.

Bjørnsgard, M. and Hauge, L. K. (2007): *Case Studies in Hydropower Scheduling.* Master thesis, Department of Industrial Economics and Technology Management, Norwegian University of Science and Technology, Norway, 2007.

Carpentier, P. L., Gendreau, M. and Bastin, F. (2012): *Midterm Hydro Generation Scheduling Under Uncertainty Using the Progressive Hedging Algorithm* Rapport de recherche CIRRELT 35, 1-18.

Cartea, A. and Villaplana, P. (2008): *Spot price modeling and the valuation of electricity forward contracts: The role of demand and capacity.* Journal of Banking & Finance, 32(12), 2502-2519.

Cheng, C. T., Wang, W. C., Xu, D. M. and Chau, K. W. (2008): *Optimizing hydropower reservoir operation using hybrid genetic algorithm and chaos.* Water Resource Management 22, 895-909.

Cortazar, G. and Schwartz, E.S. (2003): *Implementing a stochastic model for oil futures prices.* Energy Economics 25, 215-238.

Crona, M. (2009): *Evaluation of flexibility in hydropower stations.* Master thesis, Department of Engineering Sciences, Uppsala University, Sweden, 2009.

Cuthbertson, K. and Nitzsche, D. (2001): *Financial Engineering: Derivatives and Risk Management'.* 1st edition, J. Wiley.

Damodaran, A. (2008): *What is the riskfree rate? A Search for the Basic Building Block.* Stern School of Business, New York, 2008.

Dixit, A. K. and Pindyck R. S. (1994): *Investment under uncertainty.* 1st edition New Jersey: Priceton University Press.

Doorman, G. L. (2012): *Hydropower scheduling.* Compendium in course ELK15: NTNU, Trondheim..

Fleten, S. E., Tomasgard, A. and Wallace, S. W. (2001): *Produksjonsplanlegging og risikostyring i et deregulert kraftmarked med finansielle instrumenter.* Magma 4 (5), 22-33.

Fleten, S. E. and Kristoffersen, T. K. (2008): *Short-term hydropower production planning by stochastic programming.* Computers & Operations Research 35 (8), 2656-2671.

Fleten, S. E., Seim, T. O. and Thorsnes, O. R. (2010): *The relationship between prices and inflow in hydroelectric scheduling.* Modern Electric Power Systems 2010.

Fleten, S. E., Haugstvedt, D., Steinsbø, J. A. and Fleischmann, F. (2011): *Bidding hydropower generation: Integrating short- and long-term scheduling.* 17th Power System Computation Conference (August 2011).

Geman, H. and Roncoroni, A. (2006): *Understanding the Fine Structure of Electricity Prices.* Journal of Business 79 (3), 1225-1262.

Gjelsvik, A. and Wallance, S. W. (1996): *Methods for stochastic medium-term scheduling in hydrodominated power systems.* Technical Report A4438, Norwegian Electric Power Research Institute, Trondheim, Norway.

Gjelsvik, A. and Haugstad, A. (2005): *Considering head variations in a linear model for optimal hydro scheduling..* In: Proceedings, Hydropower âĂŹ05: The backbone of sustainable energy supply, International centre for hydropower, Trondheim, Norway

Gjelsvik, A., Mo, B. and Haugstad, A. (2010): *Long- and Medium-term Operations Planning and Stochastic Modeling in Hydro-dominated Power Systems Based on Stochastic Dual Dynamic Programming.* Handbook of Power Systems (I), Energy Systems 2010, 33-55.

Goulart, P. J. and Kerrigan, E. C. (2005): *Relationships between affine feedback policies for robust control with constraints.* IFAC World Congress on Automatic Control 16.

Guslitser, E. (2002): *Uncertainty-immunized solutions in linear programming.* Research Thesis, Israel Institute of Technology, Israel.

Hagem, B. (2011): *Statnetts oppdrag og nettutviklingsplaner*. Energirike, 24. juni 2011, Haugesund.

Harvey, A.C. (1989): *Forecasting, Structural Time Series Models and the Kalman Filter*. Cambridge University Press.

Higle, J. L. (2005): *Stochastic programming: optimization when uncertainty matters*. In Tutorials in Operations Research: Emerging Theory, Methods, and Applications, INFORMS, Hanover, MD, 2006.

Hiller, F.S. and Lieberman, G.J. (2001): *Introduction to Operations Research*. McGraw Hill Co. Inc., New York.

Holmqvist, E. and Engen, I. K. (2008): *Utvalg av tilsigsserier til Samkjøringsmodellen*. Norges vassdrags- og energidirektorat, rapport nr. 7 (2008).

Jain, S.K. and Singh, V.P. (2003): *Water Resources Systems planning and Management*. 1st edition, Elsevier.

Kaut, M. and Wallace, S. W. (2007): *Evaluation of scenario-generation methods for stochastic programming*. Pacific Journal of Optimization 3 (2), 257-271.

Kjærland, F. and Larsen, B. (2010): *The value of operational flexibility by adding thermal to hydropower: A real option approach*. Journal of Applied Operational Research 2(1), 43-61.

Kristiansen, T. (2004): *Pricing of Contracts for Difference in the Nordic Market*. Energy Policy 32 (9), 1075-1085.

Kuhn, D., Wiesemann, W. and Georghiou, A. (2009): *The decision rule approach to optimization under uncertainty: Methodology and applications in Operation Management*. Available on Optimization Online, submitted for publication.

Kuhn, D., Wiesemann, W. and Georghiou, A. (2011): *Primal and dual linear decision rules in stochastic and robust optimization*. Mathematical Programming 130 (1), 177-209.

Lucia, J. J. and Schwartz, E. S. (2001): *Electricity prices and power derivatives: Evidence from the Nordic Power Exchange*. Review of Derivates Research 5 (1), 5-55.

Lundgren, J., Rönnquist, M. and Peter Värbrandt, P. (2010): *Optimization*. 1st edition, Malmø: Holmsberg.

NASDAQ (2013): *NASDAQ*. Available from: `http://www.nasdaq.com/`. Last visited 31.01.2013.

Ministry of Petroleum and Energy (2013): *Energiutredningen - verdiskaping, forsyningssikkerhet og miljø*.

Nord Pool Spot (2013). Available from: `http://www.nordpoolspot.com`. Last visited 12.04.2013.

Ordóñez, F. and Zaho, J. (2007): *Robust capacity expansion of network flows*. Networks 50(2), 136-145.

Pilipovic, D. (2007): *Energy risk: Valuing and managing energy derivatives*. 2nd edition, McGraw Hill Professional.

Revelle, C., Joeres, E. and Kirby, W. (1969): *The linear decision rule in reservoir management*. Water Resources Research 5 (4), 767.

Rocha, P. and Kuhn, D. (2012): *Multistage Stochastic Portfolio Optimization in Deregulated Electricity Markets Using Linear Decision Rules*. European Journal of Operational Research 216 (2), 397-408.

Rondeel, W. G. J. (2012): *Hydro Electricity and Storage Capabilities in Norway - can they be useful for Europe?*. General annual Congress DPG Berlin March 2012, 49-59.

Schwartz, E. (1997): *The stochastic behavior of commodity prices*. The Journal of Finance 52 (3), 923-973.

Schwartz, E. and Smith, J. E. (2000): *Short-Term Variations and Long-Term Dynamics in Commodity Prices*. Management Science 46 (7), 893-911.

Shapiro, A. and Nemirovski, A. (2005): *On complexity of stochastic programming problems*. Continuous Optimization 99, 111-146.

Seim, T. O. and Thorsnes, O. R. (2007): *Analyzing the price- and inflow relationships in hydroelectric scheduling*. Master thesis, Department of Industrial Economics and Technology Management, Norwegian University of Science and Technology, Norway, 2007.

Steinsbø, J. A. (2008): *Constructing Bidding Curves for a Hydropower Producer at Nord Pool*. Master thesis, Department of Industrial Economics and Technology Management, Norwegian University of Science and Technology, Norway, 2008.

Tandberg, C. and Vefring, S. (2012): *The Linear Decision Rule Approach to the Hydrothermal Generation Planning Problem*. Master thesis, Department of Industrial Economics and Technology Management, Norwegian University of Science and Technology, Norway, 2012.

Terry, L. A., Pereira, M. V. F., Araripe Neto, T. A., Silva, L. F. C. A. and Sales, P. R. H. (1986): *Coordinating the Energy Generation of the Brazilian National Hydrothermal Electrical Generating System.* Interfaces 16 (1), 16-38.

Wallace, S. W. and Fleten, S.E. (2003): *Stochastic programming models in energy.* Handbooks in Operations Research and Management Science 10, 637-677.

Welch, G. and Bishop, G. (2001): *An Introduction to the Kalman Filter.* SIGGRAPH 2001, Los Angeles, CA, August 12-17, 2001, 1-47.

West, M. and Harrison, J. (1996): *Bayesian Forecasting and Dynamic Linear Models.* 2nd edition, Springer-Verlag.

Wolfgang, O., Haugstad, A., Mo, B., Gjelsvik, A., Wangensteen, I. and Doorman, G. (2009): *Hydro reservoir handling in Norway before and after deregulation.* Energy 34 (10), 1642-1651.

A Parameter estimation

This appendix presents the numerical results from the parameter estimations for inflow and graphically out of sample plots for relative realised inflow compared to the relative simulated inflow from Section 5. The parameters estimated from the price model is presented in the end of this appendix.

A.1 Inflow parameters

The parameters estimated from the inflow models in Section 5.3 is presented in Table A.1.1.

Table A.1.1: The estimated inflow parameters

Parameters	α	γ	τ	κ
Plant 1				
Inflow model 2				
Period 1	7.69	-5.82	-9.03	0.02
Period 2	5.06	-5.82	18.28	-0.001
Period 3	-0.19	-6.97	33.07	1.11
Inflow model 3				
	4.887	-2.75	-1.92	10.33
Plant 2				
Inflow model 2				
Period 1	18.32	13.62	-33.28	0.05
Period 2	22.76	14.48	-15.63	0.05
Period 3	9.25	-6.15	-1.60	0.001
Inflow model 3	22.26	16.70	24.72	0.06
Plant 3				
Inflow model 2				
Period 1	2.48	1.34	14.74	2.55
Period 2	-1.07	21.18	-2.10	0.38
Period 3	-0.36	-5.16	-14.97	0
Inflow model 3	8.95	-8.70	-3.26	0.31
Plant 4				
Inflow model 2				
Period 1	3.39	-1.67	41.57	0.01
Period 2	3.74	-1.42	17.92	0.97
Period 3	2.69	-2.47	41.57	0.41
Inflow model 3	3.35	-1.86	-10.81	10.30

A.1.1 Inflow simulations

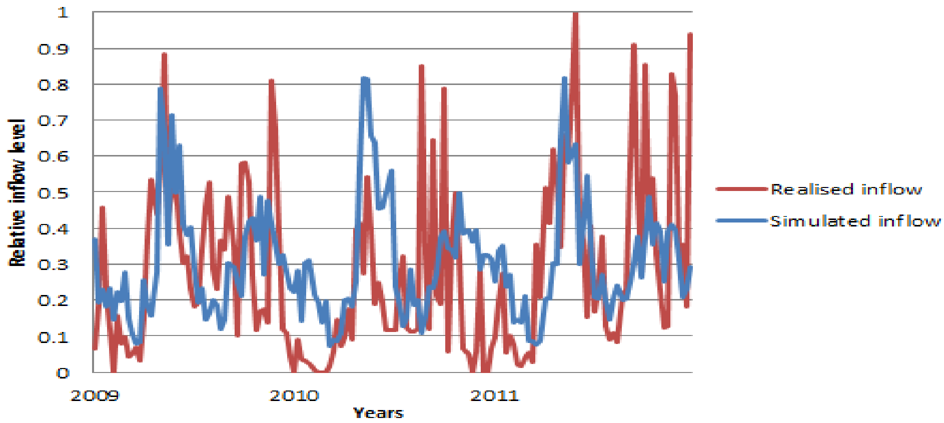

Figure A.1.1: Inflow model 1 for Plant 1 (2009-2011).

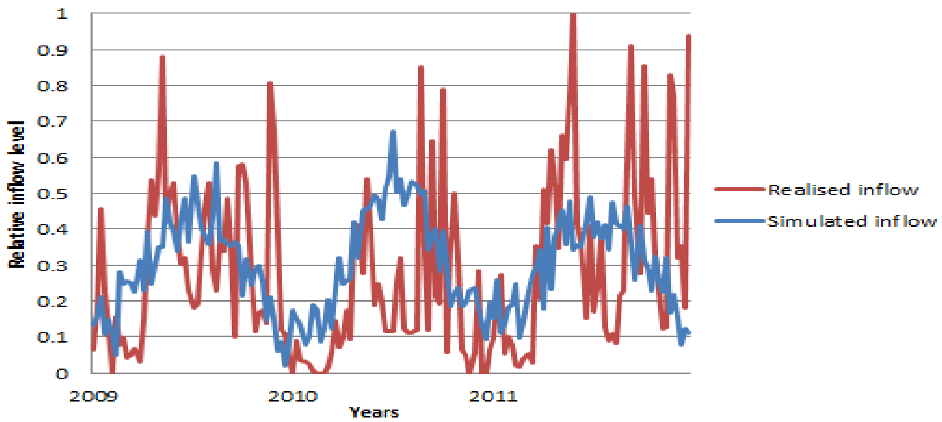

Figure A.1.2: Inflow model 3 for Plant 1 (2009-2011).

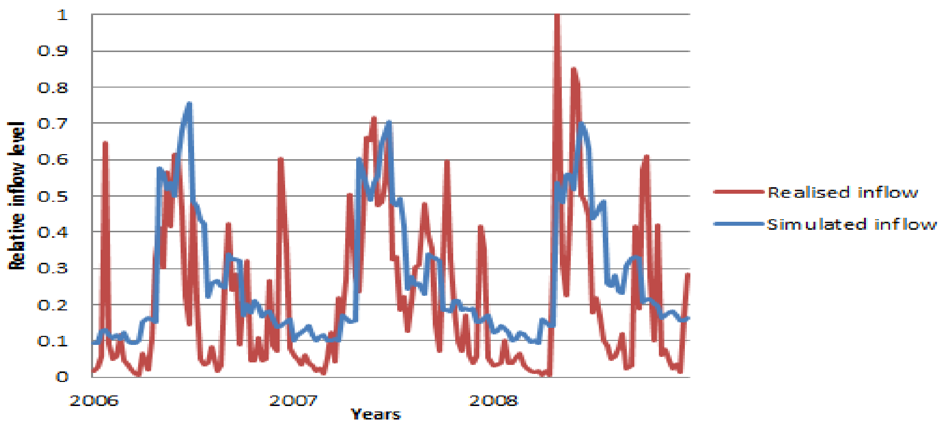

Figure A.1.3: Inflow model 1 for Plant 2 (2006-2008).

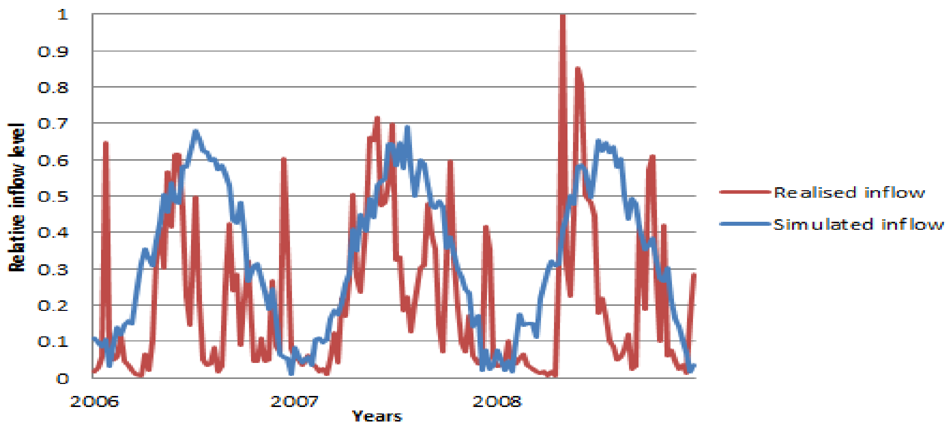

Figure A.1.4: Inflow model 3 for Plant 2 (2006-2008).

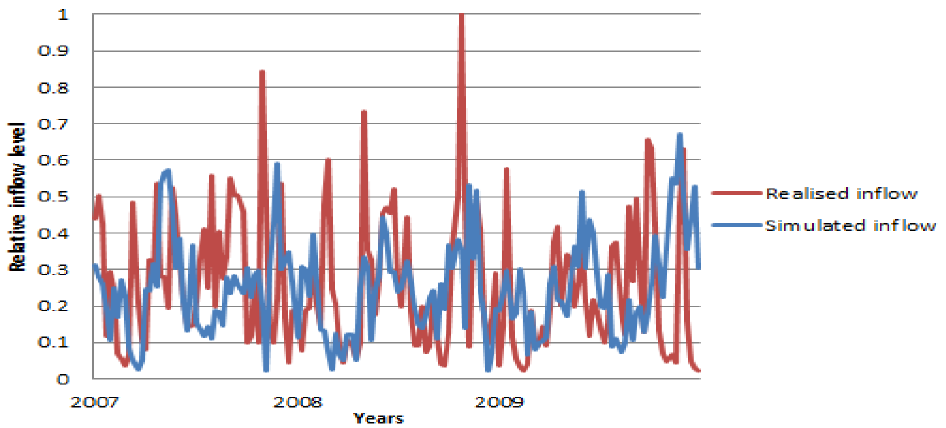

Figure A.1.5: Inflow model 1 for Plant 4 (2007-2009).

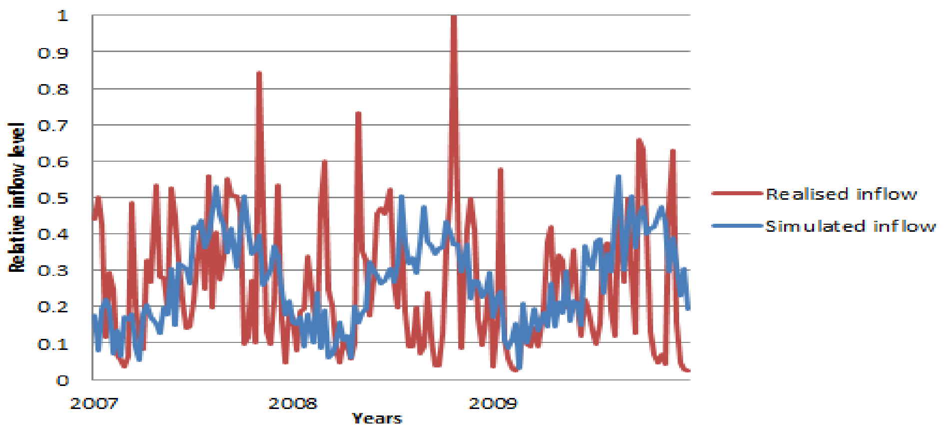

Figure A.1.6: Inflow model 3 for Plant 4 (2007-2009).

A.2 Price parameters

The parameters estimated from the price models in Section 5.4 is presented in Table A.2.1.

Table A.2.1: The estimated price parameters

Parameters	α	γ	τ	κ	α^*	μ^*	σ_x	σ_ϵ
Price model 1	309	30.27	3.96	0.01	0	0	5.77	3.10
Price model 2	11.27	-10.66	-2.74	0.12	-2.66	0.001	3.41	0.22
Price model 3	10	2.33	1	0.8	-6.25	0	5	3.99

B Primal Linear Decision Rules

This appendix presents the rewriting of a stochastic aggregated reservoir model to a LDR models. The rewritings are based on Ben-Tal et al. (2003) and Kuhn et al. (2011). The multi-reservoir model presented in Section 6.2 is developed based on the same procedure.

B.1 Aggregated reservoir model

The stochastic aggreagted reservoir model is presented as:

$$V_0 = max\ \mathbb{E}\ \left[\sum_{t=1}^{T} \frac{1}{(1+R)^t} \left(\Pi_t \cdot q_t^{(\Pi_t,\Psi_t)}\right)\right] \tag{B.1.1}$$

s.t.

$$Q_{min} \leq q_t^{(\Pi_t,\Psi_t)} \leq Q_{max}, \quad \forall t \in T \tag{B.1.2}$$

$$M_{min} \leq M_0 + \sum_{r=1}^{t} \Psi_r - \sum_{r=1}^{t} q_r^{(\Pi_r,\Psi_r)} - \sum_{r=1}^{t} s_r^{(\Psi_r)} \leq M_{max}, \quad \forall t \in T \tag{B.1.3}$$

$$q_t^{(\Pi_t,\Psi_t)}, s_t^{(\Psi_t)} \geq 0, \quad \forall t \in T \tag{B.1.4}$$

B.1.1 Affine decision rules

The decision making policies are restricted to be affine functions of the uncertain parameters, i.e. price and inflow:

$$q_t^{(\Pi_t,\Psi_t)} = \delta_t^0 + \sum_{r \epsilon I_t} (\delta_t^r \cdot \Pi_r + \gamma_t^r \cdot \Psi_r), \quad \forall t \in T \tag{B.1.5}$$

$$s_t^{(\Psi_t)} = \kappa_t^0 + \sum_{r \epsilon I_t} (\kappa_t^r \cdot \Psi_r), \quad \forall t \in T \tag{B.1.6}$$

where the coefficients are new non adjustable variables. The uncertain parameters are assumed to be within the following limits:

$$\Pi_t^*(1-\theta^\Pi) \leq \Pi_t \leq \Pi_t^*(1+\theta^\Pi), \quad \forall t \in T \tag{B.1.7}$$

$$\Psi_t^*(1-\theta^\Psi) \leq \Psi_t \leq \Psi_t^*(1+\theta^\Psi), \quad \forall t \in T \tag{B.1.8}$$

where θ^Π and θ^Ψ are nonnegative, and represent the uncertainty levels of price and inflow respectively. Π_t^* and Ψ_t^* represent the expected price and inflow in period t.

B.1.2 Substituting the affine decision rules into the stochastic model

The affine decision rules from Appendix B.1.1 are substituted into the original stochastic model from Appendix B.1. This gives:

$$V_0 = max\ \mathbb{E}\left[\sum_{t=1}^{T}\frac{1}{(1+r)^t}\left(\Pi_t\cdot\left(\delta_t^0+\sum_{r\in I_t}(\delta_t^r\cdot\Pi_r+\gamma_t^r\cdot\Psi_r)\right)\right)\right] \tag{B.1.9}$$

s.t.

$$Q_{min} \le \delta_t^0+\sum_{r\in I_t}(\delta_t^r\cdot\Pi_r+\gamma_t^r\cdot\Psi_r) \le Q_{max}, \quad \forall t\in T \tag{B.1.10}$$

$$\begin{aligned} M_{min} \le\ & M_0+\sum_{s=1}^{t}\Psi_s-\sum_{s=1}^{t}\left(\delta_s^0+\sum_{r\in I_s}(\delta_s^r\cdot\Pi_r+\gamma_s^r\cdot\Psi_r)\right)- \\ & \sum_{s=1}^{t}\left(\kappa_s^0+\sum_{r\in I_s}(\kappa_s^r\cdot\Psi_r)\right) \le M_{max}, \quad \forall t\in T \end{aligned} \tag{B.1.11}$$

$$\delta_t^0+\sum_{r\epsilon I_t}(\delta_t^r\cdot\Pi_r+\gamma_t^r\cdot\Psi_r) \ge 0, \quad \forall t\in T \tag{B.1.12}$$

$$\kappa_t^0+\sum_{r\epsilon I_t}(\kappa_t^r\cdot\Psi_r) \ge 0, \quad \forall t\in T \tag{B.1.13}$$

$$\forall\ \Pi_t \in [\Pi_t^*(1-\theta^{\Pi}),\Pi_t^*(1+\theta^{\Pi})], \quad \forall t\in T \tag{B.1.14}$$

$$\forall\ \Psi_t \in [\Psi_t^*(1-\theta^{\Psi}),\Psi_t^*(1+\theta^{\Psi})], \quad \forall t\in T \tag{B.1.15}$$

where Eq. (B.1.14) and (B.1.15) apply for all the constraints, and implies that all the constraints must remain feasible for all possible realizations of price and inflow. Splitting the equations and reorganizing the model gives:

$$V_0 = max\ \mathbb{E}\sum_{t=1}^{T}\frac{1}{(1+r)^t}\left[\Pi_t\cdot\delta_t^0+\sum_{r\in I_t}(\delta_t^r\cdot\Pi_r\cdot\Pi_t+\gamma_t^r\cdot\Psi_r\cdot\Pi_t)\right] \tag{B.1.16}$$

s.t.

$$\delta_t^0+\sum_{r\in I_t}(\delta_t^r\cdot\Pi_r+\gamma_t^r\cdot\Psi_r) \ge Q_{min}, \quad \forall t\in T \tag{B.1.17}$$

$$\delta_t^0+\sum_{r\in I_t}(\delta_t^r\cdot\Pi_r+\gamma_t^r\cdot\Psi_r) \le Q_{max}, \quad \forall t\in T \tag{B.1.18}$$

$$\sum_{s=1}^{t}\Psi_s - \sum_{s=1}^{t}\delta_s^0 - \sum_{s=1}^{t}\sum_{r\in I_s}(\delta_s^r\cdot\Pi_r + \gamma_s^r\cdot\Psi_r) - \sum_{s=1}^{t}\kappa_s^0 - \sum_{s=1}^{t}\sum_{r\in I_s}\kappa_s^r\cdot\Psi_r \geq M_{min} - M_0, \quad \forall t\in T \tag{B.1.19}$$

$$\sum_{s=1}^{t}\Psi_s - \sum_{s=1}^{t}\delta_s^0 - \sum_{s=1}^{t}\sum_{r\in I_s}(\delta_s^r\cdot\Pi_r + \gamma_s^r\cdot\Psi_r) - \sum_{s=1}^{t}\kappa_s^0 - \sum_{s=1}^{t}\sum_{r\in I_s}\kappa_s^r\cdot\Psi_r \leq M_{max} - M_0, \quad \forall t\in T \tag{B.1.20}$$

$$\delta_t^0 + \sum_{r\in I_t}(\delta_t^r\cdot\Pi_r + \gamma_t^r\cdot\Psi_r) \geq 0, \quad \forall t\in T \tag{B.1.21}$$

$$\kappa_t^0 + \sum_{r\epsilon I_t}\kappa_t^r\cdot\Psi_r \geq 0, \quad \forall t\in T \tag{B.1.22}$$

or, which is the same:

$$V_0 = max\ \sum_{t=1}^{T}\frac{1}{(1+r)^t}\left(\mathbb{E}[\Pi_t]\cdot\delta_t^0 + \sum_{r\in I_t}\delta_t^r\cdot\mathbb{E}[\Pi_r\cdot\Pi_t] + \sum_{r\in I_t}\gamma_t^r\cdot\mathbb{E}[\Psi_r\cdot\Pi_t]\right) \tag{B.1.23}$$

s.t.

$$\delta_t^0 + \sum_{r\in I_t}\delta_t^r\cdot\Pi_r + \sum_{r\in I_t}\gamma_t^r\cdot\Psi_r \geq Q_{min}, \quad \forall t\in T \tag{B.1.24}$$

$$\delta_t^0 + \sum_{r\in I_t}\delta_t^r\cdot\Pi_r + \sum_{r\in I_t}\gamma_t^r\cdot\Psi_r \leq Q_{max}, \quad \forall t\in T \tag{B.1.25}$$

$$\sum_{s=1}^{t}\Psi_s - \sum_{s=1}^{t}\delta_s^0 - \sum_{s=1}^{t}\sum_{r\in I_s}\delta_s^r\cdot\Pi_r - \sum_{s=1}^{t}\sum_{r\in I_s}\gamma_s^r\cdot\Psi_r - \sum_{s=1}^{t}\kappa_s^0 - \sum_{s=1}^{t}\sum_{r\in I_s}\kappa_s^r\cdot\Psi_r \geq M_{min} - M_0, \quad \forall t\in T \tag{B.1.26}$$

$$\sum_{s=1}^{t}\Psi_s - \sum_{s=1}^{t}\delta_s^0 - \sum_{s=1}^{t}\sum_{r\in I_s}\delta_s^r\cdot\Pi_r - \sum_{s=1}^{t}\sum_{r\in I_s}\gamma_s^r\cdot\Psi_r - \sum_{s=1}^{t}\kappa_s^0 - \sum_{s=1}^{t}\sum_{r\in I_s}\kappa_s^r\cdot\Psi_r \leq M_{max} - M_0, \quad \forall t\in T \tag{B.1.27}$$

$$\delta_t^0 + \sum_{r\in I_t}\delta_t^r\cdot\Pi_r + \sum_{r\in I_t}\gamma_t^r\cdot\Psi_r \geq 0, \quad \forall t\in T \tag{B.1.28}$$

$$\kappa_t^0 + \sum_{r\epsilon I_t}\kappa_t^r\cdot\Psi_r \geq 0, \quad \forall t\in T \tag{B.1.29}$$

$$\forall\ \Pi_t \in [\Pi_t^*(1-\theta^\Pi), \Pi_t^*(1+\theta^\Pi)], \quad \forall t\in T \tag{B.1.30}$$

$$\forall\ \Psi_t \in [\Psi_t^*(1-\theta^\Psi), \Psi_t^*(1+\theta^\Psi)], \quad \forall t\in T \tag{B.1.31}$$

Eq. (B.1.28) is dominated by Eq. (B.1.24) and can be removed.

B.1.3 Covariance

The objective function are defined such that it maximizes the expected value market value of production, and includes the terms $\mathbb{E}[\Pi_t\cdot\Pi_r]$ and $\mathbb{E}[\Pi_t\cdot\Psi_r]$. The following equivalences are used in order to rewrite the objective function in the model from Appendix B.1.2:

$$\mathbb{E}[\Pi_t] = \Pi_t^*, \quad \forall t\in T \tag{B.1.32}$$

$$\mathbb{E}[\Pi_t\cdot\Pi_r] = \mathbb{E}[\Pi_t]\cdot\mathbb{E}[\Pi_r] + \mathbb{Cov}[\Pi_t\cdot\Pi_r] = \Pi_t^*\cdot\Pi_r^* + C_{t,r}^{\Pi,\Pi}, \quad 1\leq r\leq t\leq T \tag{B.1.33}$$

$$\mathbb{E}[\Pi_t\cdot\Psi_r] = \mathbb{E}[\Pi_t]\cdot\mathbb{E}[\Pi_r] + \mathbb{Cov}[\Pi_t\cdot\Psi_r] = \Pi_t^*\cdot\Psi_r^* + C_{t,r}^{\Pi,\Psi}, \quad 1\leq r\leq t\leq T \tag{B.1.34}$$

B.1.4 Equivalences

The following equivalences from Ben-Tal et al. (2003) are used in order to rewrite the constraints in the model from Appendix B.1.2:

$$\sum_{t=1}^{T} d_t\cdot x_t \leq y, \quad \forall d_t \in [d_t^*\cdot(1-\theta), d_t^*\cdot(1+\theta)] \tag{B.1.35}$$

$$\Updownarrow$$

$$\sum_{t:x_t<0} d_t^* \cdot (1-\theta) \cdot x_t + \sum_{t:x_t>0} d_t^* \cdot (1+\theta) \cdot x_t \leq y \tag{B.1.36}$$

$$\Updownarrow$$

$$\sum_{t=1}^{T} d_t^* \cdot x_t + \theta \cdot \sum_{t=1}^{T} d_t^* \cdot |x_t| \leq y \tag{B.1.37}$$

When:

$$\sum_{t=1}^{T} d_t \cdot x_t \geq y, \quad \forall d_t \in [d_t^* \cdot (1-\theta), d_t^* \cdot (1+\theta)] \tag{B.1.38}$$

the result is:

$$\sum_{t=1}^{T} d_t^* \cdot x_t - \theta \cdot \sum_{t=1}^{T} d_t^* \cdot |x_t| \geq y \tag{B.1.39}$$

B.1.5 Additional variables

The equivalences described in Appendix B.1.4 entail a need for introducing new variables representing the absolute value of all the variables in the model from Appendix B.1.2. The new variables are defined as:

$$-d_t^r \leq \delta_t^r \leq d_t^r, \quad d_t^r = |\delta_t^r|, \quad 1 \leq r \leq t \leq T \tag{B.1.40}$$

$$-y_t^r \leq \gamma_t^r \leq y_t^r, \quad y_t^r = |\gamma_t^r|, \quad 1 \leq r \leq t \leq T \tag{B.1.41}$$

$$-k_t^r \leq \kappa_t^r \leq k_t^r, \quad k_t^r = |\kappa_t^r|, \quad 1 \leq r \leq t \leq T \tag{B.1.42}$$

B.1.6 The LDR model

Rewriting the objective function as described in Appendix B.1.3 and the constraints in the model from Appendix B.1.2 using the equivalences from Appendix B.1.4 and the new additional variables from Appendix B.1.5 results in the following aggregated reservoir LDR model:

$$\begin{aligned} V_0 = max \sum_{t=1}^{T} \frac{1}{(1+r)^t} \Bigg(& \Pi_t^* \cdot \delta_t^0 + \sum_{r \in I_t} \Pi_t^* \cdot \Pi_r^* \cdot \delta_t^r + \sum_{r \in I_t} C_{t,r}^{\Pi,\Pi} \cdot \delta_t^t \\ & + \sum_{r \in I_t} \Pi_t^* \cdot \Psi_r^* \cdot \gamma_t^r + \sum_{r \in I_t} C_{t,r}^{\Pi,\Psi} \cdot \gamma_t^r \Bigg) \end{aligned} \tag{B.1.43}$$

s.t.

$$\delta_t^0 + \sum_{r=1}^{t} \Pi_r^* \cdot \delta_t^r - \theta^{\Pi} \cdot \sum_{r=1}^{t} \Pi_r^* \cdot d_t^r + \sum_{r=1}^{t} \Psi_r^* \cdot \gamma_t^r - \theta^{\Psi} \cdot \sum_{r=1}^{t} \Psi_r^* \cdot y_t^r \geq Q_{min}, \quad \forall t \in T \tag{B.1.44}$$

$$\delta_t^0 + \sum_{r=1}^{t} \Pi_r^* \cdot \delta_t^r + \theta^{\Pi} \cdot \sum_{r=1}^{t} \Pi_r^* \cdot d_t^r + \sum_{r=1}^{t} \Psi_r^* \cdot \gamma_t^r + \theta^{\Psi} \cdot \sum_{r=1}^{t} \Psi_r^* \cdot y_t^r \leq Q_{max}, \quad \forall t \in T \tag{B.1.45}$$

$$\sum_{s=1}^{t} \Psi_s^* + \theta^{\Psi} \cdot \sum_{s=1}^{t} \Psi_s^* - \sum_{s=1}^{t} \delta_s^0 - \sum_{s=1}^{t} \sum_{r \in I_s} \Pi_r^* \cdot \delta_s^r + \theta^{\Pi} \cdot \sum_{s=1}^{t} \sum_{r \in I_s} \Pi_r^* \cdot d_s^r - \sum_{s=1}^{t} \sum_{r \in I_s} \Psi_r^* \cdot \gamma_s^r + \theta^{\Psi} \cdot \sum_{s=1}^{t} \sum_{r \in I_s} \Psi_r^* \cdot y_s^r - \sum_{s=1}^{t} \kappa_s^0 - \sum_{s=1}^{t} \sum_{r \in I_s} \Psi_r^* \cdot \kappa_s^r + \theta^{\Psi} \cdot \sum_{s=1}^{t} \sum_{r \in I_s} \Psi_r^* \cdot k_s^r \leq M_{max} - M_0, \quad \forall t \in T \tag{B.1.46}$$

$$\sum_{s=1}^{t} \Psi_s^* - \theta^{\Psi} \cdot \sum_{s=1}^{t} \Psi_s^* - \sum_{s=1}^{t} \delta_s^0 - \sum_{s=1}^{t} \sum_{r \in I_s} \Pi_r^* \cdot \delta_s^r - \theta^{\Pi} \cdot \sum_{s=1}^{t} \sum_{r \in I_s} \Pi_r^* \cdot d_s^r - \sum_{s=1}^{t} \sum_{r \in I_s} \Psi_r^* \cdot \gamma_s^r - \theta^{\Psi} \cdot \sum_{s=1}^{t} \sum_{r \in I_s} \Psi_r^* \cdot y_s^r - \sum_{s=1}^{t} \kappa_s^0 - \sum_{s=1}^{t} \sum_{r \in I_s} \Psi_r^* \cdot \kappa_s^r - \theta^{\Psi} \cdot \sum_{s=1}^{t} \sum_{r \in I_s} \Psi_r^* \cdot k_s^r \geq M_{min} - M_0, \quad \forall t \in T \tag{B.1.47}$$

$$\sum_{s=1}^{t} \kappa_s^0 + \sum_{s=1}^{t} \sum_{r \in I_s} \Psi_r^* \cdot \kappa_s^r - \theta^{\Psi} \cdot \sum_{s=1}^{t} \sum_{r \in I_s} \Psi_r^* \cdot k_s^r \geq 0, \quad \forall t \in T \tag{B.1.48}$$

$$-d_t^r \leq \delta_t^r \leq d_t^r, \quad 1 \leq r \leq t \leq T \tag{B.1.49}$$

$$-y_t^r \leq \gamma_t^r \leq y_t^r, \quad 1 \leq r \leq t \leq T \tag{B.1.50}$$

$$-k_t^r \leq \kappa_t^r \leq k_t^r, \quad 1 \leq r \leq t \leq T \tag{B.1.51}$$

C Dual Linear Decision Rules

This appendix presents the development of an aggregated reservoir dual LDR models. The dualisation is based on Lundgren et al. (2010) and the rewritings are based on Ben-Tal et al. (2003) and Kuhn et al. (2011). The multi-reservoir dual LDR model presented in Section 7.2 is developed based on the same procedure.

C.1 Aggregated reservoir model

The stochastic primal model presented in Appendix B.1 is rewritten to normal form:

$$V_0 = max \ \mathbb{E} \left[\sum_{t=1}^{T} \frac{1}{(1+r)^t} \left(\Pi_t \cdot q_t^{(\Pi_t, \Psi_t)} \right) \right] \tag{C.1.1}$$

s.t.

$$- q_t^{(\Pi_t, \Psi_t)} \leq -Q_{min}, \quad \forall t \in T \tag{C.1.2}$$

$$q_t^{(\Pi_t, \Psi_t)} \leq Q_{max}, \quad \forall t \in T \tag{C.1.3}$$

$$- \sum_{s=1}^{t} q_s^{(\Pi_s, \Psi_s)} - \sum_{s=1}^{t} s_s^{(\Psi_s)} \leq M_{max} - M_0 - \sum_{s=1}^{t} \Psi_s \quad \forall t \in T \tag{C.1.4}$$

$$\sum_{s=1}^{t} q_s^{(\Pi_s, \Psi_s)} + \sum_{s=1}^{t} s_s^{(\Psi_s)} \leq M_0 - M_{min} + \sum_{s=1}^{t} \Psi_s \quad \forall t \in T \tag{C.1.5}$$

$$q_t^{(\Pi_t, \Psi_t)}, s_t^{(\Psi_t)} \geq 0, \quad \forall t \in T \tag{C.1.6}$$

C.1.1 The stochastic dual model

The primal problem has four sets of constraints and two sets of decision variables, which gives the dual problem two sets of constraints and four sets of decision variables. The decision variables can be defined as:

$$\iota_t^{(\Pi_t, \Psi_t)}, \zeta_t^{(\Pi_t, \Psi_t)}, \nu_t^{(\Pi_t, \Psi_t)}, \mu_t^{(\Pi_t, \Psi_t)} \tag{C.1.7}$$

The duality theory from Section 7.1 and the new dual variables are used to dualize the primal problem from Appendix C.1. This gives:

$$Z_0 = min\ \mathbb{E}\ \Bigg[\sum_{t=1}^{T} \Big(-Q_{min} \cdot \iota_t^{(\Pi_t,\Psi_t)} + Q_{max} \cdot \zeta_t^{(\Pi_t,\Psi_t)} + \left(M_{max} - M_0 - \sum_{s=1}^{t} \Psi_s \right) \cdot \nu_t^{(\Pi_t,\Psi_t)} + \left(M_0 - M_{min} + \sum_{s=1}^{t} \Psi_s \right) \cdot \mu_t^{(\Pi_t,\Psi_t)} \Big) \Bigg] \tag{C.1.8}$$

$$-\iota_t^{(\Pi_t,\Psi_t)} + \zeta_t^{(\Pi_t,\Psi_t)} - \sum_{s=t}^{T} \nu_s^{(\Pi_s,\Psi_s)} + \sum_{s=t}^{T} \mu_s^{(\Pi_s,\Psi_s)} \geq \frac{1}{(1+r)^t} \cdot \Pi_t, \quad \forall t \in T \tag{C.1.9}$$

$$-\sum_{s=t}^{T} \nu_s^{(\Pi_s,\Psi_s)} + \sum_{s=t}^{T} \mu_s^{(\Pi_s,\Psi_s)} \geq 0, \quad \forall t \in T \tag{C.1.10}$$

$$\iota_t^{(\Pi_t,\Psi_t)}, \zeta_t^{(\Pi_t,\Psi_t)}, \nu_t^{(\Pi_t,\Psi_t)}, \mu_t^{(\Pi_t,\Psi_t)} \geq 0, \quad \forall t \in T \tag{C.1.11}$$

C.1.2 Affine Decision Rules

The *Affine decision Rules* for the dual sets of variables are defined as:

$$\iota_t^{(\Pi_t,\Psi_t)} = \iota_t^0 + \sum_{r \in I_t} (\iota_{1,t}^r \cdot \Pi_r + \iota_{2,t}^r \cdot \Psi_r), \quad \forall t \in T \tag{C.1.12}$$

$$\zeta_t^{(\Pi_t,\Psi_t)} = \zeta_t^0 + \sum_{r \in I_t} (\zeta_{1,t}^r \cdot \Pi_r + \zeta_{2,t}^r \cdot \Psi_r), \quad \forall t \in T \tag{C.1.13}$$

$$\nu_t^{(\Pi_t,\Psi_t)} = \nu_t^0 + \sum_{r \in I_t} (\nu_{1,t}^r \cdot \Pi_r + \nu_{2,t}^r \cdot \Psi_r), \quad \forall t \in T \tag{C.1.14}$$

$$\mu_t^{(\Pi_t,\Psi_t)} = \mu_t^0 + \sum_{r \in I_t} (\mu_{1,t}^r \cdot \Pi_r + \mu_{2,t}^r \cdot \Psi_r), \quad \forall t \in T \tag{C.1.15}$$

Remember that:

$$\Pi_t^*(1-\theta^{\Pi}) \leq \Pi_t \leq \Pi_t^*(1+\theta^{\Pi}), \quad \forall t \in T \tag{C.1.16}$$

$$\Psi_t^*(1-\theta^{\Psi}) \leq \Psi_t \leq \Psi_t^*(1+\theta^{\Psi}), \quad \forall t \in T \tag{C.1.17}$$

C.1.3 Substituting the affine decision rules into the stochastic model

The affine decision rules from Appendix C.1.2 are substituted into the stochastic dual problem from Appendix C.1.1. This gives:

$$
\begin{aligned}
Z_0 = min\ \mathbb{E} \sum_{t=1}^{T} \Bigg[-Q_{min} \cdot \left(\iota_t^0 + \sum_{r \in I_t} (\iota_{1,t}^r \cdot \Pi_r + \iota_{2,t}^r \cdot \Psi_r) \right) \\
+Q_{max} \cdot \left(\zeta_t^0 + \sum_{r \in I_t} (\zeta_{1,t}^r \cdot \Pi_r + \zeta_{2,t}^r \cdot \Psi_r) \right) \\
+ \left(M_{max} - M_0 - \sum_{s \in I_t} \Psi_s \right) \cdot \left(\nu_t^0 + \sum_{r \in I_t} (\nu_{1,t}^r \cdot \Pi_r + \nu_{2,t}^r \cdot \Psi_r) \right) \\
\left(-M_{min} + M_0 + \sum_{s \in I_t} \Psi_s \right) \cdot \left(\mu_t^0 + \sum_{r \in I_t} (\mu_{1,t}^r \cdot \Pi_r + \mu_{2,t}^r \cdot \Psi_r) \right) \Bigg]
\end{aligned}
\tag{C.1.18}
$$

$$
\begin{aligned}
- \left(\iota_t^0 + \sum_{r \in I_t} (\iota_{1,t}^r \cdot \Pi_r + \iota_{2,t}^r \cdot \Psi_r) \right) + \left(\zeta_t^0 + \sum_{r \in I_t} (\zeta_{1,t}^r \cdot \Pi_r + \zeta_{2,t}^r \cdot \Psi_r) \right) \\
- \sum_{s=t}^{T} \left(\nu_s^0 + \sum_{r \in I_s} (\nu_{1,s}^r \cdot \Pi_r + \nu_{2,s}^r \cdot \Psi_r) \right) \\
+ \sum_{s=t}^{T} \left(\mu_s^0 + \sum_{r \in I_s} (\mu_{1,s}^r \cdot \Pi_r + \mu_{2,s}^r \cdot \Psi_r) \right) \geq \frac{1}{(1+r)^t} \Pi_t, \quad \forall t \in T
\end{aligned}
\tag{C.1.19}
$$

$$
\begin{aligned}
- \sum_{s=t}^{T} \left(\nu_s^0 + \sum_{r \in I_s} (\nu_{1,s}^r \cdot \Pi_r + \nu_{2,s}^r \cdot \Psi_r) \right) \\
+ \sum_{s=t}^{T} \left(\mu_s^0 + \sum_{r \in I_t} (\mu_{1,s}^r \cdot \Pi_r + \mu_{2,s}^r \cdot \Psi_r) \right) \geq 0, \quad \forall t \in T
\end{aligned}
\tag{C.1.20}
$$

$$
\iota_t^0 + \sum_{r \in I_t} (\iota_{1,t}^r \cdot \Pi_r + \iota_{2,t}^r \cdot \Psi_r) \geq 0, \quad \forall t \in T \tag{C.1.21}
$$

$$
\zeta_t^0 + \sum_{r \in I_t} (\zeta_{1,t}^r \cdot \Pi_r + \zeta_{2,t}^r \cdot \Psi_r) \geq 0, \quad \forall t \in T \tag{C.1.22}
$$

$$
\mu_t^0 + \sum_{r \in I_t} (\mu_{1,t}^r \cdot \Pi_r + \mu_{2,t}^r \cdot \Psi_r) \geq 0, \quad \forall t \in T \tag{C.1.23}
$$

$$\nu_t^0 + \sum_{r\in I_t}(\nu_{1,t}^r \cdot \Pi_r + \nu_{2,t}^r \cdot \Psi_r) \geq 0, \quad \forall t \in T \tag{C.1.24}$$

$$\forall\, \Pi_t \in [\Pi_t^* - \theta \cdot \Pi_t^*, \Pi_t^* + \theta \cdot \Pi_t^*], \quad \forall t \in T \tag{C.1.25}$$

$$\forall\, \Psi_t \in [\Psi_t^* - \theta \cdot \Psi_t^*, \Psi_t^* + \theta \cdot \Psi_t^*], \quad \forall t \in T \tag{C.1.26}$$

where Eq. (C.1.25) and (C.1.26) apply for all the constraints, and implies that all the constraints must remain feasible for all possible realizations of price and inflow. Rewriting the model gives:

$$\begin{aligned}
&Z_0 = \\
&min \sum_{t=1}^{T} \Bigg[-Q_{min} \cdot \iota_t^0 - \sum_{r\in I_t} Q_{min} \cdot \iota_{1,t}^r \cdot \mathbb{E}[\Pi_r] - \sum_{r\in I_t} Q_{min} \cdot \iota_{2,t}^r \cdot \mathbb{E}[\Psi_r] \\
&+Q_{max} \cdot \zeta_t^0 + \sum_{r\in I_t} Q_{max} \cdot \zeta_{1,t}^r \cdot \mathbb{E}[\Pi_r] + \sum_{r\in I_t} Q_{max} \cdot \zeta_{2,t}^r \cdot \mathbb{E}[\Psi_r] \\
&+M_{max} \cdot \nu_t^0 + \sum_{r\in I_t} M_{max} \cdot \nu_{1,t}^r \cdot \mathbb{E}[\Pi_r] + \sum_{r\in I_t} M_{max} \cdot \nu_{2,t}^r \cdot \mathbb{E}[\Psi_r] \\
&-M_0 \cdot \nu_t^0 - \sum_{r\in I_t} M_0 \cdot \nu_{1,t}^r \cdot \mathbb{E}[\Pi_r] - \sum_{r\in I_t} M_0 \cdot \nu_{2,t}^r \cdot \mathbb{E}[\Psi_r] \\
&- \sum_{s\in I_t} \mathbb{E}[\Psi_s] \cdot \nu_t^0 - \sum_{s\in I_t}\sum_{r\in I_t} \nu_{1,t}^r \cdot \mathbb{E}[\Pi_s \cdot \Psi_r] - \sum_{s\in I_t}\sum_{r\in I_t} \nu_{2,t}^r \cdot \mathbb{E}[\Psi_s \cdot \Psi_r] \\
&-M_{min} \cdot \mu_t^0 - \sum_{r\in I_t} M_{min} \cdot \mu_{1,t}^r \cdot \mathbb{E}[\Pi_r] - \sum_{r\in I_t} M_{min} \cdot \mu_{2,t}^r \cdot \mathbb{E}[\Psi_r] \\
&+M_0 \cdot \mu_t^0 + \sum_{r\in I_t} M_0 \cdot \mu_{1,t}^r \cdot \mathbb{E}[\Pi_r] + \sum_{r\in I_t} M_0 \cdot \mu_{2,t}^r \cdot \mathbb{E}[\Psi_r] \\
&+ \sum_{s\in I_t} \mathbb{E}[\Psi_s] \cdot \mu_t^0 + \sum_{s\in I_t}\sum_{r\in I_t} \mu_{1,t}^r \cdot \mathbb{E}[\Psi_s \cdot \Pi_r] + \sum_{s\in I_t}\sum_{r\in I_t} \mu_{2,t}^r \cdot \mathbb{E}[\Psi_s \cdot \Psi_r] \Bigg]
\end{aligned} \tag{C.1.27}$$

$$\begin{aligned}
&-\iota_t^0 - \sum_{r\in I_t} \iota_{1,t}^r \cdot \Pi_r - \sum_{r\in I_t} \iota_{2,t}^r \cdot \Psi_r + \zeta_t^0 + \sum_{r\in I_t} \zeta_{1,t}^r \cdot \Pi_r + \sum_{r\in I_t} \zeta_{2,t}^r \cdot \Psi_r \\
&- \sum_{s=t}^{T} \nu_s^0 - \sum_{s=t}^{T}\sum_{r\in I_s} \nu_{1,s}^r \cdot \Pi_r - \sum_{s=t}^{T}\sum_{r\in I_s} \nu_{2,s}^r \cdot \Psi_r \\
&+ \sum_{s=t}^{T} \mu_s^0 + \sum_{s=t}^{T}\sum_{r\in I_s} \mu_{1,s}^r \cdot \Pi_r + \sum_{s=t}^{T}\sum_{r\in I_s} \mu_{2,s}^r \cdot \Psi_r \\
&\geq \frac{1}{(1+r)^t}\Pi_t, \quad \forall t \in T
\end{aligned} \tag{C.1.28}$$

$$
\begin{aligned}
&-\sum_{s=t}^{T}\nu_s^0 - \sum_{s=t}^{T}\sum_{r\in I_s}\nu_{1,s}^r\cdot\Pi_r - \sum_{s=t}^{T}\sum_{r\in I_s}\nu_{2,s}^r\cdot\Psi_r \\
&+\sum_{s=t}^{T}\mu_s^0 + \sum_{s=t}^{T}\sum_{r\in I_s}\mu_{1,s}^r\cdot\Pi_r + \sum_{s=t}^{T}\sum_{r\in I_s}\mu_{2,s}^r\cdot\Psi_r \\
&\geq 0, \quad \forall t\in T
\end{aligned}
\tag{C.1.29}
$$

$$
\iota_t^0 + \sum_{r\in I_t}\iota_{1,t}^r\cdot\Pi_r + \sum_{r\in I_t}\iota_{2,t}^r\cdot\Psi_r \geq 0, \quad \forall t\in T \tag{C.1.30}
$$

$$
\zeta_t^0 + \sum_{r\in I_t}\zeta_{1,t}^r\cdot\Pi_r + \sum_{r\in I_t}\zeta_{2,t}^r\cdot\Psi_r \geq 0, \quad \forall t\in T \tag{C.1.31}
$$

$$
\mu_t^0 + \sum_{r\in I_t}\mu_{1,t}^r\cdot\Pi_r + \sum_{r\in I_t}\mu_{2,t}^r\cdot\Psi_r \geq 0, \quad \forall t\in T \tag{C.1.32}
$$

$$
\nu_t^0 + \sum_{r\in I_t}\nu_{1,t}^r\cdot\Pi_r + \sum_{r\in I_t}\nu_{2,t}^r\cdot\Psi_r \geq 0, \quad \forall t\in T \tag{C.1.33}
$$

$$
\forall\, \Pi_t \in [\Pi_t^* - \theta\cdot\Pi_t^*, \Pi_t^* + \theta\cdot\Pi_t^*], \quad \forall t\in T \tag{C.1.34}
$$

$$
\forall\, \Psi_t \in [\Psi_t^* - \theta\cdot\Psi_t^*, \Psi_t^* + \theta\cdot\Psi_t^*], \quad \forall t\in T \tag{C.1.35}
$$

C.1.4 Covariance

The terms $\mathbb{E}[\Pi_t]$, $\mathbb{E}[\Psi_t]$, $\mathbb{E}[\Psi_t\cdot\Pi_r]$ and $\mathbb{E}[\Psi_t\cdot\Psi_r]$ arise in the objective function. These terms can be rewritten to:

$$
\begin{aligned}
\mathbb{E}[\Pi_t] &= \Pi_t^*, \quad \forall t\in T \\
\mathbb{E}[\Psi_t] &= \Psi_t^*, \quad \forall t\in T \\
\mathbb{E}[\Pi_t\cdot\Psi_r] &= \Pi_t^*\cdot\Psi_t^* + C_{t,r}^{\Pi,\Psi}, \quad 1\leq r\leq t\leq T \\
\mathbb{E}[\Psi_t\cdot\Psi_r] &= \Psi_t^*\cdot\Psi_t^* + C_{t,r}^{\Psi,\Psi}, \quad 1\leq r\leq t\leq T
\end{aligned}
\tag{C.1.36}
$$

C.1.5 Additional variables

In order to use the equivalences from Appendix B.1.4 new additional variables for the non-adjustable variables are defined as:

$$-l_t^r \leq \iota_t^r \leq l_t^r, \quad l_t^r = |\iota_t^r|, \quad 1 \leq r \leq t \leq T \tag{C.1.37}$$

$$-c_t^r \leq \zeta_t^r \leq c_t^r, \quad c_t^r = |\zeta_t^r|, \quad 1 \leq r \leq t \leq T \tag{C.1.38}$$

$$-v_t^r \leq \nu_t^r \leq v_t^r, \quad v_t^r = |\nu_t^r|, \quad 1 \leq r \leq t \leq T \tag{C.1.39}$$

$$-u_t^r \leq \mu_t^r \leq u_t^r, \quad u_t^r = |\mu_t^r|, \quad 1 \leq r \leq t \leq T \tag{C.1.40}$$

C.1.6 The dual LDR model

Rewriting the objective function as described in Appendix C.1.4 and the constraints in the model from Appendix C.1.3 using the equivalences from Appendix B.1.4 and the new additional variables from Appendix C.1.5 results in the following aggregated reservoir dual LDR model:

$$\begin{aligned}
& Z_0 = \\
min\ \mathbb{E} \sum_{t=1}^{T} \Bigg[& -Q_{min} \cdot \iota_t^0 - \sum_{r \in I_t} Q_{min} \cdot \iota_{1,t}^r \cdot \Pi_r^* - \sum_{r \in I_t} Q_{min} \cdot \iota_{2,t}^r \cdot \Psi_r^* \\
& +Q_{max} \cdot \zeta_t^0 + Q_{max} \cdot \sum_{r \in I_t} \zeta_{1,t}^r \cdot \Pi_r^* + Q_{max} \cdot \sum_{r \in I_t} \zeta_{2,t}^r \cdot \Psi_r^* \\
& +M_{max} \cdot \nu_t^0 + M_{max} \cdot \sum_{r \in I_t} \nu_{1,t}^r \cdot \Pi_r^* + M_{max} \cdot \sum_{r \in I_t} \nu_{2,t}^r \cdot \Psi_r^* \\
& -M_0 \cdot \nu_t^0 - M_0 \cdot \sum_{r \in I_t} \nu_{1,t}^r \cdot \Pi_r^* - M_0 \cdot \sum_{r \in I_t} \nu_{2,t}^r \cdot \Psi_r^* \\
& -\sum_{s \in I_t} \Psi_s^* \cdot \nu_t^0 - \sum_{s \in I_t} \sum_{r \in I_t} \Psi_s^* \cdot \Pi_r^* \cdot \nu_{1,t}^r - \sum_{s \in I_t} \sum_{r \in I_t} C_{s,r}^{\Pi,\Psi} \cdot \nu_{1,t}^r \\
& -\sum_{s \in I_t} \sum_{r \in I_t} \Psi_s^* \cdot \Psi_r^* \cdot \nu_{2,t}^r - \sum_{s \in I_t} \sum_{r \in I_t} C_{s,r}^{\Psi,\Psi} \cdot \nu_{2,t}^r \\
& -M_{min} \cdot \mu_t^0 - M_{min} \cdot \sum_{r \in I_t} \mu_{1,t}^r \cdot \Pi_r^* - M_{min} \cdot \sum_{r \in I_t} \mu_{2,t}^r \cdot \Psi_r^* \\
& +M_0 \cdot \mu_t^0 + M_0 \cdot \sum_{r \in I_t} \mu_{1,t}^r \cdot \Pi_r^* + M_0 \cdot \sum_{r \in I_t} \mu_{2,t}^r \cdot \Psi_r^* \\
& +\sum_{s \in I_t} \Psi_s^* \cdot \mu_t^0 + \sum_{s \in I_t} \sum_{r \in I_t} \Psi_s^* \cdot \Pi_r^* \cdot \mu_{1,t}^r + \sum_{s \in I_t} \sum_{r \in I_t} C_{s,r}^{\Pi,\Psi} \cdot \mu_{1,t}^r \\
& +\sum_{s \in I_t} \sum_{r \in I_t} \Psi_s^* \cdot \Psi_r^* \cdot \mu_{2,t}^r + \sum_{s \in I_t} \sum_{r \in I_t} C_{s,r}^{\Psi,\Psi} \cdot \mu_{2,t}^r \Bigg]
\end{aligned} \tag{C.1.41}$$

$$
\begin{aligned}
-\iota_t^0 - \sum_{r\in I_t}\iota_{1,t}^r\cdot\Pi_r^* - \theta^\Pi\cdot\sum_{r\in I_t} l_{1,t}^r\cdot\Pi_r^* - \sum_{r\in I_t}\iota_{2,t}^r\cdot\Psi_r^* - \theta^\Psi\cdot\sum_{r\in I_t} l_{2,t}^r\cdot\Psi_r^* \\
+\zeta_t^0 + \sum_{r\in I_t}\zeta_{1,t}^r\cdot\Pi_r^* - \theta^\Pi\cdot\sum_{r\in I_t} c_{1,t}^r\cdot\Pi_r^* + \sum_{r\in I_t}\zeta_{2,t}^r\cdot\Psi_r^* - \theta^\Psi\cdot\sum_{r\in I_t} c_{2,t}^r\cdot\Psi_r^* \\
-\sum_{s=t}^{T}\nu_s^0 - \sum_{s=t}^{T}\sum_{r\in I_s}\nu_{1,s}^r\cdot\Pi_r^* - \theta^\Pi\cdot\sum_{s=t}^{T}\sum_{r\in I_s} v_{1,s}^r\cdot\Pi_r^* \\
-\sum_{s=t}^{T}\sum_{r\in I_s}\nu_{2,s}^r\cdot\Psi_r^* - \theta^\Psi\cdot\sum_{s=t}^{T}\sum_{r\in I_s} v_{2,s}^r\cdot\Psi_r^* \\
+\sum_{s=t}^{T}\mu_s^0 + \sum_{s=t}^{T}\sum_{r\in I_s}\mu_{1,s}^r\cdot\Pi_r^* - \theta^\Pi\cdot\sum_{s=t}^{T}\sum_{r\in I_s} u_{1,s}^r\cdot\Pi_r^* \\
+\sum_{s=t}^{T}\sum_{r\in I_s}\mu_{2,s}^r\cdot\Psi_r^* - \theta^\Psi\cdot\sum_{s=t}^{T}\sum_{r\in I_s} u_{2,s}^r\cdot\Psi_r^* \geq \frac{1}{(1+r)^t}(\Pi_t^* + \theta^\Pi\cdot\Pi_t^*), \\
\forall t\in T
\end{aligned}
\tag{C.1.42}
$$

$$
\begin{aligned}
-\sum_{s=t}^{T}\nu_s^0 - \sum_{s=t}^{T}\sum_{r\in I_s}\nu_{1,s}^r\cdot\Pi_r^* - \theta^\Pi\cdot\sum_{s=t}^{T}\sum_{r\in I_s} v_{1,s}^r\cdot\Pi_r^* \\
-\sum_{s=t}^{T}\sum_{r\in I_s}\nu_{2,s}^r\cdot\Psi_r^* - \theta^\Psi\cdot\sum_{s=t}^{T}\sum_{r\in I_s} v_{2,s}^r\cdot\Psi_r^* \\
+\sum_{s=t}^{T}\mu_s^0 + \sum_{s=t}^{T}\sum_{r\in I_s}\mu_{1,s}^r\cdot\Pi_r^* - \theta^\Pi\cdot\sum_{s=t}^{T}\sum_{r\in I_s} u_{1,s}^r\cdot\Pi_r^* \\
+\sum_{s=t}^{T}\sum_{r\in I_s}\mu_{2,s}^r\cdot\Psi_r^* - \theta^\Psi\cdot\sum_{s=t}^{T}\sum_{r\in I_s} u_{2,s}^r\cdot\Psi_r^* \\
\geq 0, \quad \forall t\in T
\end{aligned}
\tag{C.1.43}
$$

$$
\begin{aligned}
\iota_t^0 + \sum_{r\in I_t}\iota_{1,t}^r\cdot\Pi_r^* - \theta^\Pi\cdot\sum_{r\in I_t} l_{1,t}^r\cdot\Pi_r^* + \sum_{r\in I_t}\iota_{2,t}^r\cdot\Psi_r^* - \theta^\Psi\cdot\sum_{r\in I_t} l_{2,t}^r\cdot\Psi_r^* \\
\geq 0, \quad \forall t\in T
\end{aligned}
\tag{C.1.44}
$$

$$
\begin{aligned}
\zeta_t^0 + \sum_{r\in I_t}\zeta_{1,t}^r\cdot\Pi_r^* - \theta^\Pi\cdot\sum_{r\in I_t} c_{1,t}^r\cdot\Pi_r^* + \sum_{r\in I_t}\zeta_{2,t}^r\cdot\Psi_r^* - \theta^\Psi\cdot\sum_{r\in I_t} c_{2,t}^r\cdot\Psi_r^* \\
\geq 0, \quad \forall t\in T
\end{aligned}
\tag{C.1.45}
$$

$$
\begin{aligned}
\nu_t^0 + \sum_{r\in I_t}\nu_{1,t}^r\cdot\Pi_r^* - \theta^\Pi\cdot\sum_{r\in I_t} v_{1,t}^r\cdot\Pi_r^* + \sum_{r\in I_t}\nu_{2,t}^r\cdot\Psi_r^* - \theta^\Psi\cdot\sum_{r\in I_t} v_{2,t}^r\cdot\Psi_r^* \\
\geq 0, \quad \forall t\in T
\end{aligned}
\tag{C.1.46}
$$

$$\mu_t^0 + \sum_{r \in I_t} \mu_{1,t}^r \cdot \Pi_r^* - \theta^\Pi \cdot \sum_{r \in I_t} u_{1,t}^r \cdot \Pi_r^* + \sum_{r \in I_t} \mu_{2,t}^r \cdot \Psi_r^* - \theta^\Psi \cdot \sum_{r \in I_t} u_{2,t}^r \cdot \Psi_r^* \geq 0, \quad \forall t \in T \tag{C.1.47}$$

$$-l_t^r \leq \iota_t^r \leq l_t^r, \quad 1 \leq r \leq t \leq T \tag{C.1.48}$$

$$-c_t^r \leq \zeta_t^r \leq c_t^r, \quad 1 \leq r \leq t \leq T \tag{C.1.49}$$

$$-v_t^r \leq \nu_t^r \leq v_t^r, \quad 1 \leq r \leq t \leq T \tag{C.1.50}$$

$$-u_t^r \leq \mu_t^r \leq u_t^r, \quad 1 \leq r \leq t \leq T \tag{C.1.51}$$

D Results from the primal models

This appendix presents figures showing expected production strategies for all the hydropower plants evaluated in this thesis. Figures showing the lowest possible, the expected and the highest possible reservoir levels are presented for Plant 2 for uncertainty levels of 5 % and 15 %. All figures are operating with relative numbers, in which 1 corresponds to the maximum production level and maximum reservoir capacity.

D.1 Hydropower plant 1

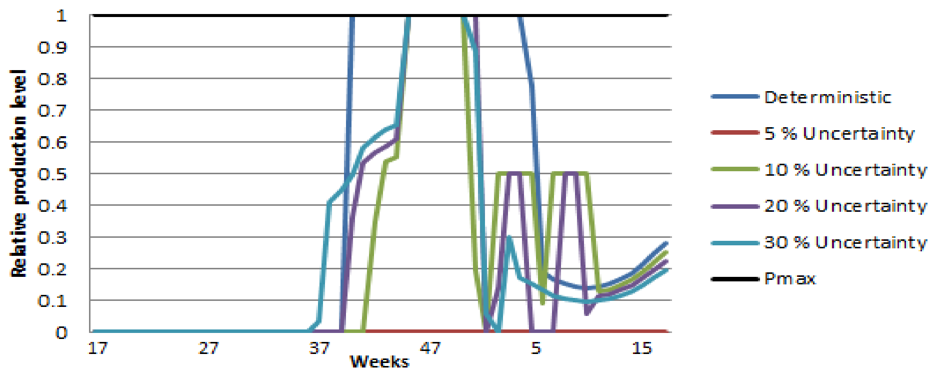

Figure D.1.1: Relative expected production levels for Plant 1

D.2 Hydropower plant 2

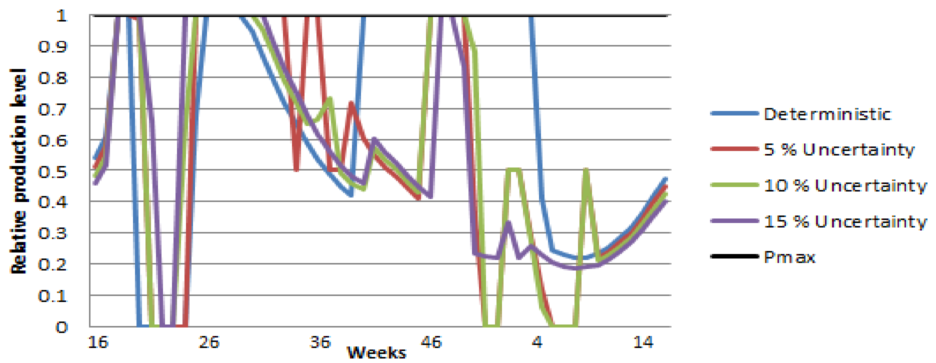

Figure D.2.1: Relative expected production levels for Plant 2

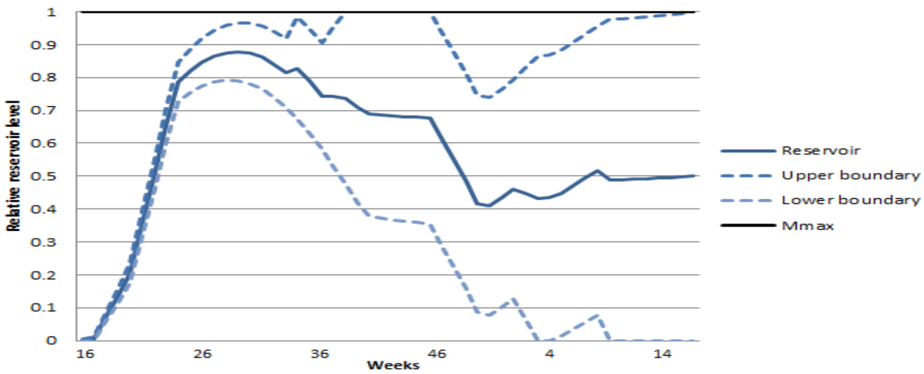

Figure D.2.2: The figure show the lowest possible, the expected and the highest possible reservoir level for an uncertainty level of 5 %.

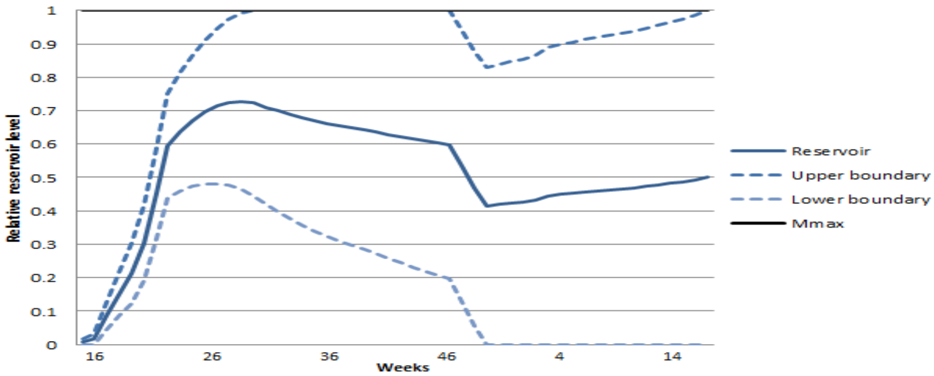

Figure D.2.3: The figure show the lowest possible, the expected and the highest possible reservoir level for an uncertainty level of 15 %.

D.3 Hydropower plant 3

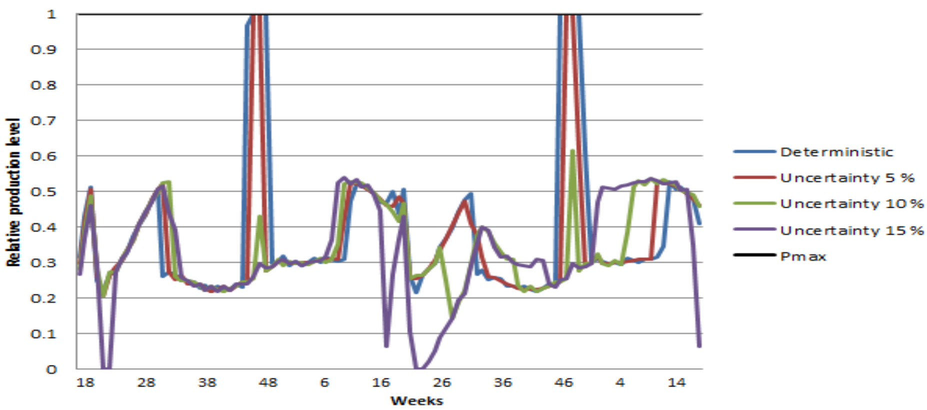

Figure D.3.1: Relative expected production levels for Power Station 1

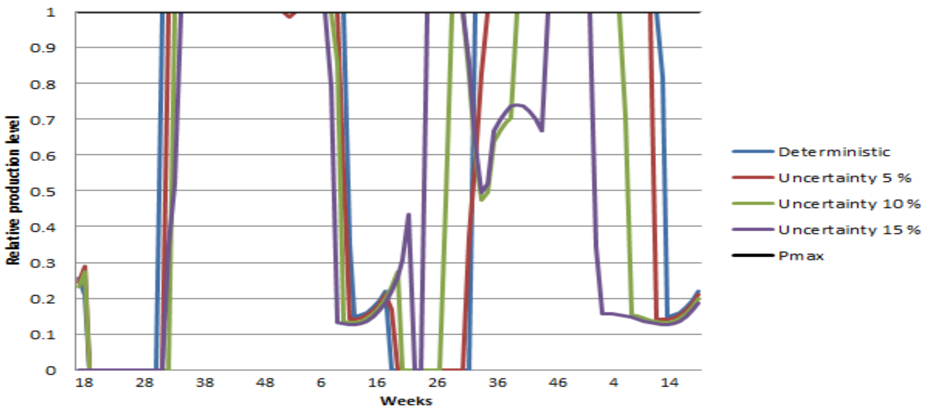

Figure D.3.2: Relative expected production levels for Power Station 2

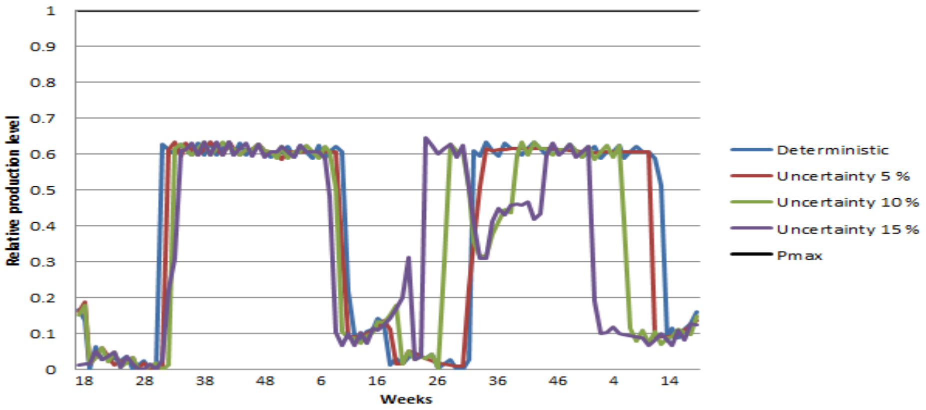

Figure D.3.3: Relative expected production levels for Power Station 3

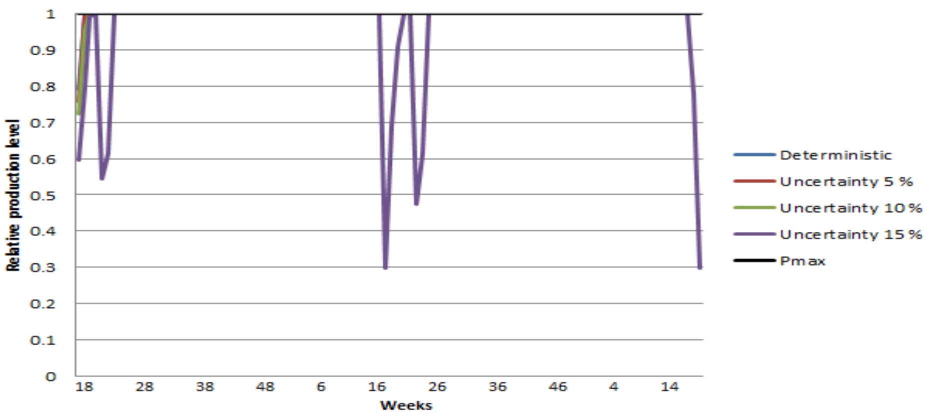

Figure D.3.4: Relative expected production levels for Power Station 4

D.4 Hydropower plant 4

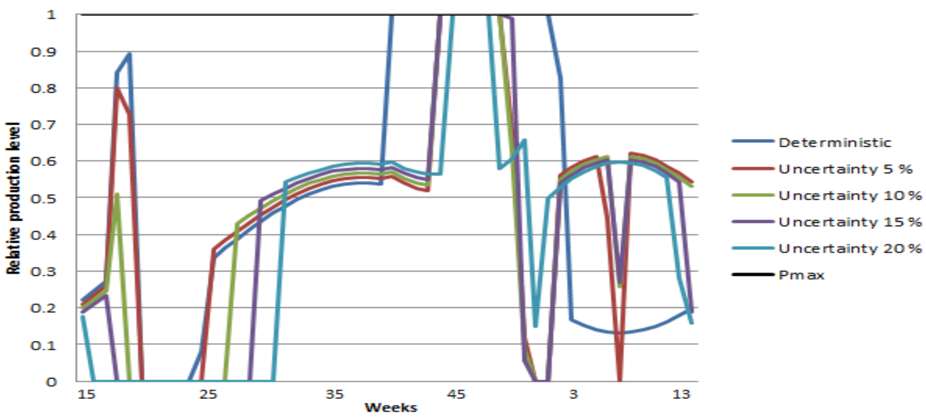

Figure D.4.1: Relative expected production levels for Power Station 1

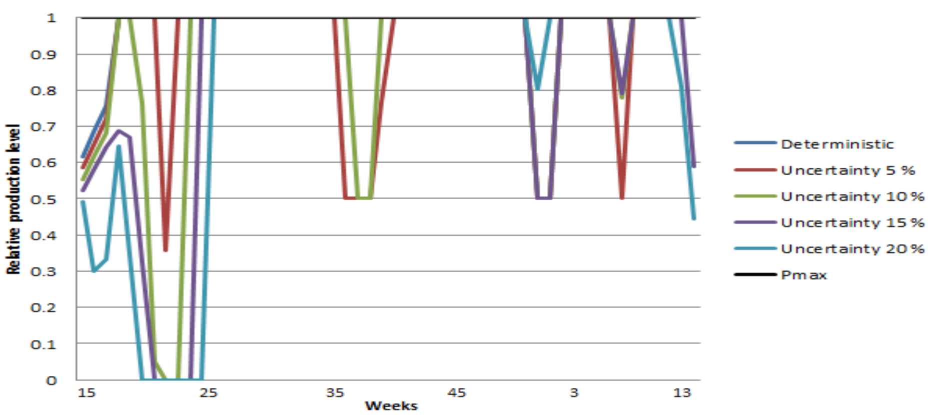

Figure D.4.2: Relative expected production levels for Power Station 2

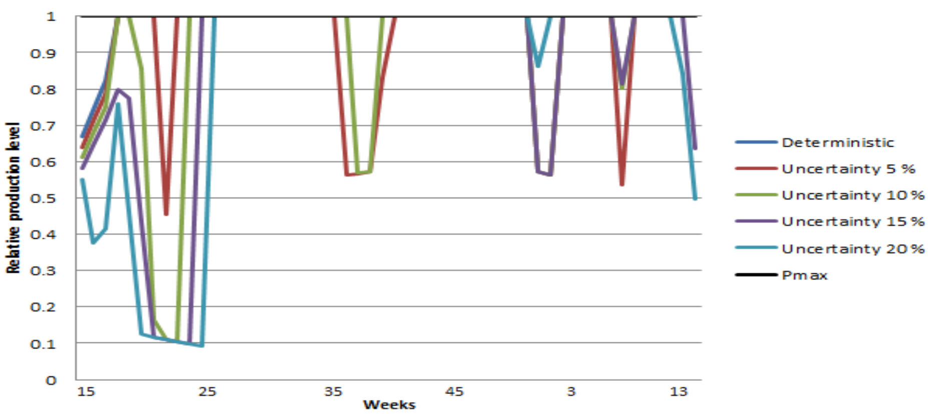

Figure D.4.3: Relative expected production levels for Power Station 3

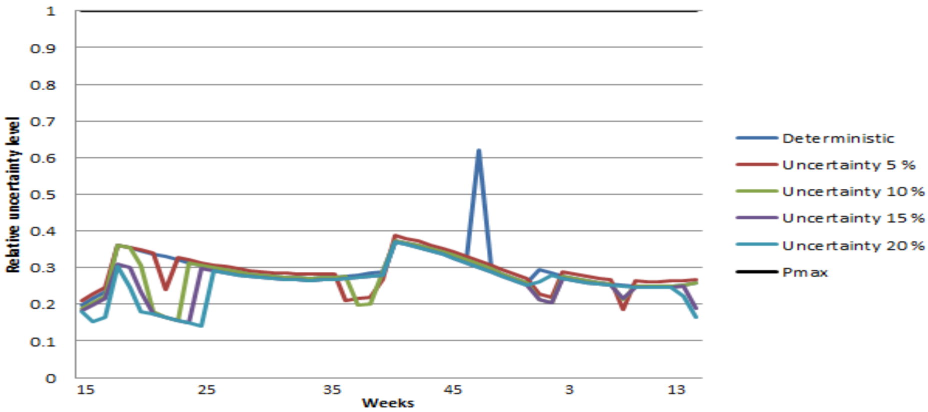

Figure D.4.4: Relative expected production levels for Power Station 4